Fall 2013

Observation-Based Algorithm Development For Subsurface Hydrology In Northern Temperate Wetlands

Chun-Mei Chiu
Purdue University

Graduate School ETD Form 9
(Revised 12/07)

PURDUE UNIVERSITY
GRADUATE SCHOOL
Thesis/Dissertation Acceptance

This is to certify that the thesis/dissertation prepared

By CHUN-MEI CHIU

Entitled : OBSERVATION-BASED ALGORITHM DEVELOPMENT FOR SUBSURFACE HYDROLOGY IN NORTHERN TEMPERATE WETLANDS

For the degree of Doctor of Philosophy

Is approved by the final examining committee:

LAURA C. BOWLING Chair	DEVDUTTA S. NIYOGI
PHILIP R. OWENS	QIANLAI ZHUANG

To the best of my knowledge and as understood by the student in the *Research Integrity and Copyright Disclaimer (Graduate School Form 20)*, this thesis/dissertation adheres to the provisions of Purdue University's "Policy on Integrity in Research" and the use of copyrighted material.

Approved by Major Professor(s): LAURA C. BOWLING

Approved by: JOSEPH M. ANDERSON 10/10/2013
Head of the Graduate Program Date

OBSERVATION-BASED ALGORITHM DEVELOPMENT FOR SUBSURFACE HYDROLOGY IN NORTHERN TEMPERATE WETLANDS

A Dissertation
Submitted to the Faculty
of
Purdue University
by
Chun-Mei Chiu

In Partial Fulfillment of the
Requirements for the Degree
of
Doctor of Philosophy

December 2013
Purdue University
West Lafayette, Indiana

To my parents, 邱世昆 (Chiu Shih-Kun) and 陳麗存 (Chen Li-Tsun), and siblings – for their unconditional love and support of all that I do.

ACKNOWLEDGEMENTS

Completing my PhD degree has probably been the most challenging mission of my life. The best and worst moments of my doctoral journey have been shared with many people. It has been a great privilege to spend several years in the Department of Agronomy at Purdue University, and its members will always remain dear to me.

My first debt of gratitude is to my advisor, Dr. Laura C. Bowling. She patiently provided the vision, encouragement and advice necessary for me to carry out the doctoral program and complete my dissertation. I want to thank her for her never giving up encouragement and for serving as a role model to me as a member of academia. She has been a brilliant, tough and supportive adviser to me throughout my graduate school career, while always giving me great freedom to pursue independent work. Her mentorship has been paramount in providing a well-rounded experience consistent my long-term career goals. For everything, you have done for me, Dr. Bowling, I give you my most sincere thanks.

Special thanks to my committee, Dr. Dev Niyogi, Dr. Philip Owens, Dr. Qianlai Zhuang for their support, guidance and helpful suggestions. Their guidance has served me well and I owe them my heartfelt appreciation. I also would like to thank Dr. Ron Turco and Dr. Darrell Schulze for providing me with great teaching opportunities and guidance while serving as a Teaching Assistant.

The current and former members of the Hydrologic Impacts Group also deserve my sincerest thanks; their friendship and assistance has meant more to me than I could ever express. I could not have completed my work without the invaluable and friendly assistance of the participants of the NEESPI, Wabash, and CSCAP projects. I should also mention the entire body of graduate students and staff in the Department of Agronomy for involving me as part of this great professional community. I also would like to thank the Purdue water community for providing chance to let me involving the greater Lafayette community.

My friends in the US, Taiwan and other parts of the world were sources of laughter, joy, and support. Special thanks go to Glenn Rowland for proofreading this thesis in a short time frame, providing his input and constantly giving mental support. I would also like to mention the members of I Love Taiwan Club for their friendship, allowing me to lead the club and providing the opportunity to grow in leadership. These experiences have and will extend well beyond our shared time in West Lafayette.

I wish to thank my parents, 邱世昆 (Chiu Shih-Kun) and 陳麗存 (Chen Li-Tsun) and my grandparents. Their love provided my inspiration and has been my driving force. I owe them everything and wish I could show them just how much I love and appreciate them. I hope that this work makes you proud. I also want to thank my two brothers and sister, whose love and encouragement allowed me to finish this journey. Finally, I want to thank my extended family, especially my sisters-in-law, for their unconditional support.

TABLE OF CONTENTS

Page

Page

Page

LIST OF TABLES

Table Page

LIST OF FIGURES

Figure Page

Figure Page

Figure Page

Figure Page

Figure Page

ABSTRACT

Chiu, Chun-Mei. Ph.D., Purdue University, December 2013. Observation-based algorithm development for subsurface hydrology in northern temperate wetlands. Major Professor: Laura C. Bowling.

This study investigates wetland subsurface hydrology, as well as biogeochemistry - which is strongly influenced by water and temperature dynamics - as these interactions are expected to be highly significant, yet remain poorly represented in current ecosystem and climate models.

Northern wetlands have received widespread public attention due to steadily increasing summer mean global temperatures, extreme precipitation events and higher rates of natural greenhouse gas emissions, as well as the significant impacts on them due to human activities. The goal of my graduate research has been to improve quantification of the role of subsurface hydrology in northern wetlands by using a macroscale hydrological model, the Variable Infiltration Capacity (VIC) model. The existing VIC model was modified to better represent the effect of surface and subsurface water storage in managed wetlands. An improved water table depth calculation, based on a drained to equilibrium assumption, was incorporated into a new subsurface drainage algorithm. The spatial variability of water table depth across landscape positions has been represented

using a topographic index approach. By incorporating a water table gradient into the VIC grid cell, subsurface-surface water exchange within the wetland can also be represented, dependent on land surface class. This algorithm was developed and evaluated using data at scales ranging from field to small watershed, which included a small wetland at the Agronomy Center for Research and Education (ACRE), the long-term drainage experiment at the Davis-Purdue Agricultural Center (DPAC), and a cooperators mint farm in Pulaski, Indiana.

The improved model has been used at larger scales - from large watersheds to regional scale - to better understand the subsurface hydrology affected by drainage practices throughout the poorly-drained Midwest agricultural regions. Recent concern regarding high rates of soil organic matter decomposition due to artificial drainage enhancements motivated an integrated field and modeling experiment to quantify the influence of water management on cultivated organic soils in the Kankakee River basin, a flat outwash plain covered with relatively deep, poorly drained soil with high organic matter content. Methane and carbon dioxide emissions were simulated by using soil temperature, water table position and net primary production generated from the VIC model and evaluated using CO_2 flux measurements, water table height and soil moisture measurements. The model simulations do support the high rates of subsidence previously reported for these high organic matter soils, but most of the subsidence took place soon after the introduction of agricultural drainage. Another case study evaluated the role of anthropogenic modifications to drainage conditions and wetland extent on streamflow in the upper Wabash River basin. An initial test case demonstrated that a depressional

wetland perched on the Tipton Till Plain tends to recharge soil moisture in riparian areas by late summer, reducing the volume of baseflow downstream. When scaled up to the upper Wabash River basin , the study demonstrated that wetlands provided more temporal surface water storage and served to reduce peak flows. Subsurface drainage increased the high flow, mean flow, and Richard-Baker flashiness Index (RBI), and reduced the low flow and flow distribution. Stream network density analysis showed that simulations with lower drainage density (representing historic, natural conditions) had relatively lower high flow and smaller RBI. These results provide evidence that although drainage creates more pore space in the soil profile - reducing surface runoff - it also creates more flow paths, allowing water to travel to the watershed outlet more quickly.

1. INTRODUCTION

1.1 Introduction

Much of the landscape of the northern high latitudes reflects the history of repeated glaciations. The nature of the landscape may include low topographic gradients and underlying dense till which restricts vertical water movement. Also within this landscape, there are kettle depressions formed by large blocks of ice that were surrounded by till or stratified drift during the retreat of the glacier and there are smaller depressions that were controlled by differences in the underlying structure, all of which lead to poorly drained soils. The relatively recent glaciation in some parts of the artic and northern temperate zone means that the landscape is less dissected than older landscapes, and therefore less hydrologically connected. As a result, two of the most common landscape features in the northern high latitudes are wetlands and lakes (Figure 1-1). The majority of the world's wetlands are located between 45 and 70 ^{o}N (Lehner & Döll, 2004), an area which we refer to generally as the northern high latitudes.

The United States EPA estimates that Alaska has approximately 175 million acres (~0.708 million km^2) of wetlands, comprising approximately 43% of the surface area of the state, more wetland acreage than the rest of the United States combined. Natural Resources Canada estimates that 14% of Canada (1.27 million km^2) is occupied by wetlands. The Wetland International Russia office estimates that most of western Russia is categorized as flat lowlands with a humid climate that includes a vast area of wetlands

(~1.8 million km^2), as well as 120,000 rivers with a total length of 2,300,000 km and approximately 2 million lakes with total volume of 370,000 km^3. In the conterminous U.S., there were an estimated 0.446 million km^2 (46.6 million ha or 110.1 million acres) of wetland in 2009 with an estimated 0.422 million km^2 (42.2 million ha or 104.3 million acres) of freshwater wetlands and 0.024 million km^2 (2.4 million ha or 5.8 million acres) of intertidal (saltwater) wetlands (Dhal, 2011). Wetlands compose 5.5 % of the surface area of the conterminous U.S with an estimated 95 % of all wetlands being fresh-water.

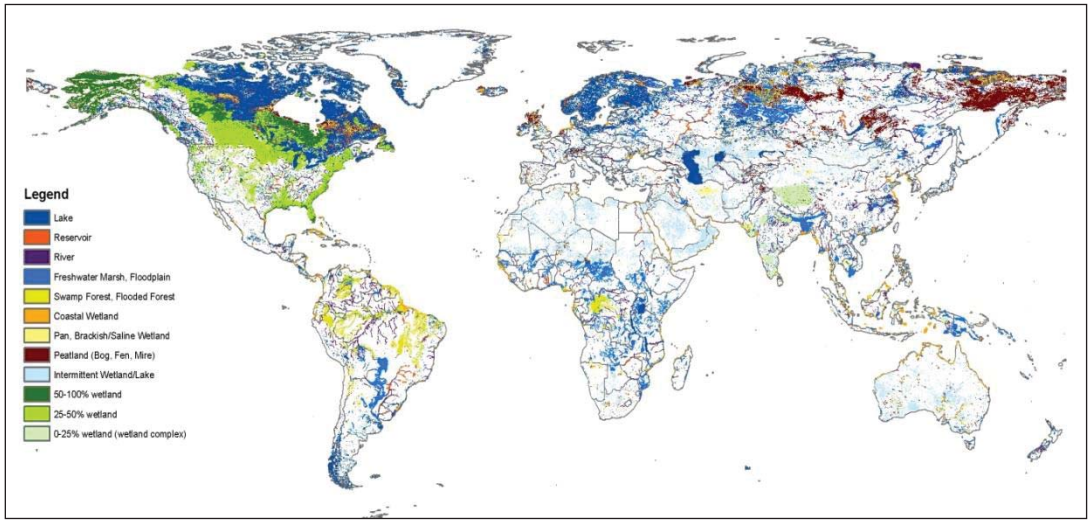

Figure 1-1. The global lake and wetland extent from Global Lakes and Wetlands Database (GLWD) (Lehner & Döll, 2004).

Wetlands are sensitive ecosystems affected by weather and climate conditions and human activities. It is well-established that the global mean temperature has been increasing for several decades (Christensen et al., 2007). Regional changes observed in the northern high latitude climate include warmer spring and summer temperatures and increased annual precipitation (Hinzman et al., 2005; Serreze and Barry, 2005; Forbes, 2001; Kudeyarov et al., 2009; Khon et al., 2007). The average temperature of northern permafrost has increased, resulting in massive ground ice thawing (Forbes, 2001;

Anisimov and Nelson, 1997; Nelson and Anisimov, 1993, William, 1995). USGCRP (2009) showed that observed average temperature in the Midwest has noticeably increased, despite the strong year-to-year variations. The largest increase has been observed in winter, extending the length of the frost-free season by more than one week due to earlier dates for the last spring frost. Heavy rainfall is now twice as frequent as it was a century ago. The more intense rainfall can lead to more frequent floods that cause significant impacts locally and even nationally. Recent historical observations in the wetland-rich North Central US also indicate that winter and spring precipitation is increasing, while summer precipitation remains unchanged (Mishra et al, 2010). There is an increase in surface soil temperature leading to a decrease in the number of soil frost days (Sinha et al., 2008; 2010).

Loss of wetlands is increasing due to human activities such as agricultural applications and development of land for urban and industrial use as shown in Figure1-2 (Dahl, 2011). However, the impact of global change on the extent and function of northern wetlands is still uncertain. A feedback loop between climate change and changes in wetlands exists because moisture availability in lakes and wetlands can impact the rate and speciation of carbon release from both natural wetlands and lakes. However, the magnitude of the interaction between hydrological perturbations, streamflow and water quality and the carbon cycle is not yet well studied in northern latitudes.

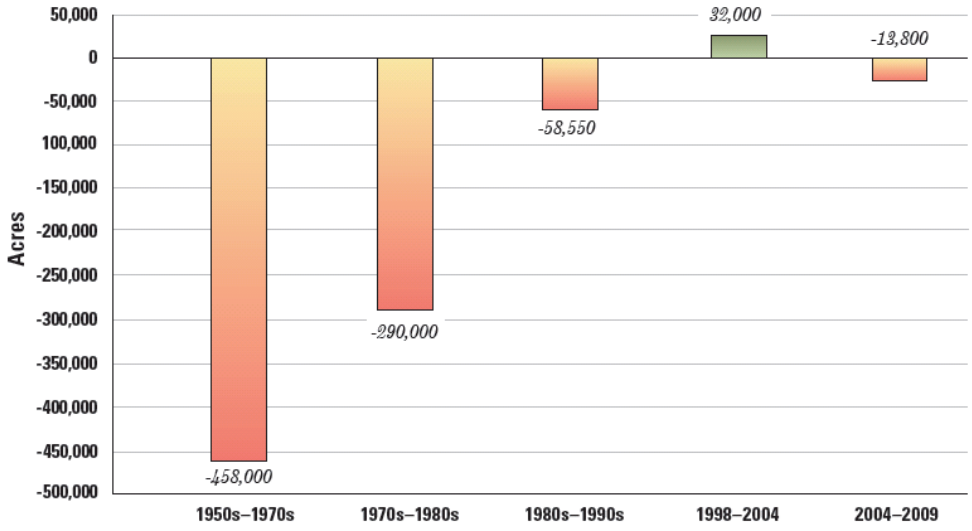

Figure 1-2. Average annual net loss and gain estimates for conterminous United Stated from 1954 to 2009. (Courtesy Dahl, 2011)

1.1.1. Wetland classification, functions and importance

Various terms are used to describe wetlands including marshes, swamps, bogs, small ponds, sloughs, potholes, mudflats, peatlands and wet meadows. Generally, wetlands are any land that is saturated most of time and for which water is the main factor determining the nature of soil development and the types of plants and animal communities living in the soil and surface region (Cowardin et al., 1979). Wetlands are the lands in the transitional zone between terrestrial and aquatic systems, where the water table is usually at or near the surface and which may be covered by shallow water. Usually, wetlands must have one or more the following characteristics: (1) the land periodically or predominantly supports hydrophytes; (2) predominantly undrained hydric soil; and (3) water-saturated soil or covered by shallow water during the growing season of each year (Cowardin et al., 1979). Wetlands can be classified into two broad classes by their geographic location: coastal wetlands and inland wetlands. We mainly focus on inland wetlands located in northern latitudes in this study.

Wetland hydrologic functions play important roles in modifying or controlling the water quality and quantity of water moving through watersheds as well as in the global water cycle, such as (1) flood storage and stormflow modification, (2) mediating the balance of ground water discharge and recharge, (3) modifying the precipitation and evaporation balance, (4) providing flood protection and erosion reduction, and (5) maintenance of water quality and water balance (Carter, 1996). Wetlands can store floodwaters by spreading water out over a huge flat area before it moves into lakes or streams. This storage function decreases the surface flow velocity, reduces the peak flows and then distributes stormflow over longer periods, resulting in delayed stream peak flow with consequent reduction in the risk of flood (Leibowitz et al., 1992). When the surface water level of a wetland is lower than the water table of the surrounding land, nearby groundwater inflows can recharge this wetland. Recharge or discharge of wetlands is strongly influenced by the local hydrology, topography, evapotranspiration, precipitation, soil types, and climate.

Wetlands can moderate air temperature fluctuations and feedback into regional climate systems (Carter, 1996). During winter, relatively warm and wet wetlands tend to prevent rapid freezing at night. In summer, wetlands tend to stay at lower temperatures because evapotranspiration - from either the wetland itself or from the vegetation - converts latent heat and releases water vapor into the atmosphere, moderating the temperature fluctuations. By modifying local climates, wetlands can affect cloud formation, thunderstorms and precipitation patterns (Carter, 1996; Jacobs and Grandi, 1988; Jefferies et al., 1999). With regard to their effect on water quality, wetlands can trap waste water and precipitate, transform, recycle, or export many harmful components.

When water flows through a wetland, its' quality can be altered remarkably (Mitsch and Gosselink, 2000). Fisher and Acreman (2004) collected data from 57 natural wetlands from around the world and found that the majority of wetlands reduced nutrient loading and there was little difference in the proportion of wetlands that reduced N to those that reduced P loading.

1.1.2. The impact human activities and global climate change on wetlands

Wetlands can be significantly affected by both human activities and global climate change. Agricultural land use has been a major factor in the loss of wetland function. For example, Wilen and Frayer (1990) demonstrated that the massive losses of wetlands in the conterminous United States from 1950's to 1970's were primarily due to human activities. Agricultural development was responsible for 87% of wetland losses and 90% of the losses of forested wetlands. Urban and other development caused only 8% and 5% of the losses, respectively. Forested-wetland losses caused by urban development and other industrial development were 6% and 4%, respectively. Natural Resources Canada also found that agricultural expansion is the cause of 85% of Canada's wetland losses. Agricultural drainage (such as ditches and subsurface tile) is mainly used to lower water table depth, and increase the rate of water movement flowing away from the land. Loss of wetlands can result in changes in flood timing and an increase in the magnitude and likelihood of severe and costly flood damage occurring in low-lying areas of a basin. Besides of the hydrological impacts, changing streamflow pattern, surface and subsurface drainage also contribute to significant water quality impairment. Drainflow plays an important role in short circuiting the natural cleaning mechanism of riparian wetlands. The tile drainflow containing primarily nitrates from excess fertilizer can bypass riparian

wetlands and directly enter ditches and small creeks. Rabalais et al. (2002) found that nitrate loss from extensive agricultural application in the Mississippi River Basin is one of the major contributors to the Gulf of Mexico's oxygen depletion.

Climate variability and change can also have a substantial impact on wetlands, particularly those that exist in areas of seasonally or permanently frozen soil. Recently, increases in the temperature of both permanently and seasonal frozen ground have been observed in conjunction with other global climate changes. Romanovsky et al. (2001) indicated that permafrost temperature in northern Russia had increased by 1 to 2^{o}C during the last 30 to 35 years, while temperature has increased by 0.03 ^{o}C at depths up to 15 m in the Central Mackenzie basin, Canada (Couture et al. 2002). Sinha et al. (2008; 2010) showed that there has been an increase in surface soil temperature leading to a decrease in the number of soil frost days in the Midwest United States.

Several studies have shown that lake and wetland extent above the continuous permafrost has increased, but decreased above discontinuous permafrost (Smith et al., 2005 and Grippa et al., 2007). It is hypothesized that the initial warming of permafrost can lead to development of thermokarst (commonly known as thaw lake) and - in the beginning stage – results in expansion of the lake area. In addition, melting ground ice may lead to addition of water volume to lakes, streams or oceans from in response to warming. However, further warming leads to thinning and eventual puncture of the permafrost, allowing drainage to occur and resulting in permanently drained lakes (Smith et al., 2005). Seasonal soil frost can also play a substantial role in wetland hydrology. For example, the winter and spring storage capacity of wetlands may be limited by frozen ground, so flood peak reduction is often greatest for summer rainfall events (Roulet and Woo, 1986; Woo

1988). Since high ice content wetland soils are slower to thaw, the presence of frozen wetlands may increase the surface water response of frozen ground (Woo and Winter 1993; Woo and Xin, 1996). In regions with mid-winter thaw events the tendency towards high ice content wetland soils may be reversed, as winter flooding of wetlands can prevent or limit frost formation (Woo and Winter, 1993).

In addition to their hydrological responses to climate change, wetlands are significant due to their role as carbon sinks. A large amount of prehistoric organic matter is stored, especially in peatlands in vast areas of partially decomposed organic material. Globally, peatlands are found in over 175 countries, at both tropical and high latitudes, and cover approximately 3% of the world's land areas (IUCN 2011). Boreal ecosystems are estimated to store between 25 to 30% of the global soil carbon pool (McGurie et al., 1995; 1997), largely in the poorly drained wetland and permafrost forests distributed throughout Siberia, Alaska, Canada, and Scandinavia. By another estimate, approximately 30% of the world's peat stocks are found in the West Siberian peat basin, where the peat is up to 10 m thick (Zhulidov et al., 1997). Natural wetlands (bogs, swamps, tundra) are large natural sources of atmospheric methane (Matthews and Fung, 1987; Houghton et al., 2001), releasing an estimated 30 to 50 Tg CH_4 y^{-1} (Zhuang et al., 2004, 2006). The interaction between many factors of soil, hydrology, and vegetation must be considered when predicting carbon dynamics (Zhang et al., 2002). Among these many factors, there are three major parameters that control the rate and amount of methane emission from wetlands (Christensen et al., 1996, 2003). Firstly, the position of the water table determines the extent of anaerobic soil, where methane is produced, and the aerobic soil zone, where methane is restrained and carbon dioxide is produced. Secondly, methane

production is controlled by the availability and quality of suitable substrate with high organic matter content. Finally, the soil temperature controls the rates of microbiological processes including organic matter degradation, methane production, and methane oxidation. Bohn et al. (2007) showed that temperature and precipitation variability also play an essential role in predicting methane emissions in permafrost free regions in northern Eurasia because of their direct influence on the position of the water table. A shift from anaerobic to aerobic soil conditions, resulting from changes in water table, will effectively stop methane emission but increase the rate of carbon dioxide production, primarily by near surface respiration by living roots and heterotrophic organism (Elberling et al., 2008).

1.1.3. The need for understanding hydrological process and carbon dynamics of wetlands using models

Wetlands are an important natural resource globally, with an especially high distribution in the northern temperate and artic zones, making simulation of wetland feedbacks to climate and runoff to oceans particularly important for the Northern Hemisphere. In addition, loss of wetlands has been substantial due to human activities such as agriculture application and development of land for urban and industrial use. However, the impact of global change on the extent of northern wetlands is still uncertain.

Despite the observed influence of lakes, bogs and other surface water storage on the attenuation of streamflow globally, surface storage and subsurface recharge associated with wetland environments are not represented in many of the land surface schemes (LSS) used for regional and global weather and climate prediction. At the time of the PILPS 2e model intercomparison project, only two of the 21 models that participated had any

representation of surface water storage (MATSIRO model – Takata et al., 2003 and VIC model - Liang et al., 1994; Bowling et al. 2003). Seven of the models represented evaporation from surface water bodies. Since that time other LSS have continued to develop wetland representation, mostly emphasizing organic soil representation such as in the Canadian Land Surface Scheme (Comer et al. 2010) and the Community Land Model (Lawrence and Slater, 2008).

Therefore, a greatly improved simulation capacity for wetland hydrology and coupled carbon dynamics on the large scale is needed. The overall goal of this study is to improve our understanding of wetland hydrological processes impacted by global change and human activities. This study was accomplished using the Variable Infiltration Capacity (VIC) model as a tool for examining the hydrological response to perturbation of wetlands and using a simplified carbon dioxide and methane model for examining the carbon dynamics.

1.2 **Hypotheses and Objectives**

The northern mid-latitudes provide a great testing ground for understanding and evaluating water, energy and carbon balance dynamics of wetlands on regional scales. The air temperature has increased over the past several decades due to global climate change. In particular, northern regions have warmed strongly in winter and summer. The associated change in the extent of lakes and wetlands in northern regions as ground warms is uncertain. Meanwhile, human activities and agricultural construction such as surface ditches, and subsurface drainage tiles are used to drain wetlands and improve annual crop yields. These activities can alter the local or regional hydrology compared to historical patterns and concurrently change greenhouse gas emissions. Consequently, the

magnitude of greenhouse gas emissions, such as carbon dioxide and methane, in northern wetland regions is uncertain. There are several specific science questions to be addressed by this proposed research:

1. What is the role of natural, depressional wetlands in the Wisconsin till plain that is heavily influenced by agricultural drainage in recharging local soil moisture and ground water?

   Hypothesis: groundwater flow and subsurface drainage from the adjacent land areas both serve to recharge surface water storage in wetlands during the winter and spring; however during the drier summer season wetlands serve to recharge local soil moisture, reducing streamflow at the outlet.

   Wetlands can help to maintain the water table and exert control on hydraulic gradients to provide the force for groundwater recharge and discharge to adjacent areas. The constant inflow from tile drainage in the surrounding agricultural land also provides the force for recharging or discharging. In the winter, soil surrounding the wetland has been saturated due to snow melt and rainfall, so the hydraulic head is higher at the upland and water flows into the wetland. In the summer, evapotranspiration increases, decreasing the water table depth of the surrounding area. Higher hydraulic head in the center of wetland allows water flow from wetland to upland.

2. How has organic matter content and depth, which affects thermal and hydraulic properties, and drainage conditions, affected the surface thermal and moisture regime in managed peatlands in Northern Indiana over the past several decades?

Furthermore, how have agricultural drainage applications affected methane and carbon dioxide emissions from these high organic matter soils?

Hypothesis: Soils with high organic matter content with high drainage have lower average annual surface moisture and higher annual surface temperature, resulting in higher annual CO_2 emissions and lower methane emissions. Furthermore northern wetlands experiencing intense human activities such as cultivation and drainage experience faster organic matter degradation rates.

The higher porosity of organic matter reduces surface thermal conductivity and acts as insulation. The organic matter layer also has high hydraulic conductivity and weak suction for retaining water. Surface ditches and subsurface tiles can increase the rate of water movement and decrease surface soil moisture. Thus, soils with high organic matter and high drainage will be drier than those with low organic matter with low drainage. Without this organic layer cover, the heat from the atmosphere will be more easily transferred to deeper depths, resulting in a deeper thermal damping depth and less soil ice. Meanwhile, methane and carbon dioxide emissions are governed by whether the soil condition is anaerobic or aerobic, soil temperature and organic matter content. Both emissions are strongly correlated with temperature. Methane is produced under anaerobic and wet conditions, whereas carbon dioxide production is favored under aerobic and dry condition. Wetland and lakes provide a reducing environment that produces methane under saturated conditions.

3. How have agricultural applications such as surface ditches or subsurface tiles altered hydrological patterns and reduced the magnitude (volume and duration) of surface water storage in the Wabash River Basin, Indiana?

Hypothesis: The use of drainage applications has increased surface and subsurface flow and lowered the water table depth, consequently increasing stream flashiness and flood frequency.

Wetlands are hydrologically dynamic systems, which have the potential to improve water quality, reduce the risk of flood, and provide habitat for wildlife. Agricultural drainage such as surface ditches or subsurface tiles are used to lower the water table depth, reduce the degree of water saturation and increase the crop yield in cultivated areas. The ability of water movement is increased and further alters runoff, baseflow and streamflow and decreases the duration of soil saturation across wide areas. Therefore, I hypothesize that the intense drainage system in the Wabash watersheds reduced the average storage volume in wetlands and increased the variability of the streamflow patterns compared with their pre-drainage condition.

The overall goal of this study is to understand the interaction of surface hydrology, surface energy balance and carbon dynamics with surface physical properties in northern wetlands. This study primarily focuses on the continued development of a land surface model for northern wetlands that utilizes remote sensing products and directly observed measurements to i) evaluate the model performance and ii) quantify the relationship between surface water, energy balance and carbon dynamics.

This work was accomplished with respect to four primary objectives:

1. Modify the Variable Infiltration Capacity (VIC) model to better represent wetland processes;
2. Quantify the importance of agricultural drainage relative to subsurface moisture exchange to the water balance of a natural, depressional wetland;

3. Estimate the effect of drainage condition alterations on CO2 and CH4 emission exchange in the Kankakee watersheds with high organic matter soils; and
4. Evaluate the role of anthropogenic modifications to drainage conditions on streamflow variability in the Wabash River basin.

1.3 **Thesis Format**

This thesis is divided into six chapters. This first chapter provides a general motivation of the need for enhanced modeling tools to support wetland-related research. Chapter 2 describes the extensive model development and evaluation activities undertaken as part of this research to improve our ability to simulate the water, energy and carbon cycle of non-riparian wetlands. Wetland dynamics in the face of environmental change are then explored through three case studies. Chapter 3 provides a field-scale simulation using a lumped modeling approach for a managed wetland in West Lafayette, IN heavily influenced by agricultural drainage inputs and highlights the importance of surface-subsurface water exchange in wetland hydrology. In Chapter 4, the cumulative impact of agricultural drainage practices on carbon emissions from peat soils in the Kankakee River Basin, IN are evaluated. The cumulative impacts of subsurface agricultural drainage, wetland depressional storage and surface network enhancements are explored in Chapter 5, which includes a case study of historic changes in the Wabash River basin, IN. It is anticipated that Chapters 3 -5 will be submitted for publication in peer-reviewed journals in the near future. Finally, Chapter 6 provides and overall summary and conclusions from this research.

1.4 **References**

Anisimov, O. A., and Nelson, F. E. 1997. Permafrost zonation and climate change in the Northern Hemisphere: results from transient general circulation models. *Climate change* 35:241-258.

Bohn, T. J., D. P. Lettenmaier, K. Sathulur, L. C. Bowling, E. Podest, K. C. McDonald, and T. Friborg, 2007: Methane emissions from western Siberian wetlands: heterogeneity and sensitivity to climate change, *Env. Res. Lett.*, 2, 045015, doi: 10.1088/1748-9326/2/4/045015.

Bowling, L.C. and 25 others, 2003. Simulation of high-latitude hydrological processes in the Torne-Kalix basin: PILPS hase 2(e) 1: Experiment description and summary intercomparisons, Global and Planetary Change, 38, 1-30.

Carter, V., 1996. Technical Aspects of Wetlands: Wetland Hydrology, Water Quality, and Associated Functions, *In* J. D. Fretwell, J. S. Williams, and P. J. Redman (compilers) National Water Summary on Wetland Resources. U.S. Geological Survey, Reston, VA, USA. Water-Supply Paper 2425. p. 261–266

Christensen, T. R., I. C. Prentice, J. Kalpan, A. Haxeltine, and S. Sitch, 1996. Methane flux from northern wetlands and tundra: An ecosystem source modeling approach, Tellus, ser. B, 48:652-661.

Christensen, T. R., A. Ekberg, L. Strom, M. Mastepanov, N. Panikov, M, Oquist, B. H. Sevenson, H. Nykanen, P. J. Martikainen, and H. Oskarsson, 2003. Factors controlling large scale variations in methane emission from wetlands. Geophys. Res. Lett., 30, 1414, doi:10.1029/2002GL016848.

Christensen, J.H.; B. Hewitson; A. Busuioc; A. Chen, X. Gao, I. Held, R. Jones, R.K. Kolli, W.-T. Kwon, R. Laprise, V. Neil T. Comer , Peter M. Lafleur , Nigel T. Roulet , Matthew G. Letts , Michael Skarupa & Diana Verseghy (2000) A test of the Canadian land surface scheme (class) for a variety of wetland types, Atmosphere-Ocean, 38:1, 161-179, DOI: 10.1080/07055900.2000.9649644.

Comer, N.T.; P.M. Lafleur, N.T. Roulet, M.G. Letts, M. Skarupa and D. Verseghy. 2000. A test of the Canadian Land Surface Scheme (CLASS) for a variety of wetland types. atmosphere-ocean, 38(1)

Couture, R., S. Smith, S.D. Robinson, M.M. Burgess and S. Solomon, 2003. On the hazards to infrastructure in the Canadian North associated with thawing of permafrost. Proceedings of Geohazards 2003, Third Canadian Conference on Geotechnique and Natural Hazards, pp. 97-104. Canadian Geotechnical Society.

Cowardin, L.M., V. Carter, F.C. Golet, and E.T. LaRoe. 1979. Classification of Wetlands and Deepwater Habitats of the United States. U. S. Department of the Interior, Fish and Wildlife Service, Washington, DC. FWS/OBS-79/31.

Dahl, T.E. 2011. Status and trends of wetlands in conterminous United States 2004 to 2009. U.S. Department of the Interior, Fish and Wildlife Service, Washington, D.C. 108 p

Elberling, B., Nordstrøm, C., Grøndahl, L., Søgaard, H., Friborg, T., Christensen, T.R., Ström, L., Marchand, F. and Nijs, I. 2008. High-Arctic Soil CO2 and CH4 Production Controlled by Temperature, Water , Freezing and Snow. *In Meltofte, H., Christensen, T. R., Elberling, B., Forchhammer, M.C. and Rasch, M. (eds.). High-Arctic Ecosystem Dynamics in a Changing Climate. Advances in Ecological Research 40: 441 – 472.*

Fisher, J., and M.C. Acreman, 2004, Wetland nutrient removal: a review of the evidence, Hydrology and Earth System Sciences. 8(4), 673-685.

Forbes, B.C., 2001, Change in permafrost landscapes under global change, R. Raepe and V. Melnikov (eds.), Permafrost response on Economic development, Environmental Security and Natural Resources, p:333-339.

Grippa M, Mognard N M, Le Toan T and Biancamaria S 2007 Observations of changes in surface water over the western Siberia lowland *Geophys. Res. Lett.* 34 1–5

Hinzman, L. D., N. D. Bettez, W. R. Bolton, F. S. Chapin, M. B. Dyurgerov, C. L. Fastie, B. Griffith, R. D. Hollister, A. Hope, H. P. Huntington, A. M. Jensen, G.J. Jia, T. Jorgenson, D. L. Kane,D. R. Klein, G. Kofinas, A. H. Lynch, A. H. Lloyd, A. D. McGuire, F. E. Nelson, W. C. Oechel, T. E. Osterkamp, C. H. Racine, V. E. Romanovsky, R. S. Stone, D. A. Stow, M. Sturm, C. E. Tweedie, G. L. Vourlitis, M. D. Walker, D. A. Walker, P. J. Webber, J. M. Welker, K. S. Winker, K. Yoshikawa, 2005. Evidence and implications of recent climate change in northern Alaska and other arctic regions. Climate Change. 72: 251-298.

Houghton, J. T., et al. (Eds.) 2001. Projections of future climate change, Climate Change 2001: The Scientific Basis, Contribution of Working Group I to the Third Assessment Report of the Intergovernmental Panel on Climate Chage, 881 pp., Cambridge Uni. Press, New York.

IUCN, 2011. IUCN UK Commission of Inquiry on Peatlands Full Report, IUCN UK Peatland Programme October 2011.

Jacobs, J.D. and Grandin, L.D. (1988) The influence of an Arctic large-lakes system on mesoclimate in south-central Baffin Island, N.W.T., Canada, Arctic and Alpine Research 20, 212-219.

Jeffries, M.O., Zhang, T., Frey, K. and Kozlenko, N. (1999) Estimating late winter heat flow to the atmosphere from the lake-dominated Alaskan north slope,. J. Glaciol., 45, 315–324, 1999.

Khon,V. C., I. I. Mokhov, E. Roeckner, V. A. Semenov, 2007. Regional changes of precipitation characteristics in Northern Eurasia from simulations with global climate model. Global and Planetary change, 57:118-123.

Kudeyarov, V. N., V. A. Demkin, D. A. Gilichinskii, S.V. Goryachkin, and V. A. Rozhkov, 2009. Global Climate and soil cover. Euraisan Soil Science. 42:953-966.

Lawrence, D. M., and A . G. Slater, 2008. Incorporating organic soil into a global climate model. Climate Dyn. 30,145-160.

Lehner, B. and P. Döll (2004): Development and validation of a global database of lakes, reservoirs and wetlands. Journal of Hydrology 296/1-4: 1-22.

Leibowitz, S.G., Abbruzzese, Brooks, Adamus, P.R.,Hughes, L.E., Iris, J.T., 1992, A synoptic approach to cumulative impact assessment--A proposed methodology, in McCannell, S.G., and Hairston, A.R., eds.: U.S. Environmental Protection Agency, EPA/600/R-92-167, 127 p.

Liang, X., D. P. Lettenmaier, E. F. Wood, and S. J. Burges, 1994, A simple hydrologically based model of land surface water and energy fluxes for general circulation models. *J. Geophys. Res.* 99:14,415-14,428.

Matthews, E., and I. Fung, 1987. Methane emission from natural wetland: global distribution, area, and environmental characteristics of sources. Glob. Biogeochem. Cycle, 1:61-86.

McGuire, A. D., J. M. Melillo, D. W. Kicklighter, and L. A. Joyce, 1995, Equilibrium responses of soil carbon to climate change: Empirical and process-based estimates, *J. Biogeogr.,* 22:785-796.

McGuire, A. D., J. M. Melillo, D. W. Kicklighter, Y. Pan, X. M. Xiao, J. Helfrich, B. Moore, C. J. Vorosmarty, and A. L. Schloss, 1997, Equilibrium response of global net primary production and carbon storage to doubled atmospheric carbon dioxide: Sensitivity to changes in vegetation nitrogen concentration. *Global Biogeochem. Cycles,* 11:173-189.

Mishra, V., K. A. Cherkauer, and S. Shukla (2010), Assessment of Drought due to Historic Climate Variability and Projected Future Climate Change in the Midwestern United States, Journal of Hydrometeorology, 11(1), 46-68, doi: 10.1175/2009JHM1156.1.

Mitsch, W.J. and J.G. Gosselink, 2000. Wetlands. John Wiley & Sons, Inc. New York, NY.

Nelson, F. E., and Anisimov, O. A. 1993. Permafrost zonation in Russia under anthropogenic climate change. *Permafrost and Periglacical Processes* 4:137-148.

Rabalais, N. N., R. E. Turner, and W. J. Wiseman. 2002. Gulf of Mexico hypoxia, aka "The Dead Zone." Annu. Rev. Ecol. Syst.33: 235-263.

Romanosky V. E., and T. E. Osterkamp, 2001, Permafrost: Changes and impacts. Permafrost response on economic development environmental security and natural resources. Raepe and Melnikov. 2001. 297-315

Romanovsky, V. E., Shender, N. I., Sazonova, T. S., Balobaev, V. T., Tipenko, G. S. and Rusakov, V. G., 2001. Permafrost Temperatures in Alaska and East Siberia: Past, Present and Future, in: Proceedings of the Second Russian Conference on Geocryology (Permafrost Science), Moscow, June 6-8, pp. 301-314.

Roulet, N.T. and Woo, M.K. (1986) Hydrology of a wetland in the continuous permafrost region, *Journal of Hydrology* 89, 73-91.

Serrerze, M. C., and R. G. Barry, 2005. The Arctic Climate system. Cambridge. P 295.

Sinha, T., and K. A. Cherkauer, 2008. Time series analysis of soil freeze and thaw processes in Indiana, Journal of Hydrometeorology, *9*(5), 936-950.

Sinha, T., K.A. Cherkauer, and V. Mishra (2010), Impacts of historic climate variability on seasonal soil frost in the Midwestern United States, J. Hydrometeorology, doi: 10.1175/2009JHM1141.1.

Smith, L. C., Y. Sheng, G. M. MacDonald, and L. D. Hinzman, 2005, Disappearing Arctic Lakes. Science,vol: 308:1429.

Takata, K., S. Emori, and T. Watanabe, 2003: Development of minimal advanced treatments of surface interaction and runoff. Global Planet. Change, 38, 209–222, doi: 10.1016/S0921-8181(03)00030-4.

USGCRP (2009). *Global Climate Change Impacts in the United States* . Karl, T.R., J. M. Melillo, and T. C. Peterson (eds.). United States Global Change Research Program. Cambridge University Press, New York, NY, USA.

Wilen, B. O., and W. E. Frayer, 1990, Status and trends of U.S. wetlands and deepwater habitats. Forest Ecology and Management, Volumes 33-34, P. 181-192.

William, P.J., 1995. Permafrost and climate change: geotechnical implication. *Phil Trans. Roy. Soc. Lond.* A352:347-258.

Woo, M.K. and Winter, T.C. (1993) The role of permafrost and seasonal frost in the hydrology of northern wetlands in North America, *Journal of Hydrology* 141, 5-31.

Woo, M.K. (1988) Wetland runoff regime in northern Canada, in *Permafrost: fifth international conference* 1, Proceedings, International conference on permafrost, pp. 644-649.

Woo, M.K. and Xia, Z. (1996) Effects of hydrology on the thermal conditions of the active layer, *Nordic Hydrology* 27, 129-142.

Zhang, Y., C. Li, C. C. Trettin, H. Li, and G. Sun, 2002. An integrated model of soil, hydrology and vegetation for carbon dynamics in wetland ecosystems. Global Biogeochem. Cycles, 16(4), 1061, doi:10.1029/2001GB001838.

Zhuang, Q., J. M. Melillo, D. W. Wicklighter, R. G. Prinn, A. D. McGuire, P. A. Steudler, B. S. Felzer, and S. Hu, 2004. Methane fluxes between terrestrial ecosystems and the atmosphere at northern high latitudes during the past century: A retrospective analysis with a process-based biogeochemistry model. Global Biogeochem. Cycles. 18, GB3010, doi:10.1029/2004GB002239.

Zhuang, Q., J. M. Melillo, M.C. Sarofim, D. W. kicklighter, A. D. McGurie, B. S. Felzer, A. Sokolove, R. G. Prinn, P. A. Steudler and S. Hu, 2006. CO_2 and CH_4 exchanges between land ecosystems and the atmosphere in northern high latitudes over the 21st century. Geophys. Res. Lett. 33, L17403, doi:10.1029/2006GL026972.

Zhulidov, A.V., J.V. Headley, R.D. Robarts, A.M. Nikanorov and A.A.. Ischenko, 1997. Atlas of Russian wetlands: biogeography and metal concentrations. National Hydrology Research Institute, Environment Canada, Saskatoon, SA., Canada. 312p.

2. MODEL DESCRIPTIONS AND DEVELOPMENT

As described in Chapter 1, wetlands represent an influential portion of the northern landscape that is undergoing on-going and dramatic change. Our ability to represent the flow attenuation, evaporation and groundwater recharge aspects of wetland hydrology within the context of land surface simulations is still limited at large scale. This chapter describes several enhancements to the VIC model to improve the representation of wetland hydrology.

2.1 Model Descriptions

2.1.1. Variable Infiltration Capacity (VIC) model

The Variable Infiltration Capacity model (VIC) is a macroscale hydrological model simulating hydrologic fluxes and moisture storage in response to input meteorological variability (Liang et al., 1994). It is utilized at grid cell scales with typical dimensions from 1/8 to 2 degree latitude by longitude (or 12 to 100 km). The VIC model characterizes multiple vegetation classes as fractions within a grid cell and utilizes three or more soil layers to calculate the energy and water balance (Liang et al., 1999). A variable infiltration curve is used to represent surface runoff processes. The base flow is represented as a function of the unfrozen soil moisture in the lowest soil layer. To represent the hydrology of northern wetlands, the VIC model includes representation of

soil freeze/thaw, interception of snow by forest canopies (Cherkauer and Lettenmaier, 1999 and Cherkauer et al., 2003), and surface storage in lakes and wetlands (Bowling and Lettenmaier, 2010).

The lake and wetland model developed by Bowling and Lettenmaier (2010) represents the effects of small (sub-grid) lakes and wetlands by creating a surface wetland land class that can be added to the grid cell mosaic, in addition to the vegetation and bare surface land classes. The wetland class represents seasonally flooded ground as well as permanent water bodies, and requires specification of the lumped bathymetric profile of all lakes and wetlands within the model grid cell. The specification of a variable depth-area relationship is used for representation of the reduction in surface water extent and the emergence of wetland vegetation type following seasonally flooded wetlands. Subsurface outflow from the lake is calculated using the VIC model ARNO baseflow curve, and surface outflow from the lake is calculated from the depth based on the equation for flow over a broad-crested weir. Bowling and Lettenmaier (2010) showed that the interaction between surface water storage and soil moisture storage in adjacent uplands is not simulated and possibly leads to an overestimation of late summer recharge to lake and wetland storage.

2.1.2. VIC Routing Model

Streamflow routing at the basin scale is usually separate from the land surface simulation. Typically the routing model of Lohmann et al. (1996; 1998) is coupled with the VIC model to produce streamflow hydrographs. This algorithm is limited in its ability to capture differences in the timing of water movement through headwater streams using a

constant unit hydrograph to route the simulated runoff and baseflow to the outlet of each grid cell. Yang et al. (2011) developed a GIS-based routing model that preserves the spatially distributed travel time information in a finer-resolution flow network than the VIC model grid cell size. By using a finer resolution DEM, the cell response functions (CRFs) are derived for the VIC model grid cells as their unit hydrograph. Streamflow is calculated by convolution integral of the runoff for all VIC cells with their CRFs. This GIS-based unit hydrograph approach makes the model more responsive to drainage network enhancement.

2.1.3. Methane model

The methane model, based on Walter and Heimann (2000), consists of a hypothetical one-dimensional soil column divided into 1 cm thick parallel layers. The boundary between anaerobic and aerobic soil zones is taken to be the position of the water table. Methane is only produced in layers below the water table; oxidation occurs in the layers above the water table. There are three different transport mechanisms for emitting methane into the atmosphere (Figure 2-1). The first is molecular diffusion through water or soil pores filled with air and standing water. Second is bubble ebullition from depths where bubbles are produced to the water table. Third is the uptake through vegetation from the soil layer directly up to the atmosphere. Combining these gives us the numerical one-dimensional continuity equation within the entire soil/water column shown below:

$$\frac{\partial}{\partial t} C_{CH_4}(t,z) = -\frac{\partial}{\partial} F_{diff}(t,z) + Q_{ebull}(t,z) + Q_{plant}(t,z) + R_{prod}(t,z) + R_{oxid}(t,z) \quad (\mathbf{2\text{-}1})$$

Where $C_{CH4}(t,z)$ is the methane concentration at the depth z and time t, $F_{diff}(t,z)$ is the methane flux diffused through the soil, $Q_{ebull}(t,z)$ is the methane flux through ebullition, $Q_{plant}(t,z)$ is the methane flux from the plant-mediated transport, $R_{prod}(t,z)$ is methane production rate and $R_{oxid}(t,z)$ is the methane oxidation rate. The daily values of water table position, soil temperature profile and the net primary productivity (NPP) are the forcing of the methane model and are generated as outputs from the VIC model. The soil temperature algorithm is described by Cherkauer and Lettnemaier (1999), while the water table algorithm is a new feature described in Section 2.2.2, NPP is also one output of the VIC model adapted from the Biosphere-Energy-Transfer-Hydrology (BETHY) model (Knorr, 1997), as described by Bohn et al.(2007) and summarized in Section 2.1.4. The model output is the methane fluxes to the atmosphere and methane concentration in the soil profile, both daily values generated by solving the one-dimensional continuity equation within the entire soil/water column.

2.1.4. Soil respiration sub-model

The soil respiration (CO_2) sub-model is adapted from the BETHY model (Knorr, 1997). The net ecosystem exchange with the atmosphere is computed as the difference between soil respiration and NPP. In order to spin up the equilibrium status of the soil carbon pools, this CO_2 sub-model is calculated outside the VIC model. The CO_2 sub-model requires three forcings: daily soil moisture content, soil temperature profile, and NPP, which quantifies the availability of organic matter for methane production. NPP is an output of the VIC model adapted from the BETHY model; the water table position and

soil temperature profiles for the soil respiration model are also outputs from the VIC model.

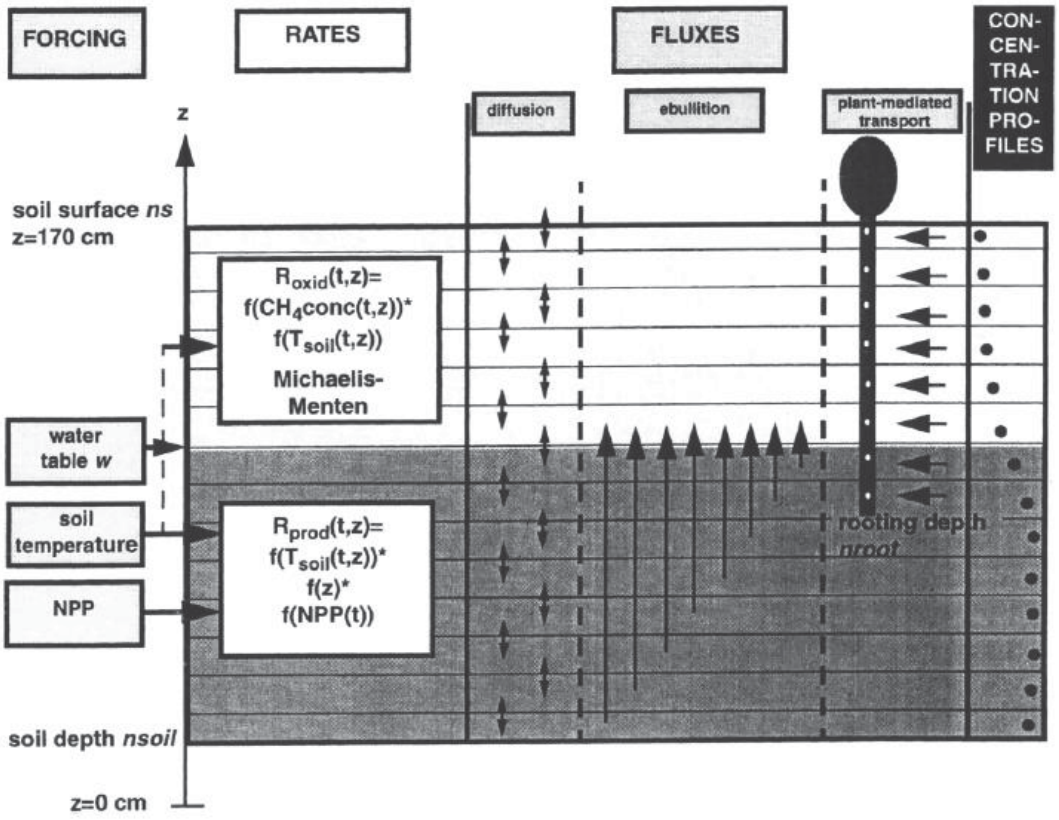

Figure 2-1. Schematic representation of methane model structure. (Courtesy from Walter and Heimann, 2000).

2.2 VIC Model Development

2.2.1. Organic Matter Representation

Wetlands often contain a high content of organic matter which controls the surface temperature and moisture with its low thermal properties and high hydraulic conductivity and water holding capacity. Organic matter may act as a natural insulator that buffers the energy transfer into soil during spring and summer and out of soil during fall and winter

(Bonan and Shugart 1989). Lawrence and Slater (2008) found that organic matter provided limited insulation from surface warming using the Community Land Model (CLM). Previous versions of the VIC model did not represent the effect of organic material on soil moisture and thermal properties. As illustrated in Figure 2-2, Chiu et al. 2008 identified a warm bias in the simulation of summer wetland soil temperatures in the Arctic.

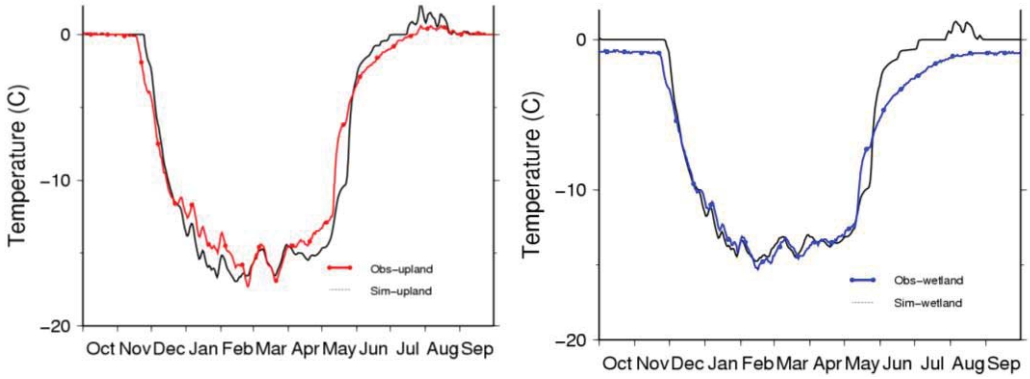

Figure 2-2. Observed and simulated 60 cm soil temperature at (a) upland and (b) wetland, averaged from 10/1/1996 to 9/30/2001 at Betty Pingo, Alaska

The thermal conductivity calculation of the VIC model was improved so that the thermal and hydraulic conductivity and heat capacity are calculated as a weighted average of the mineral and organic soil fractions. For each soil layer, for each grid cell, the effective thermal conductivity of a dry soil is calculated as the weighted average of the dry mineral soil conductivity and the fixed dry organic soil conductivity (0.25 W/mK) based on Farouki (1981). The thermal conductivity of mineral soil is based on knowledge of quartz fraction (Cherkauer and Lettenmaier 1999). The dry soil conductivity is adjusted for moisture content using the Kersten number approach of Johansen (1975).

Total soil volumetric heat capacity (J/m^3 K) is calculated as a fraction of the volume fractions of solid, water, organic matter and air components present in a unit soil volume and the respective heat capacities per unit volume of solids, water, organic matter, and air. The heat capacity of pure organic material is set equal to 2.7x10^6 J/m^3 K. All other values are as reported in Cherkauer and Lettenmaier (1999). Improvements to the simulation of soil temperature profile associated with these model changes are shown in Chapter 4.

2.2.2. Equilibrium Water Table Algorithm

The volume of drained pore space for different water table positions is calculated assuming the soil water in a homogeneous soil is in equilibrium with the water table and therefore follows the soil water characteristic curve as estimated using the Brooks and Corey (1964) model. The calculation is adapted from the DRAINMOD model (Skaggs, 1980) to the VIC model to determine how the water table moves when a given amount of water is removed or added to the soil column, and is described in Chiu et al. (2013) and summarized here.

Soil moisture content for different water table positions is calculated as follows (Brooks and Corey, 1964):

$$\theta = \left(\frac{h_b}{h}\right)^{\lambda} * (\theta_s - \theta_r) + \theta_r \quad \textbf{(2-2)}$$

Where θ is water content (volumetric water content), λ is pore –size index, θ_s is saturated water content (volumetric water content), θ_r is residual water content (volumetric water content), $h_b$is air bubbling pressure (cm); value must be greater than 0, and h is soil water pressure (suction), determined by the water table position (cm).

The volume drained per unit area, V_d, when the water table falls from the surface to depth y_1, is expressed as.

$$v_d = \int_0^{y_1} \left(\theta_0(y) - \theta_i(y)\right) dy \qquad \textbf{(2-3)}$$

Where $\theta_0(y)$ is the soil water content at depth *y* prior to drainage (zero pressure), usually assumed to be constant at the saturated soil water content (porosity (θ)) , and $\theta_i(y)$ is the equilibrium water content (eq 2-2) for soil layer *i* at depth *y* for a water table depth of y_1. For a layered soil integration will proceed in parts for each soil layer above the water table (Figure 2-3).

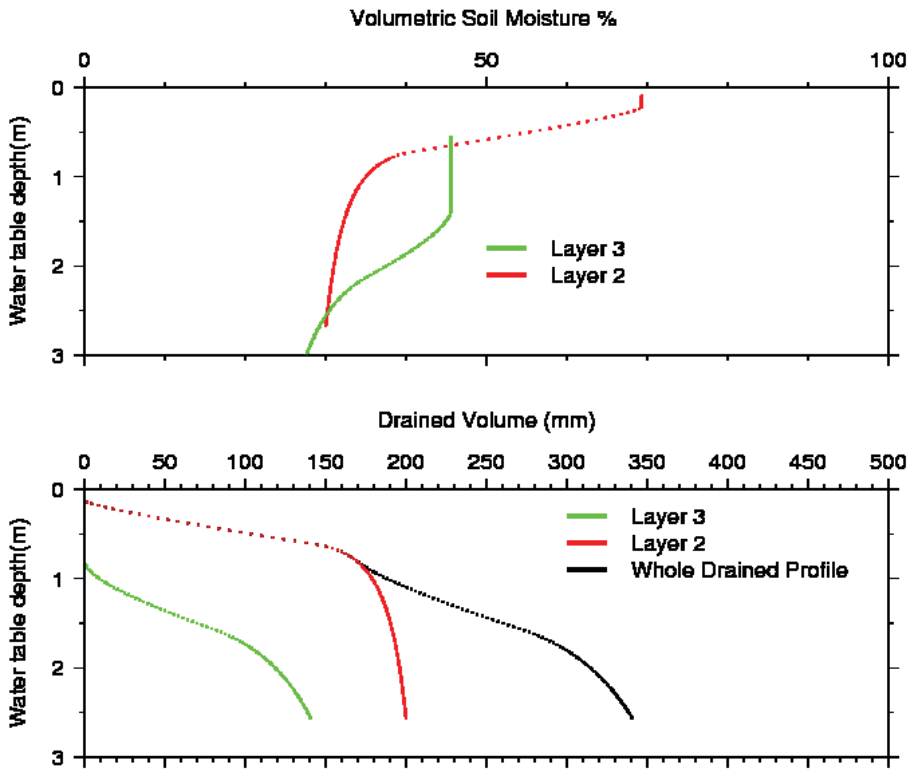

Figure 2-3. The soil water characteristic curve of each soil layer (upper). The drainage volume vs water table depth is calculated by combining the soil water characteristic curves (lower).

2.2.3. Drainage Algorithm

In order to estimate subsurface (tile) drainage, a new tile drainage algorithm has been developed and tested for Indiana field drainage locations (Bowling et al., 2013, in preparation). The tile drainage component of subsurface flow is calculated when the simulated water table rises above a specified drain or ditch depth.

Subsurface flow (baseflow) is generated in the VIC model by the empirical Arno equation, which is a function of soil moisture in the bottom soil layer (Todini, 1996; Gao et al., 2010). Baseflow response follows a linear relation under low soil moisture levels and a non-linear profile at high soil moisture content, allowing a much faster baseflow response when soil moisture reaches this threshold. Following Liang et al. (1994):

$$R_b = D_{min}\left(\frac{\theta_b}{W_s\theta_m}\right) \qquad 0 \le \theta_b \le W_s\theta_m \qquad \textbf{(2-4a)}$$

$$R_b = D_{min}\left(\frac{\theta_b}{W_s\theta_m}\right) + (D_{max} - \frac{D_{min}}{W_s}) \cdot \left(\frac{\theta_b - W_s\theta_m}{\theta_m - W_s\theta_m}\right)^c \qquad W_s\theta_m < \theta_b \le \theta_m \qquad \textbf{(2-4b)}$$

where θ_m is the maximum soil moisture of the lower soil layer in millimeters and W_s is the fraction of θ_m where nonlinear baseflow begins, θ_b is the soil moisture content of the lower soil layer in millimeters, and n is the exponent, usually taken as 2 in VIC baseflow calculations. D_s is the fraction of D_{max} where nonlinear baseflow begins. D_{max} represents the maximum drainage rate per unit surface area (in mm/hr) for fully saturated conditions (Figure 2-4).

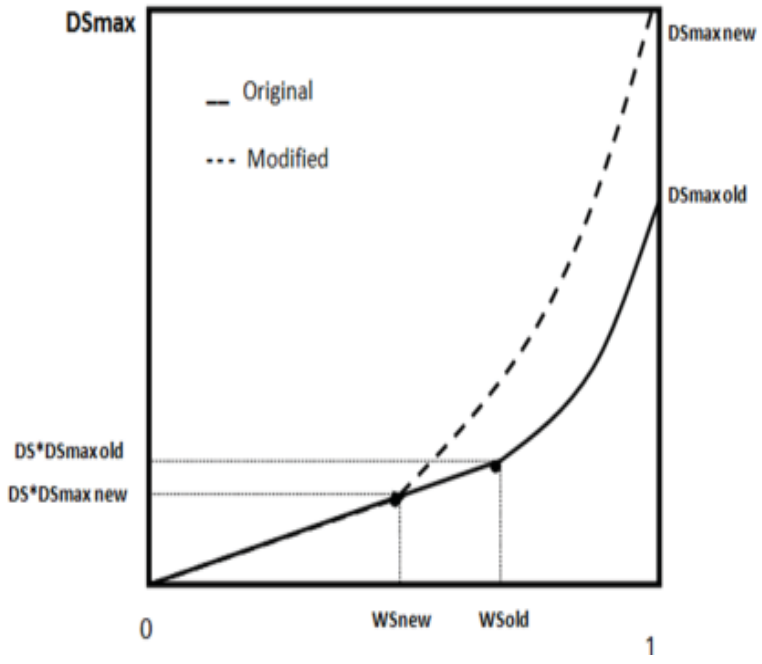

Figure 2-4. The Arno baseflow curve as used in the VIC model, and internal modifications to the curve for tile-drained land.

With the drainage algorithm, the classic ellipse equation for drainflow is solved in terms of VIC input parameters, by equating the maximum baseflow rate in the VIC model with the ellipse equation during maximum flow conditions. The ellipse equation is a simplified version of the Houghoudt steady state equation that assumes an elliptical water table depth between the subsurface drains and steady state drainage under constant drain spacing and drain depth. Dsmax and Ws are modified internally to the model to more accurately represent the baseflow of artificially drained soil, as a function of two new drainage parameters: drain spacing (S) and drain depth (d_d). These two parameters can be defined by the user and stored in the vegetation parameter file so that one or more drained land use types can be developed. The drain depth is used to modify Ws, such that the

transition to non-linear baseflow begins at the soil moisture value which corresponds to the point where the water table will first rise above the drain depth.

Subsurface flow from tiles in the ellipse equation (equation 2-5) is a function of saturated lateral hydraulic conductivity (*k*), drain spacing (*S*), depth from the drain to the impermeable soil layer (*d*), and water table height above the drain depth (*m*) at the middle of parallel drain pipes (Bouwer and Schilfgaarde, 1963).

$$q = \frac{4k * m * (2 * d + m)}{S^2} \qquad (\mathbf{2\text{-}5})$$

In order to equate Arno baseflow and ellipse equation, the DSmax parameter describing the maximum baseflow rate predicted by the VIC model per unit surface area can be rewritten in terms of Darcy's law:

$$DS_{\max} = \frac{k * \tan_{\beta} * D_b}{a} \qquad (\mathbf{2\text{-}6})$$

Where D_b is the depth of the bottom soil layer, a is the contributing drainage area, and $\tan_{\beta}$ is the slope of the unit area. The contributing drainage area, and land slope can vary within a study area and are currently assigned values of a =375 and $\tan_{\beta}$=0.05 for agricultural land.

The saturated conductivity (from eq. 2-6) was substituted into the ellipse equation (2-5) to produce a drainage equation from model input shown in Equation (2-7)

$$DS'_{\max}(1 - DS'Ws') = \frac{m(2 * (d_t - d_d) + m)}{s} = \frac{2 * DS_{\max}}{D_b * \tan\beta} \qquad (\mathbf{2\text{-}7})$$

Where d_d is the drain depth, d_t is the total soil depth of all three layers, m is the average water table height (the average water table height between tiles). It is assumed that the maximum drainage rate occurs when the bottom soil layer is saturated because lateral flow is assumed to only occur from the bottom soil layer in the VIC model. There is only active tile drainage when water table reaches or rises above the level of the drain which must be placed in the bottom soil layer in the model above the impermeable bottom boundary.

This algorithm was evaluated using data from the on-going drainage water management field experiment at the Davis Purdue Agricultural Center (PAC) in Farmland, IN. The simulated and observed water tables from two fields are shown in Figure 2-5. Simulated and observed drainflow from the Davis PAC is shown in Figure 2-6.

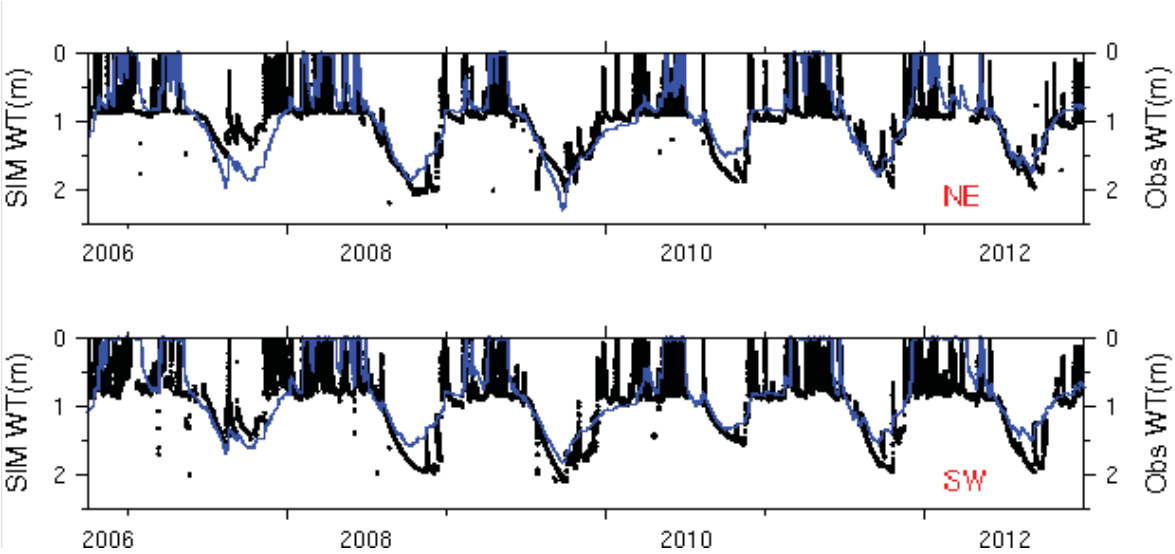

Figure 2.-5. Simulated and observed water table for two subsurface drained fields at the Davis PAC, 2006 -2012.

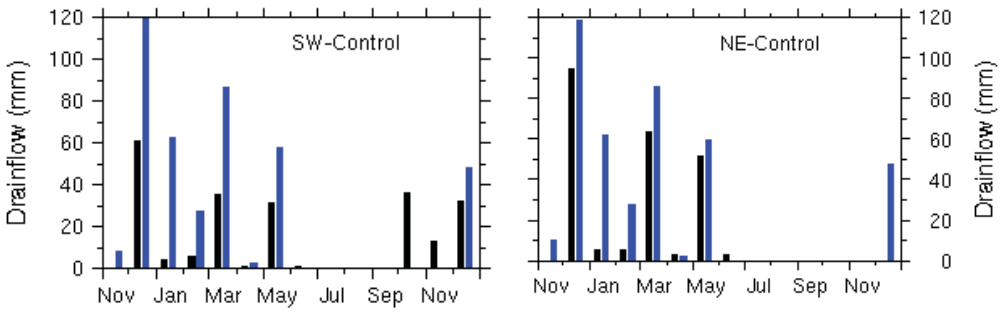

Figure 2-6. Simulated (blue) and observed (black) monthly drainflow for the Davis Purdue Agricultural Center in 2012. Only one year of drainflow is currently available, and monitoring equipment was malfunctioning in several months of the year.

2.2.4. Subsurface Exchange Algorithm

One of the key limitations of the original VIC lake and wetland algorithm described by Bowling and Lettenmaier (2010) is that there was no two-way coupling between the simulated surface water feature and its local watershed. Surface and subsurface water could flow into the wetland, but there was no mechanism for the wetland to recharge adjacent land areas. Two major improvements to the VIC lake and wetland algorithm were first proposed by Sathulur (2008) and have been extensively tested and modified since that time. The first improvement parameterizes a sub-grid spatially variable soil water distribution within the VIC model, while the second improvement allows the exchange of subsurface moisture between the upland and water fractions. Therefore, these improvements allow us to examine changes in soil moisture between upland and wetland regions.

2.2.4.1. Distribution of Moisture Deficit

Distributed hydrologic models can predict temporally and spatially variable saturated thickness due to flow convergence and divergence between individual pixels based on digital elevation models (e.g. DHSVM, THALES, TOPOG) (Wigmosta et al., 1994;

Grayson et al., 1992, Vertessy and Elsenbeer, 1999; Wigmosta and Lettenmaier, 1999). Alternatively, the TOPMODEL approach utilizes a topographic index, a DEM derived quantity which takes into account slope and accumulated upslope area, to provide a temporally-fixed spatial distribution of relative saturation (Beven et al., 1979). The strength of the topographic index is that it can be used to identify hydrologically similar areas prior to model simulation, to simplify model implementation. The topographic index was incorporated into the VIC model lake and wetland algorithm, to represent spatial variability in water table depth, and subsurface/surface moisture exchange between surface water and riparian areas. The revised depth-fractional area curve of the lake and wetland class, segregated based on hydrologically similar areas, rather than elevation alone, is described in Section 2.2.5.

As described above, subsurface flow in the VIC model is generated by the semi-empirical Arno curve (equation 2-4), which is a parabolic function of soil moisture in the bottom layer. The original TOPMODEL storage deficit calculations are not appropriate in the VIC model, since the underlying assumption is not that of an exponentially decreasing transmissivity. Based on the work of Ambroise et al. (1996) and Duan and Miller (1997), the spatial variability of storage deficit in the bottom soil layer for high soil moisture deficit (linear transmissivity) and low soil moisture deficit (hyperbolic transmissivity) in the VIC model was derived. The two portions of the profile are treated independently, such that the total storage deficit is equal to the sum of the deficits in the linear and nonlinear portions of the soil profile.

Using the TOPMODEL spproach, the soil moisture deficit (drained volume) is calculated for each node as a function of the node topographic wetness index, the average wetland moisture content and the average wetland topographic index.. The water table depth for each node is then calculated by the look-up table from the equilibrium water table algorithm. The mean storage deficit is used to find the average water table thickness for the grid cell and land class type. This algorithm has been evaluated using data from multiple long-term observation wells at the Valdai Water Balance Experiment Station in Valdai, Russia. The simulated and observed range in water table position across different landscape positions is illustrated in Figure 2-7.

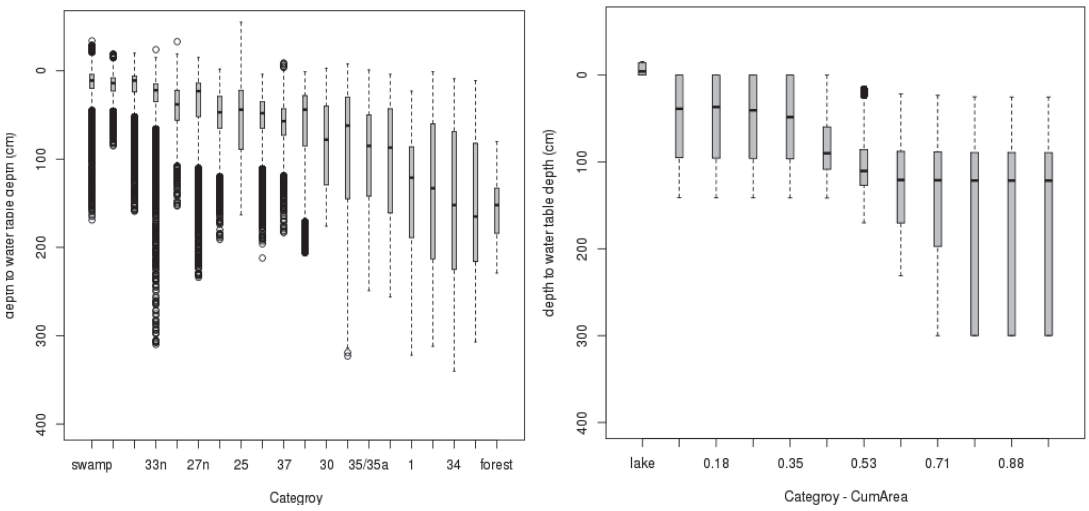

Figure 2-7. Box plots of daily water table position (1966-1983). (left) Observed water table depth from 23 different wells in the Usadievskiy catchment at Valdai, Russia and (right) simulated water table depth for eleven different wetland nodes from lower landscape position to high landscape position (Box plot presents 25%, 50 %, 75 %, minimum, maximum and outliers).

2.2.4.2. Subsurface/Surface Moisture Exchange within the Lake/Wetland Class

In the original implementation of the VIC wetland algorithm (Bowling and Lettenmaier, 2010), soil moisture in the wetland upland class adjacent to the open water was

independent of the surface water storage. Surface and subsurface moisture could flow into the grid cell lake, and lake water was used to recharge subsurface moisture during lake expansion, but the subsurface moisture in the wetland was not in equilibrium with the adjacent lake. With the introduction of a spatially variable water table in the riparian zone, the model has also been modified to relate the soil moisture content of the adjacent land class fraction to the surface water level variations. Subsurface water flows into or out of the lake class based on the hydraulic gradient between the surface water and the elevation of the water table in the element immediately adjacent to the lake, as illustrated in Figure 2-8.

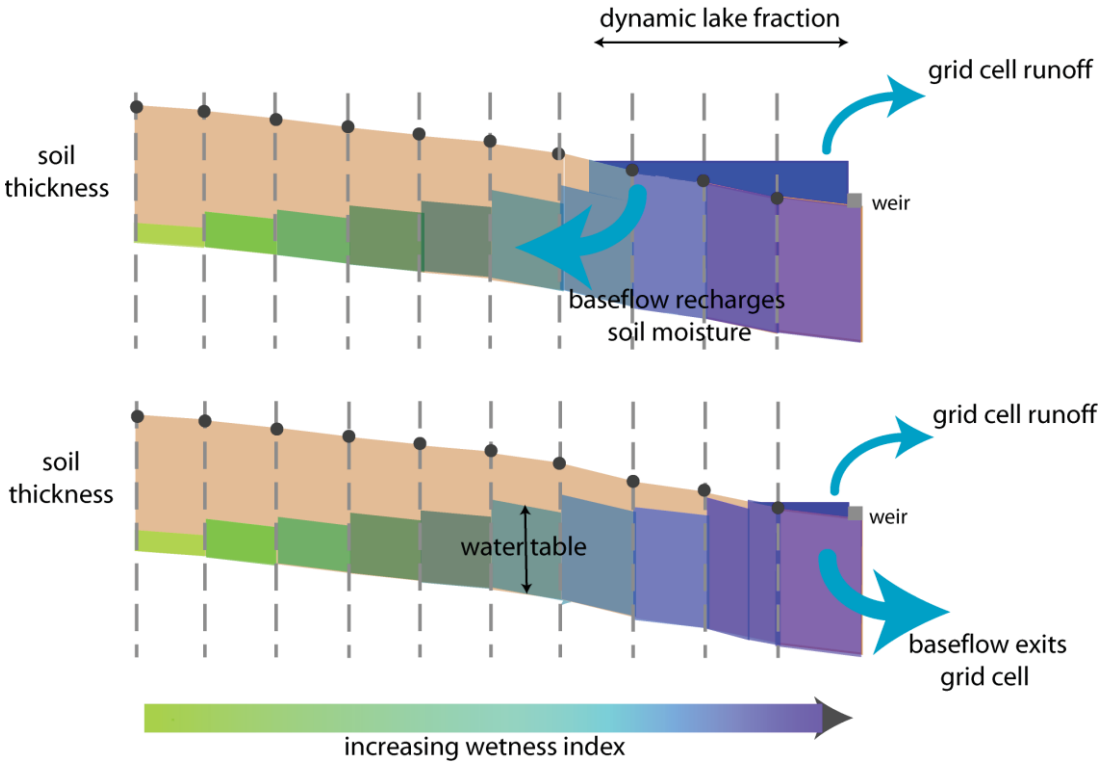

Figure 2-8. (a) Distributed water table resulting from the fractional area topographic index curve that illustrates the baseflow from upland to lake and (b) the baseflow from lake to upland.

For each topographic index class *i*, for *i*=1…*N*, the water table elevation above datum (datum is taken relative to the maximum lake depth L_{depth}) is:

$$E_i = L_{depth} \qquad z_i \le L_{depth} \qquad \textbf{(2-9a)}$$

$$E_i = \left(\frac{z_i - l_{depth}}{z_i - z_{i-1}}\right)\left[\frac{(z_i + z_{i-1})}{2} - (d - h_i)\right] + \left(\frac{l_{depth} - z_{i-1}}{z_i - z_{i-1}}\right)L_{depth} \qquad z_i > L_{depth} > z_{i-1} \qquad \textbf{(2-9b)}$$

$$E_i = \frac{(z_i + z_{i-1})}{2} - (d - h_i) \qquad z_{i-1} \ge L_{depth} \qquad \textbf{(2-9c)}$$

Where $(z_i + z_{i-1})/2$ is the average surface elevation of each topographic index class.

The downslope subsurface flow rate for each hydrologic element in the wetland is calculated based on the VIC baseflow curve, with D_{max} and total soil moisture adjusted for each element. The maximum velocity of baseflow, $D_{max,i}$ for each lake/wetland element is estimated using the grid cell average VIC input parameter, D_{max}, and the average topographic gradient of the wetland. In each time step, baseflow per unit area from the wetland into (out of) the lake is calculated as follows:

$$Q_b = \frac{\sum_{i=1}^{N-N_l} f_i Q_{b,i}}{\sum_{i=1}^{N-N_l} f_i} \qquad E_l > L_{depth} \qquad \textbf{(2-10)}$$

$$Q_b = -1 \cdot D_{max} \qquad E_l < L_{depth}$$

$$Q_b = 0.0 \qquad E_l = L_{depth}$$

Where f_i is the fractional area of element *i*, $E_{l,}$ is the water table elevation of the element adjacent to the lake (equation 2-8b). The influence of this mechanism to allow surface water to recharge adjacent soil moisture is illustrated in the simulation of the watershed average water table for the Valdai test case, in Figure 2-9.

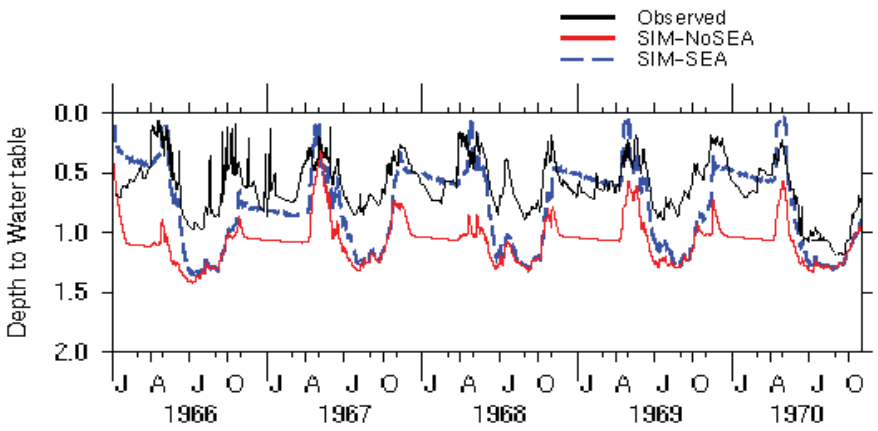

Figure 2-9. Comparison of the watershed average depth to water table in the Usadievskiy catchment at Valdai, Russia using the new Subsurface Exchange Algorithm (SEA) to allow groundwater recharge and using the traditional VIC model (No SEA).

2.2.5. Wetland and Lake Model Parameterization

The expansion and contraction of surface water extent or the inundated portion of wetlands with changes in surface water volume was represented previously in VIC in the form of a hypsometric curve. The hypsometric curve is a non-dimensional curve relating area against relative elevation, yielding the fraction of land area at various elevations. It accounts for elevation only and does not capture the influence of the spatial distribution of the topography on flow convergence. In areas with moderate to steep topography contributing area and the slope (gradient) are key variables determining the distribution and redistribution of water (Anderson and Kneale, 1982).

This means that areas with different elevations may exhibit the same potential for saturation. In order to represent this spatial variation in surface wetness the previously defined hypsometric curve is modified to include the topographic index. It is assumed that locations in the catchment having similar topographic index are hydrologically

similar and will have the same water table depth; the topographic index is therefore expressed as distribution function for the entire catchment.

The generalized topographic index is a function of the ratio of specific accumulated drainage area per unit contour length, a, to the surface slope, tan β, represented as (a/tanβ). The specific accumulated area is the total flow accumulation area (or upslope area), normalized by the unit contour length, L. For input to the VIC model, the generalized topographic index is calculated according to Wolock and McCabe (1995), utilizing the multiflow directional algorithm (Pelletier, 2008) for all fine resolution wetland pixels within a coarser resolution model grid cell. First, depression areas in the DEM dataset are filled. Second, the generalized topographic index (a/tanβ) was calculated for each grid cell DEM using the multiflow algorithm of Pelletier (2008). Third, the average slope (□) and average elevation change between current finer pixel and any adjacent pixels at lower elevation (delta Z) were calculated. Fourth, those generalized topographic index (TI) from only those pixels falling into wetland classes from land cover use dataset are ranked from highest to lowest. Then ranked list is divided into 14 classes (approximately equal area). The average TI, and average slope, and elevation increment and total area are calculated for each wetland class (Figure 2-10).

Permanent open water features (lakea) are assumed to have a bathymetric profile defined by a parabolic relationship, with maximum depth determined as a function of lake area by regional curves. This parameterization approach can be used to estimate maximum surface storage capacity for large regional domains, as illustrated in Figure 2-11.

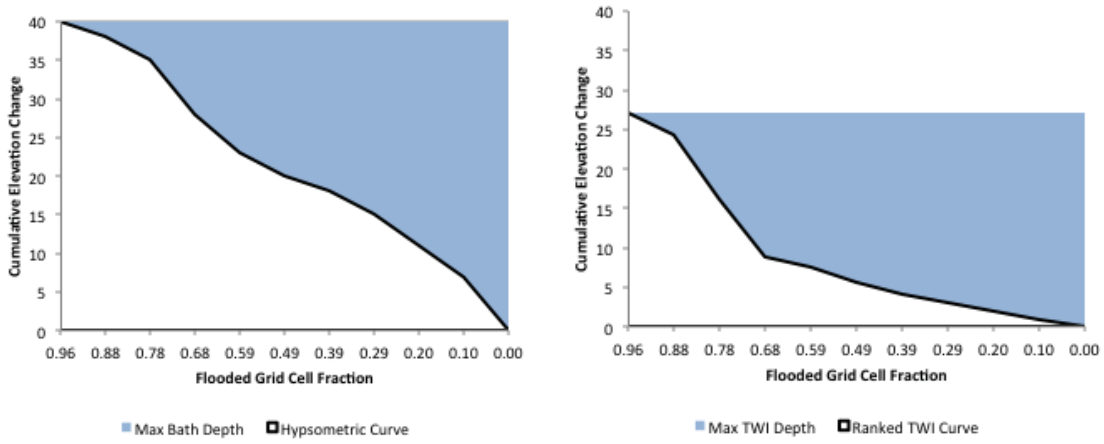

Figure 2-10. The lake and wetland elevation file created using the conventional hypsometric curve (left) and the ranked topographic wetness index (right). The total surface water storage capacity (shaded area) is the same in each case. The TWI curve reflects the face that initial surface flooding is not control by absolute elevation alone, as water collects in local low spots

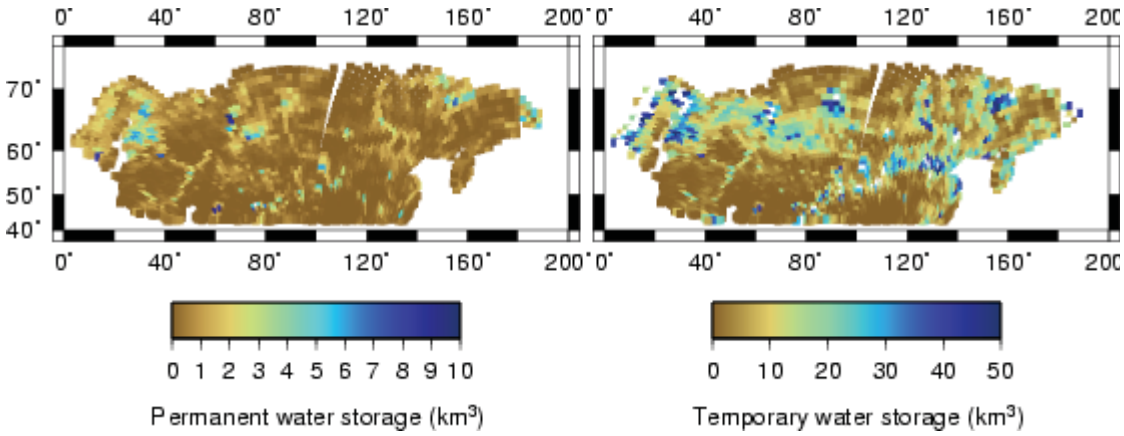

Figure 2-11. Estimates of maximum permanent and temporary water storage based on the lake and wetland parameterization in Northern Eurasia used with the revised lake and wetland algorithm with subsurface exchange.

2.3 **Summary**

The modifications that have been made to the model greatly expand the range of applications and problems that can be investigated with the VIC model, with specific

regard to providing a robust methodology for answering questions about the hydrologic response of wetlands to environmental changes or stresses. Firstly, including the organic matter fraction allows the effect of organic matter on soil moisture regime and thermal properties to be probed, and permits the investigation of the specific behavior of soil with high organic matter content, such as peat land, swamps, or marshes, with a greater degree of control.

The equilibrium water table algorithm, which combines the soil's ability to store and release water (split between soil water content and soil suction, i.e. matric potential) and a drained volume calculation adapted from the DRAINMOD model, allows the modeler to determine how the water table moves when a given amount of water is removed or added to the soil column. This modification provides greater ability to investigate changes in the water table depth than the soil saturation thickness.

A new drainage algorithm has been developed within the VIC model to estimate subsurface tile drainage, using the classic drainflow ellipse equation. This modification makes the model more robust for areas with intense agricultural tile drain practices.

The distributed water table allows the model to account for the variation of water table depth at different positions within a watershed. A lake-wetland parameterization was developed utilizing the generalized topographic index and is used for preparing a wetland parameter file in order to estimate the distributed water table. The subsurface/surface moisture exchange algorithm now also takes into account the lake and wetland algorithm to represent the equilibrium condition for subsurface moisture in a wetland with an adjacent lake. This development provides a highly relevant and applicable tool for understanding subsurface water movement within a natural wetland.

Each of these improvements, taken separately, provides an incremental improvement in the VIC model. When combined, they offer a much-improved representation of the water balance in wetland locations and its response to external forcing events. The model is now much more capable of answering science questions about the effects of drainage and other agricultural modifications on wetlands, and provides a starting point for evaluating the resulting effect on carbon dynamics.

2.4 **References**

Ambroise, B., Beven, K. J., and Freer, J., 1996, "Towards a Generalization of the TOPMODEL Concepts: Topographic Indices of Hydrological Similarity", Water Resources Research, Vol. 32, No. 7, pp. 2135–2145.

Anderson, M. G., and P. E. Kneale, 1982, "The Influence of Low-Angled Topography on Hillslope Soil-Water Convergence and Stream Discharge", Journal of Hydrology, Vol. 57, pp. 65– 80.

Beven, K. and Kirkby, M. J., 1979, "A Physically Based, Variable Contributing Area Model of Basin Hydrology", Hydrological Sciences Bulletin, Vol. 24, pp. 43–69.

Bohn, T. J., D. P. Lettenmaier, K. Sathulur, L. C. Bowling, E. Podest, K. C. McDonald, and T. Friborg, 2007: Methane emissions from western Siberian wetlands: heterogeneity and sensitivity to climate change, *Env. Res. Lett.*, 2, 045015, doi: 10.1088/1748-9326/2/4/045015.

Bonan, G. B. and H. H. Shugart, 1989: Environmental-Factors and Ecological Processes in Boreal Forests. Ann.Rev. Ecol. Syst.,20, 1–28.DOI:10.1146/ annurev.es.20.110189.00024.

Bowling, L. C. and Lettenmaier, D. P.: Modeling the Effects of Lakes and Wetlands on the Water Balance of Arctic Environments, Journal of Hydrometeorology, 11, 276–295, 2010.

Bowling L. C., and Chiu, C.M.,2013, In preparation, The influence of artificial drainage on streamflow variability in the Wabash River basin, *J. of hydrology*.

Chiu, C.M., and L. C. Bowling, In preparation, Lake parameterization across NEESPI domain, *Climate dynamics*, Expect to submit in November 2013

Brooks, R. H., and A. T. Corey, 1964: Hydraulic properties of porous media, *Hydrology Paper no. 3*, Civil Engineering Department, Colorado State University.

Cherkauer, K. A., and D. P. Lettenmaier, (1999) Hydrologic effects of frozen soils in the upper Mississippi River basin, J. Geophys. Res., 104: 19,599–19,610.

Cherkauer, K. A., and D. P. Lettenmaier, 2003. Simulation of spatial variability in snow and frozen soil, J. Geophys. Res.,108(D22), 8858, doi:10.1029/2003JD003575.

Duan, J., and Miller, L. N., 1997, "A Generalized Power Function for the Subsurface Transmissivity Profile in TOPMODEL", Water Resources Research, Vol. 33, No. 11, pp. 2559–2562.

Farouki, O. T., 1981: The thermal properties of soils in cold regions, *Cold Reg. Sci. Technol.*, **5**(1), 67-75, doi: 10.1016/0165-232X(81)90041-0

Gao, H., Q. Tang, X. Shi, C. Zhu, T. Bohn, F. Su, J. Sheffield., M. Pan, D.P Lettenmaier, and E.F. Wood (2010) . Water Budget Record from Variable Infiltration Capacity (VIC) Model. In Algorithm Theoretical Basis Document for Terrestrial Water Cycle Data Records (in review)

Grayson, R. B., Moore, I. D., and McMahon, T. A., 1992, ‘‘Physically Based Hydrological Modeling. I: A Terrain-based Model for Investigative Purposes,’’ Water Resources Research., Vol. 28, No. 10, pp. 2639–2658.

Johansen, O., 1975, Thermal conductivity of soils, Ph.D. thesis, Trondheim, Norway. (CRREL Draft Translation 637, 1977). ADA 044002.

Knorr, W. 1997: *Satellite Remote Sensing and Modelling of the Global CO2 Exchange of Land Vegetation: A Synthesis Study.* Max-Planck-Institut für Meteorologie, Examensarbeit Nr. 49 (in German), Hamburg, Germany. ISSN 0938-5177.

Liang, X., D. P. Lettenmaier, E. F. Wood, and S. J. Burges, 1994, A simple hydrologically based model of land surface water and energy fluxes for general circulation models. *J. Geophys. Res.* 99:14,415-14,428.

Liang, X., E. F. Wood, and D. P. Lettenmaier, 1999. Modeling ground heat flux in land surface parameterization schemes. *J Geophys. Res*. 104:9,581-9,600.

Liang, X., and Xie, Z., 2003, “Important Factors in Land–atmosphere Interactions: Surface Runoff Generations and Interactions between Surface and Groundwater”, Global and Planetary Change, Vol. 38, pp. 101– 114.

Lawrence, D. M., and A . G. Slater, 2008. Incorporating organic soil into a global climate model. Climate Dyn. 30,145-160.

Lohmann, D., R. Nolte-Holube, and E. Raschke, 1996: A large-scale horizontal routing model to be coupled to land surface parametrization schemes, *Tellus*, **48**(A), 708-721.

Lohmann, D., E. Raschke, B. Nijssen and D. P. Lettenmaier, 1998: Regional scale hydrology: I. Formulation of the VIC-2L model coupled to a routing model, *Hydrol. Sci. J.*, 43(1), 131-141.

Pelletier, J.D., 2008, Quantitative Modeling of Earth Surface Processes, Cambridge University Press.

Sathulur, K. (2008). The spatial distribution of water table position in northern Eurasian wetlands using the Variable Infiltration Capacity Model, Master of Science in Engineering Thesis, Purdue University.

Skaggs, R.W., Gilliam, J.W., Sheets, T.J., and Barnes, J.S. (1980) Effect of Agricultural Land Development on Drainage Waters in the North Carolina Tidewater Region, Water Resour. Res. Inst., Rep. No. 159, Univ. of North Carolina, Raleigh.

Todini, E., 1996. The ARNO rainfall-runoff model. J Hydrol.,175: 339-382.

Vertessy, R. A., and Elsenbeer, H., 1999, “Distributed Modeling of Storm Flow Generation in an Amazonian Rain Forest Catchment: Effects of Model Parameterization” Water Resources Research, Vol. 35, No. 7, pp. 2173–2187.

Walter, B. P., and M. Heimann, 2000. A process-based, climate-sensitive model to derive methane emissions from natural wetlands: Application tp five wetland sites, sensitivity to model parameters, and climate. Global Biogeochem. Cycles, 14(3), 745-765.

Wigmosta, M.S. and Lettenmair, D. P., 1999, "A comparison of simplified methods for routing topographically driven subsurface flow", Water Resources Research, Vol. 35, No. 1, pp. 255-264.

Wigmosta, M. S., Vail, L. W. and Lettenmair, D. P., 1994, "A Distributed Hydrology-Vegetation Model for Complex Terrain", Water Resources Research, Vol. 30, No. 6, pp. 1665-1679.

Wolock,D.M.,andG.J.McCabe(1995),Comparisonofsingleandmultiple-flow direction algorithms for computing topographic parameters inTOPMODEL, Water Resour. Res.,31(5), 1315–1324.

Yang G., L.C. Bowling, K. A. Cherkauer, B. C. Pijanowski, and D. Niyogi (2010), Hydroclimatic Response of Watersheds to Urban Intensity- An Observational and Modeling Based Analysis for the White River Basin, Indiana, J. Hydrometeorology, 11(1), 122-138.

Yang, G., L. C. Bowling; K. A Cherkauer, and B. C Pijanowski (2011), The impact of urban development on hydrologic regime from catchment to basin scales, Landscape and Urban Planning, doi: 10.1016/j.landurbplan.2011.08.003.

3. CHARACTERIZATION AND ANALYSIS OF A NATURAL WETLAND RECEIVING AGRICULTURAL RUNOFF

3.1 Abstract

Wetlands in Midwestern agricultural landscapes have great potential to attenuate runoff response and assimilate nutrients, reducing the load that passes through these areas, eventually reaching the Gulf of Mexico where seasonal hypoxia from nutrients has become a concern. In this study, the Variable Infiltration Capacity (VIC) hydrologic model is used to investigate the hydrology of a natural wetland at Purdue's Agronomy Center for Research and Education in West Lafayette, Indiana. From June 2007 to June 2013, the wetland was monitored for stage in the two main inlet channels and outlet channel; piezometers were installed and monitored on the western side of the wetland. The model was evaluated with respect to these observations of drainage inputs, hydraulic gradients and total outflow from October 1, 2007 to September 30, 2010. The natural watershed for the wetland is 314,000 m^2 (0.31 km^2), while the area of tile drainage which contributes drainage to the wetland is a combined 730,000 m^2 (0.73 km^2) for two separate tile drain systems. The water balance is dominated by the amount of water coming in through the tile drainage. Tile drainage and direct precipitation are the major water source into the wetland. The primary outflow is through the outlet channel. The hydraulic

gradient showed that water moved toward the wetland from upper landscape positions most of the time, but in later summer the hydraulic gradient favors water movement from the wetland to the upland.

3.2 **Introduction**

Wetlands are unique environments that provide habitat for a variety of plants and animals, help to reduce downstream flooding, recharge groundwater, retain sediments, and offer sites for chemical transformations to take place (Kent, 2001). By retaining sediments and hosting chemical transformations the quality of water flowing through a wetland can improve by the time it leaves (DeBusk and DeBusk, 2001; Fisher and Acreman, 2004; Mitsch and Gosselink, 2007; Vymazal, 2007). Recently, water from agricultural sources has been a greater concern because of the hypoxic zone in the Gulf of Mexico (Howarth et al., 2002). The hypoxic zone disrupts the ecosystem, either forcing migrations away from the hypoxic zone or killing those organisms that are unable to migrate (Rabalais et al., 2002a). The nutrients are entering the Gulf from various sources and source areas. Multiple studies and models have attempted to determine the delivery method of nutrients to the Gulf (Goolsby et al., 1999, 2001; Howarth et al., 2002; Justic et al., 2007). One of the more recent studies (Alexander et al., 2008) used a model to estimate the sources and transportation methods of nitrogen and phosphorus and found nitrogen and phosphorus originated predominately from agricultural sources from 1975-1995. Alexander et al., (2008) found nine states (Illinois, Iowa, Indiana, Missouri, Arkansas, Kentucky, Tennessee, Ohio, and Mississippi) contributed 75% of the nutrients delivered to the Gulf of Mexico.

In order to improve the conditions in the Gulf and in local waterways, it is necessary to understand how the water and nutrients are making their way from agricultural areas into rivers and streams. Tile drainage, where land is artificially drained through the subsurface, can modify the hydrologic response and also heavily contributes to the problem of nitrates entering the surface water. Subsurface tile drains can reduce runoff since the water will move more quickly into the subsurface (Skaggs and Van Schilfgaarde, 1999). Many studies have shown, however, that tile drains accelerate the transport of soluble nutrients to waterways by increase subsurface water movement (Willrich, 1969; Jackson, 1973). NO_3 is flushed from the surface and into tile drains, which quickly carry it to local waterways.

The hydrology of a wetland defines the major characteristics of a specific wetland (Cowardin et al., 1979). The soil properties, types of plant and even wildlife are influenced by the water flowing through the wetlands (Mitsch and Gosselink, 2007).The hydrology of wetlands can be diverse due to its topographic position, and micro-climate (regional weather). It can vary seasonally and annually for a specific wetland (Mitsch and Gosselink, 2007). Wetlands have their own unique set of components for the water budget that govern how water flows in and out of their individual wetland ecosystem (Tiner, 2005). Water budgets provide a basis for understanding how hydrologic processes of a wetland vary with topography and climate. The accuracy of each component is dependent on the measurement and the magnitude of associated errors (Winter, 1981; Carter 1986; Cowardin et al., 1979). Precipitation, surface water flow, ground water flow, and evapotranspiration (ET) are the major components of the natural wetland hydrologic cycle (Tiner, 2005). The residence time of a wetland is also a way to represent how long

water stays in the wetland and strongly depends on the time of year and wetland geomorphology.

Because of the benefits wetlands can supply, restored or constructed wetlands make good options for treating water from different sources. As water from agricultural sources in the Midwest seems to be the source of the hypoxia problem more studies are needed on wetlands in this region (Mitsch and Day, 2006). Few hydrologic models have been applied to forested wetlands to date. Mansell et al. (2000) studied cypress pine flatwood forest wetlands in the lower Altantic and Gulf coastal Plain provinces of southeastern US with a land VS2DT model (Variably Saturated Two-dimensional Transport) and they have found that there was a relatively small variation in daily pond water and ground water table elevations. They found that 80% of annual precipitation returned to the atmosphere by evapotranspiration pathway, especially in spring and summer. Skaggs at al. (2005) and Philip et al. (2010) have developed a method to predict the lateral effect of a drainage ditch on wetland hydrology in two wetland mitigation sites in eastern North Carolina using the DRAINMOD model. The results showed that the model slightly over-predicted the lateral effect and since the shallow ditch did not penetrate the tight clay layer near the soil surface the effect of the ditch on the hydrology of adjacent wetlands was limited.

This study will add to the growing number of wetland studies in the Midwest, as it focuses on a small, natural wetland in Indiana that receives a large amount of tile drained water from the surrounding agricultural fields. The main objective of this research is to

investigate the hydrology and physical characteristics of the wetland through application of the Variable Infiltration Capacity (VIC) model with the enhanced wetland algorithm.

3.3 Methodology

3.3.1. Site description

The 1.3 hectare (3.3 acres or 0.013 km^2) wetland is located in West Lafayette, Indiana at Purdue University's Agronomy Center for Research and Education (ACRE) shown in Figure 3-1. This wetland is also listed in the U.S. Fish and Wildlife Service (FWS) National Wetland Inventory with a wetland classification code of PAB4F based on Cowardin et al.'s (1979) classification system. This indicates a lacustrine system with an aquatic bed and floating vascular plants that are semi-permanently flooded. Most of Indiana has been glaciated and there is a thick layer of glacial till deposits at a depth of about 45 to 60 centimeters in the area of ACRE wetland underlain by the New Albany Shale (Wayne, 1952). The dominant soils in the wetland itself are poorly drained. According to the National Resources Conservation Service's (NRCS) Soil Survey Geographic (SSURGO) information, the soil series in the center of this natural, depressional wetland is a Milford series (Mu - Milford silty clay loam, pothole: Fine, mixed, superactive, mesic Typic Endoaquolls) which is classified as a hydric soil. Most other soils in the area surrounding the wetland are moderately well drained soils (Figure 3-2).

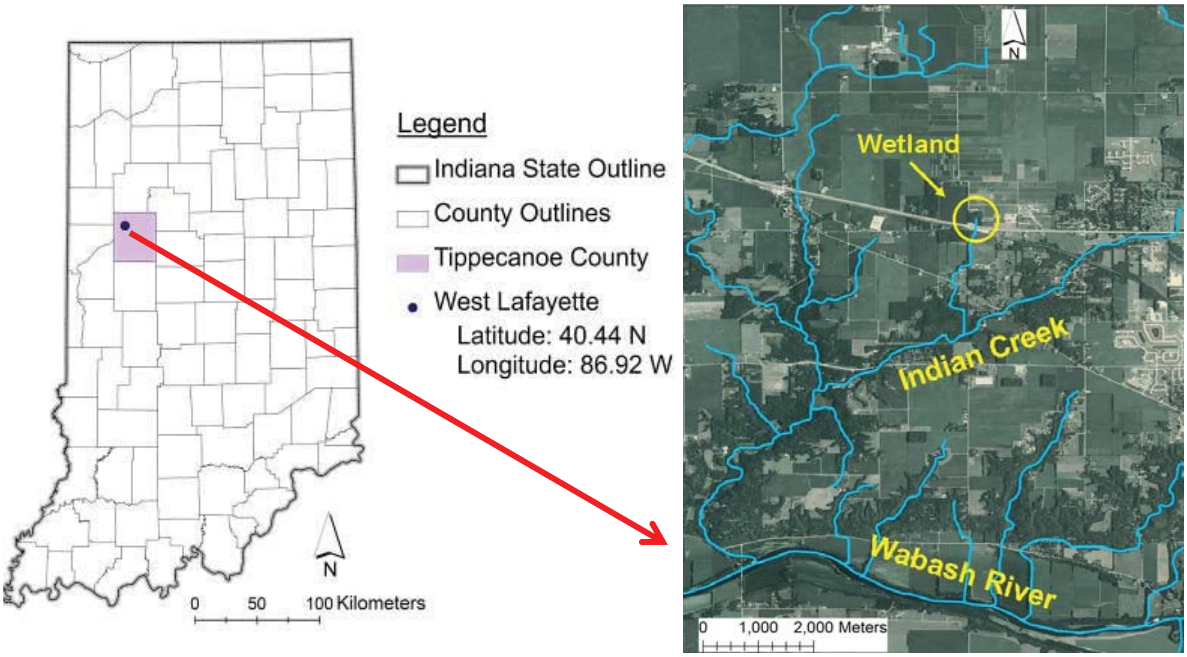

Figure 3-1. Location of the Oak's Wood Wetland in Tippecanoe County, Indiana.

In wetland delineation, the presence of hydrophytic vegetation is one of three important criteria. Tiner (2005) summarized all wetland plant species compiled by U.S. Fish and Wildlife service (FWS) into four major categories: a) Obligate wetland (OBL), b) Facultative wetland (FACW), c) Facultative (FAC), and d) Facultative upland (FACU). A plus or minus next to the abbreviation is used to indicate whether the plants falls into the upper and lower part of the range. The wetland itself is currently covered extensively with Reed Canary Grass (*Phalaris arundinacea*), an emergent vascular plant with obligate wetland status. Although Reed Canary Grass is native in the Midwest, some cultivars are considered invasive because of its aggressive growth habits. Algae are also found on the still wetland's water surface, especially during the summer.

In the adjacent woodland both native and invasive wetland species can still be found in and near the wetland edge, including Swamp rose (OBL), wild hyacinth (FAC+), May

apply (FACU), Jack in the pulpit (FACW-), jewelweed (FACW) and garlic mustard (FAC; invasive species). Overall, more than 75% of the wetland watershed contains cultivated row crops (primarily corn and soybean), with regularly-spaced subsurface drains. Twenty percent of the watershed is wooded and the rest of the watershed is open water area covered extensively with reed canary grass.

The geographic information for the data layers in this study came predominately from the Indiana Spatial Data Portal (ISDP). The aerial photographs were from the 2006 IndianaMap Reflight Orthophotography and the 2007 National Agriculture Imagery Program for Tippecanoe County (both have a resolution of two meters). Quarter-quad aerial images from the 2006 IndianaMap Reflight were also used (with a resolution of one meter). High resolution aerial images (6 inch or 15.24 cm) were used from the 2006 IndianaMap Reflight to get close-up images of the wetland.

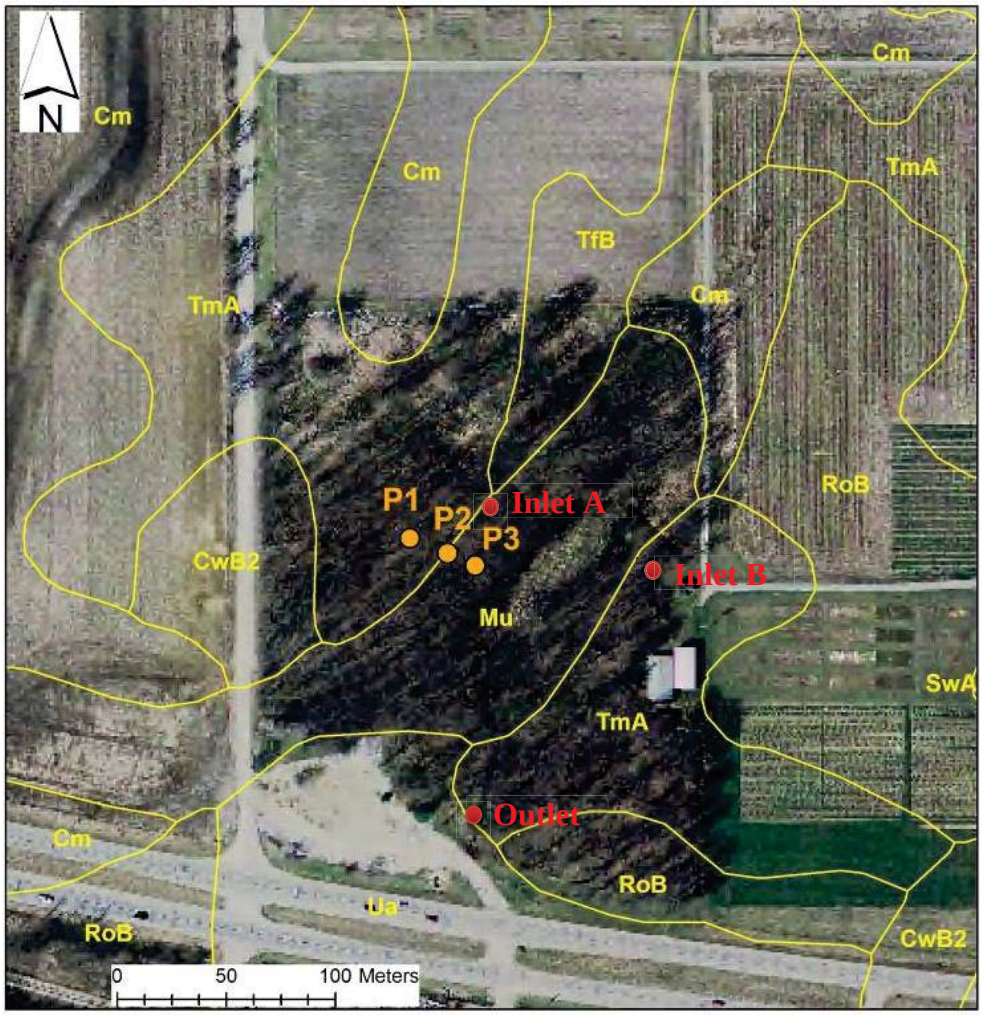

Figure 3-2. Soil series in the ACRE wetland area, with indicating three nest piezometers location (P1, P2 and P3), Inlet A, Inlet B and Outlet location. The soil series are indicated by the polygon overlay, and include: Milford silty clay loam (Mu), Toronto-Millbrook complex (TmA), Throckmorton silt loam (TfB), Chalmers silty clay loam (Cm), Rockfield silt loam (RoB) and Udorthents (Ua).

The delineated watershed for the wetland based on the 10 meter resolution National Elevation Dataset (NED) DEM is 31.4 hectares (77.5 acres or 0.314 km^2). The wetland receives much of its water from the surrounding subsurface tile drainage, some of which lies outside the natural watershed. Two artificial inlet channels flow into the wetland from the subsurface drainage system at ACRE (Figure 3-3). A channelized outlet directs

water leaving the wetland into a culvert, where it flows into Indian Creek and eventually the Wabash River (Figure 3-3). As originally digitized by Naz and Bowling (2008), the larger tile drain network flows into the western portion of the wetland (Inlet A), which receives drainage from 60.4 hectares (149.3 acres or 0.604 km^2) of drained agricultural land. Inlet B, on the eastern side of the wetland receives water from 12.6 hectares (31.1 acres or 0.126 km^2). The natural watershed area that is not included in the drainage area to Inlet A and Inlet B is 15.7 hectares (38.7 acres or 0.157 km^2).

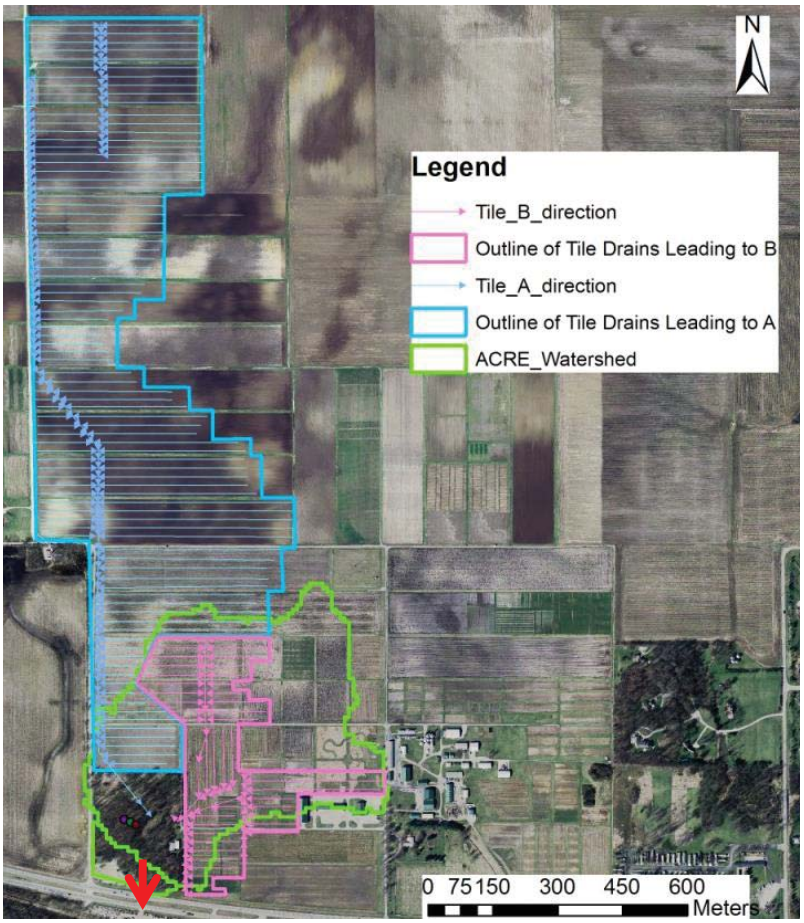

Figure 3-3. Location of subsurface tile drainage systems at ACRE that drain into the wetland (tile drain data described in Naz and Bowling, 2008). The tile drain network flows into two artificial inlet channels: Inlet A (western portion) and Inlet B (eastern portion).

3.3.2. Stage and Discharge measurements

Stilling wells were installed to monitor continuous water level in June 2007 at the two inlet channels and the outlet channel, see Figure 3-2 for locations. Initially, weekly manual readings were taken from the stilling wells. In November 2007, three Global Water pressure transducers combined with data loggers (model series: WL14, or WL15, or WL16) were installed and replaced the manual measurements. The water level data were downloaded in the field onto a laptop. The value recorded by the data logger in the stilling wells is adjusted by the difference between the bottom of channel and the bottom of the sensor to generate a stage above a fixed datum.

Repeated field discharge measurements were taken in all three channels using a Marsh-McBirney Model 2000 Flo-mate flowmeter attached to a top-setting wading rod using the Watson and Burnett (1995) discharge method. In order to determine the discharge at any particular stage with continuous water level data, a stage-discharge relationship was developed. BARC v2.3 is a program developed by Brian Loving, USGS, to provide an aid in development of new stage-discharge rating curves by hand in log space. Rating curves will take the general form of a power law relationship, as follows:

$$Q = A(gh\text{-}offset)^{B} \qquad (\mathbf{3\text{-}1})$$

Where Q is the calculated discharge (in cfs), gh is the gauge height (in in), A and B are constants and offset can be considered a physical offset between stage readings at the sensor at the stage experienced by the channel. Figure 3-4 illustrates why multiple curves may be necessary for different stage readings, as the feature exerting hydraulic control in the channel changes as water levels rise.

Different offsets, end points and break points were explored to develop the best curve relative to the field measured discharges. The final stage-rating curve's equations for each channel are given by the following:

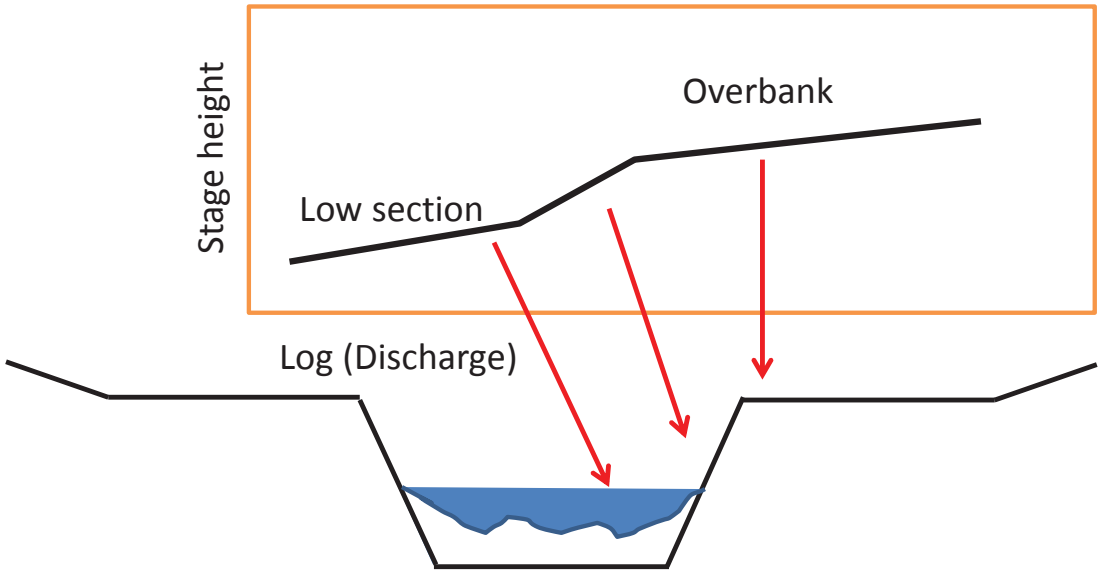

Figure 3-4. An example of the channel and the stage-discharge curve relationship at the related channel position.

Inlet A rating curve:

$$Q = \begin{cases} 0 & gh < 1.17 \\ 1.1e^{-3}(gh - 1.1)/(8.85 - 1.1) & 1.17 \le gh < 8.85 \\ 8.78e^{-4}(gh - 7.75)^{2.37} & 8.85 \le gh < 10.0 \\ 5.35e^{-12}(gh - 7.75)^{25.70} & 10.0 \le gh < 10.4 \\ 3.8e^{-4}(gh - 7.75)^{7.15} & 10.4 \le gh < 11.3 \\ 0.88(gh - 7.75)^{1.03} & 11.3 \le gh < 12.0 \\ 3.93 & gh \ge 12.0 \end{cases} \quad \textbf{(3-2)}$$

Inlet B rating curve:

$$Q = \begin{cases} 0 & gh < 3.6 \\ 0.3e^{-3}(gh - 3.6)/(5.8 - 3.6) & 3.6 \le gh < 5.8 \\ 1.33e^{-18}(gh - 4.0)^{60.14} & 5.8 \le gh < 5.9 \\ 1.53e^{-2}(gh - 4.0)^{2.53} & 5.9 \le gh < 6.83 \\ 2.54e^{-6}(gh - 4.0)^{10.89} & 6.83 \le gh < 7.37 \\ 0.50(gh - 4.0)^{0.86} & 7.37 \le gh < 7.71 \\ 0.41 & gh \ge 7.71 \end{cases} \quad \textbf{(3-3)}$$

Outlet Rating Curve:

$$Q = \begin{cases} 0 & gh < 8.95 \\ 0.1e^{-2}(gh - 8.95)/(9.45 - 8.95) & 8.95 \le gh < 9.45 \\ 2.24(gh - 9.36)^{2.27} & 9.45 \le gh < 10 \\ 9.92e^{-2}(gh - 0.0)^{0.94} & 10 \le gh < 13 \\ 2.62e^{-2}(gh - 6.41)^{1.98} & 13 \le gh < 20 \\ 4.62 & gh \ge 20 \end{cases} \quad \textbf{(3-4)}$$

where gh is stage height in inches and Q is discharge in cfs (ft^3/s).

3.3.3. Hydraulic head monitoring

The hydrology of the Oak's Wood wetland was known to be influenced heavily by the drainage water coming in through tile drainage from the surrounding agricultural land. The relationship of the wetland with the riparian woodland was less certain. A transect of nested piezometers (50cm, 100cm, 200cm) were installed on the west side of the wetland at three locations (P1, P2, and P3) to determine water table position and the direction of movement of subsurface water to and from the wetland and to allow access to sample the subsurface water (Sylvester, 2008). The details of piezometers installation can be found in Sylvester (2008). Piezometers were measured manually approximately weekly between 8/21/2007and 6/2/2011. Only the observed period from 10/1/2007 9/30/2010 was used to compare to model simulation. Hydraulic head and hydraulic

gradients were calculated to represent the direction of subsurface water movement above the till layer, near the boundary of the dense till layer, and within the till layer. The lateral gradient is the change in hydraulic head divided by the distance. The lateral hydraulic gradient is calculated at the same depth between P1 and P2, P1 and P3, and P2 and P3. The distance between P1 and P2 is19.63 m, between P1 and P3 is 41.27 m, and between P2 and P3 is 21.64 m. The vertical gradient is the change in hydraulic head divided by the change in the elevation. The vertical hydraulic gradient is calculated at the same location between 50cm and 100cm, 50cm and 200cm, and 100cm and 200cm.

3.4 **Model Description**

In order to create an integrated understanding of the hydrology of the wetland, the VIC hydrology model (Liang et al. 1994) is used to simulate the wetland watershed. As described in Chapter 2, the VIC model is a land surface scheme that closes a full water and energy balance for each computational unit. The model is typically applied for large regional simulations. In this application, the wetland watershed is represented as a single model grid cell using a lumped modeling approach. Different contributing areas to the wetland can be represented as distinct vegetation zones that are each solved separately. The combined runoff, baseflow and drainflow from each vegetation zone serve as influent to the wetland. The VIC wetland algorithm solves for the water and energy exchange of this surface water element, ultimately calculating surface water discharge at the wetland outlet. This application serves as a case study to evaluate new model algorithms including:

- Water table representation using a drained to equilibrium profile;

- Subsurface agricultural drainage from the surrounding fields; and
- The direction of subsurface water movement between wetland and surrounding area with the subsurface exchange algorithm.

The model requires four types of input data: meteorological observations, soil characteristics, vegetation and lake-wetland, each of which is described below.

3.4.1. Model set up

3.4.1.1. Vegetation Description

The entire contributing drainage area through the outlet, including the topographic watershed and the tile drainage contributions has three primary land uses: semi-permanent open water, wooded wetland and cropland. The VIC wetland algorithm simulates open water areas as spatially dynamic within their defined maximum wetland extent, so the open water wetland and adjacent wooded area are simulated as one coupled land element. Therefore, the land area was divided into four distinct vegetation 'tiles', including: the land area draining to Inlet A (68% of watershed area), land area draining to Inlet B (15% of watershed area), natural watershed area that does not contribute to inlet A or B (16% of watershed area) and open water/wooded wetland (1.5% of watershed area). Vegetation details, drain spacing and drain depth are summarized in Table 3-1. Leaf area indices and crop heights for each vegetation type were extracted from a regional vegetation library for each month of the year based on MODIS imagery (Myneni et al. 1998).

Table 3-1. Drain spacing and drain depth for each vegetation type

Vegetation type	deciduous broadleaf forest	Corn (Tile A)	Soybean (Tile B)	Cropland (rest of watershed)
Vegetation no	1	15	11	11
Area (%)	0.015	0.676	0.146	0.163
Drain spacing (m)	0	20	20	0
Drain depth (m)	0	1.0	1.0	0
Root depth (layer1) m	0.1	0.1	0.1	0.1
Root depth (layer2) m	1	0.75	0.35	0.35
Root depth (layer3) m	5	0.5	1.0	1.0
Root fraction (layer 1)	0.10	0.1	0.2	0.2
Root fraction (layer 2)	0.50	0.6	0.7	0.7
Root fraction (layer 3)	0.40	0.3	0.1	0.1

3.4.1.2. Weather Data

A meteorological observation file containing hourly precipitation, relative humidity, air temperature, wind speed, and precipitation from 7/1/1996 through 12/31/2010 was compiled using observations from the Purdue Automated Station located at the main ACRE meteorological station. Missing precipitation data was estimated using observations from the co-located National Climatic Data Center (NCDC) daily coop station. Other missing data was estimated using the VIC model pre-processing algorithms, based on the MTCLIM model.

3.4.1.3. Soil Parameters

The VIC model assumes one soil type for each model cell, so the soil information does not vary across the vegetation fractions defined above. The physical soil constants were set based on field soil profile descriptions that were made in the Toront-Millbrook complex at the time of piezometer installation (Sylvester, 2008). This complex includes silt loams to clay loams on till plains and is frequently poorly drained. The entire list of soil physical constants used for the model inputs are shown in Table 3-2. The soil profile was divided into the following depths: Layer 1 (0.1 m), Layer 2 (0.6 m), and Layer 3 (1.3

m). The texture of each layer is determined by the field soil profile description based on the majority fraction: Layer 1 (Silt loam), Layer 2 (Silty Clay loam), and Layer 3 (Clay loam). Saturated vertical conductivity, bubbling pressure, residual moisture, and porosity were estimated based on soil texture (Maidment et al. 1993). Field capacity and wilting point moisture were calculated using the Brooks-Corey model (Brooks and Corey 1964). The particle density was set to 2.65 g/cm^3 for all three layers.

Table 3-2. Soil physical constants used for the initial model input based on field soil profile description (Sylvester, 2008)

Soil parameters	Layer 1	Layer 2	Layer 3
Soil Type	Silt loam	Silty clay loam	Clay loam
Soil layer thickness (m)	0.1	0.6	1.3
Saturated vertical conductivity (mm/day)	163.2	48	48
λ	0.234	0.177	0.242
Exponent	11.55	14.30	11.26
Bubble pressure	20.76	32.56	25.89
Field capacity moisture*(fraction)	0.384	0.509	0.477
Wilting point moisture*(fraction)	0.237	0.393	0.340
Residual moisture (fraction)	0.015	0.04	0.075
Porosity fraction (cm^3/cm^3)	0.501	0.471	0.464
Particle density	2685	2685	2685
Soil bulk density	1339.8	1420.4	1439.1

3.4.1.4. Wetland Parameterization

The wetland parameter file describes the variation of surface water area with wetland stage, as well as the slope and topographic index of each bin. The finer resolution (1.5m) DEM from the 2006 reflight of the 2005 IndianaMap Orthophotography project was used and clipped to the same extent as the wooded wetland area. The generalized wetness index and land surface slope were calculated using the SAGA program (Conrad, 2011). The average wetness index, slope, and the area were determined using statistics tool in

ArcMap for each depth bin at depth increments of 0.5 m. Figure 3-5 gives an idea how the surface area of water will increase with depth, while the wetness index decreases.

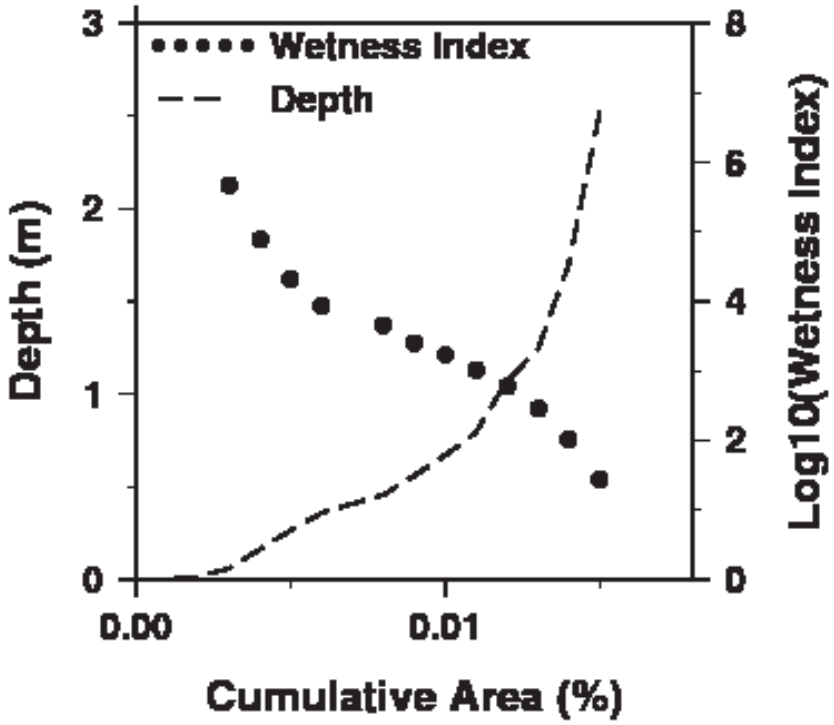

Figure 3-5. The cumulative wetland area of total grid cell vs wetness index and cumulative wetland area of total grid cell vs depth increment. (Note: wetness index is presented as log in order to have better visualization)

3.4.2. Calibration and Evaluation

Application of the VIC model commonly involves calibration of four parameters: the infiltration parameter (bi); Ws (the fraction of maximum soil moisture of the third layer when non-linear baseflow occurs), Ds (the fraction of maximum baseflow velocity), and Dsmax (maximum baseflow velocity) which are the baseflow parameters. Calibration involved the visual determination and the manual adjustment of these parameters via a trial and error procedure that leads to an acceptable match of model simulation with observations of water table, drainflow and wetland outflow (Table 3-3).

Table 3-3. Parameters used for calibrating the subsurface drainage algorithm.

Parameters	Initial value	Calibrated value
bi	0.01	0.05
Ds	0.01	0.01
Dsmax	0.0085	0.1585
Ws	0.99	0.9999

Initial Dsmax = Ksat * tanB * db / a = Ksat*0.05*Depth3/365

3.5 **Results and Discussions**

3.5.1. Model Evaluation

3.5.1.1. Discharge

Even though the wetland was still being monitored, the limited period of filled weather data was from 7/1/1996 to 12/31/2010. The monitored 15 minute stage data from 10/1/2007 to 9/30/2010 are shown in Figure 3-6. A large winter flood event in this year was followed by multiple freeze-thaw cycles, which may have affected the channel shape. In general, the water levels for all three channels are lower in the summer and higher in the winter. In Inlet B, the channel usually was muddy with soft sediment, and covered by algae most of the year which increased the difficulty and error of measuring discharge.

Observed discharge at 15 minute intervals was calculated using equations (3-2) – (3-4).

The 15 minute discharge was summed to monthly values and normalized by the appropriate contributing drainage area for each channel to get a monthly runoff depth. The monthly simulated drainflow from the area of tile drain A, from the area of tile drain B, the outflow of the wetland and precipitation are shown in Figure 3-8. It is assumed that the influent to Inlets A and B that emerges from subsurface corrugated culverts is coming only from subsurface drains. There are no known surface inlets in these fields.

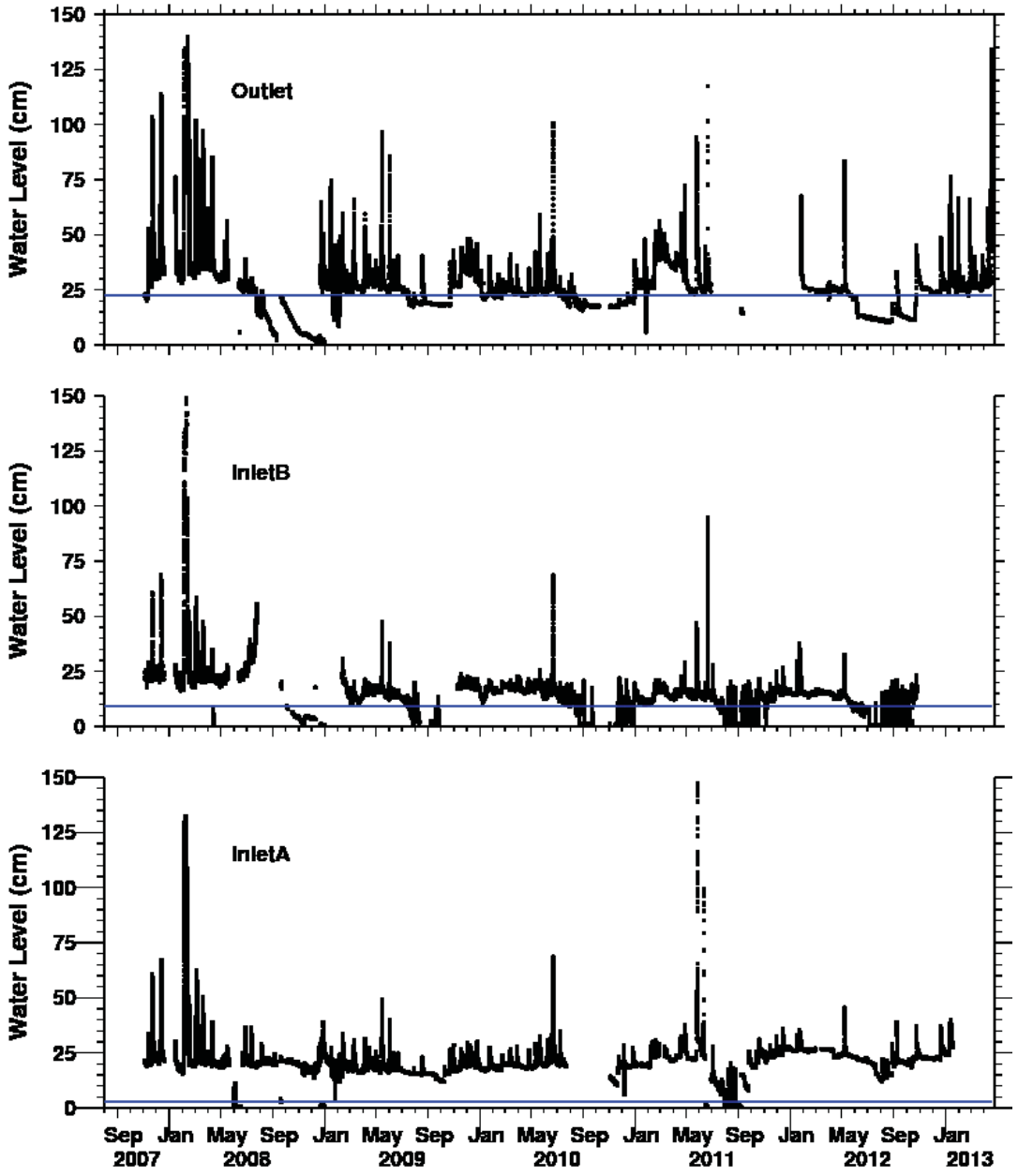

Figure 3-6. Observed stage height from three stilling wells for the time period from 8/1/2007 to 4/25/2013 at 15 or 6 minute record interval. The blue line is the baseline where there is no flowing water.

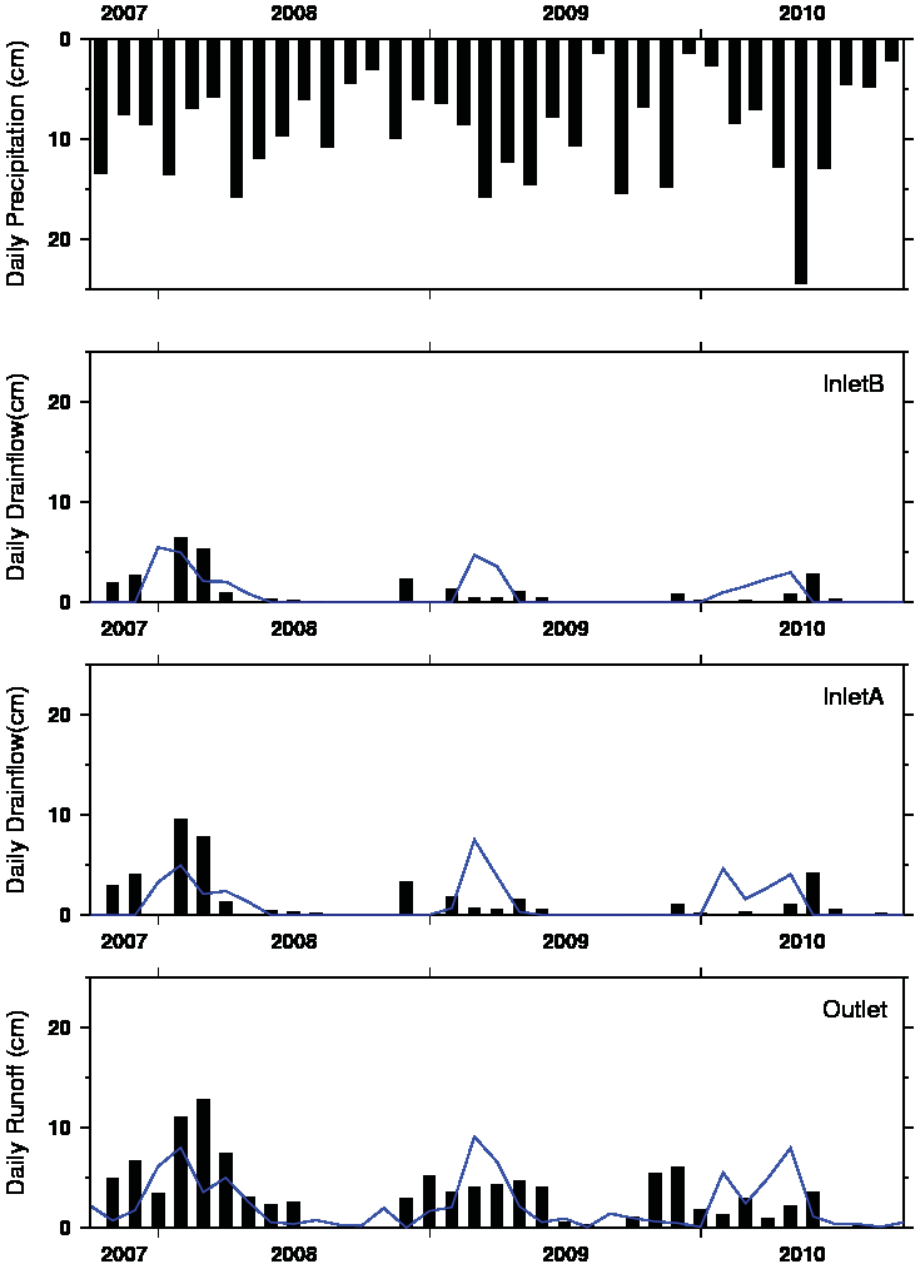

Figure 3-7. Monthly precipitation, monthly drainflow from Inlet B, monthly drainflow from Inlet A and monthly runoff through outlet channel from 10/1/2007 to 9/30/2010. The solid blue line is the simulation, and bar is observation.

Therefore, only the drainflow estimates from the VIC model for these two vegetation types were compared to the observed discharge from Inlet A and Inlet B. Total grid cell runoff is compared to the outlet channel discharge. The monthly simulated drainflow from Inlet A and Inlet B responded to rain events during the spring but drainflow during the fall (November/December) was under predicted.

The mean bias is used to do quantitative assessment of model performance by comparing monthly observed inflow water depth and outflow water depth with simulations. The mean bias for outflow, drainflow A and drainflow B is -19.2%, -35.3%, and -36.2% respectively.

3.5.2. Wetland Water Level

The model provides the ability to estimate the water depth, water area and water volume in the wetland. The monitored water level in the center of the wetland is used to calibrate the model. Figure 3-8 shows the daily observed water depth in the center of wetland. The simulation time period fell on limited observed water level data. The data logger didn't work correctly during the early installation period (Jan to May, 2009) and during (Sep to Jun, 2010).

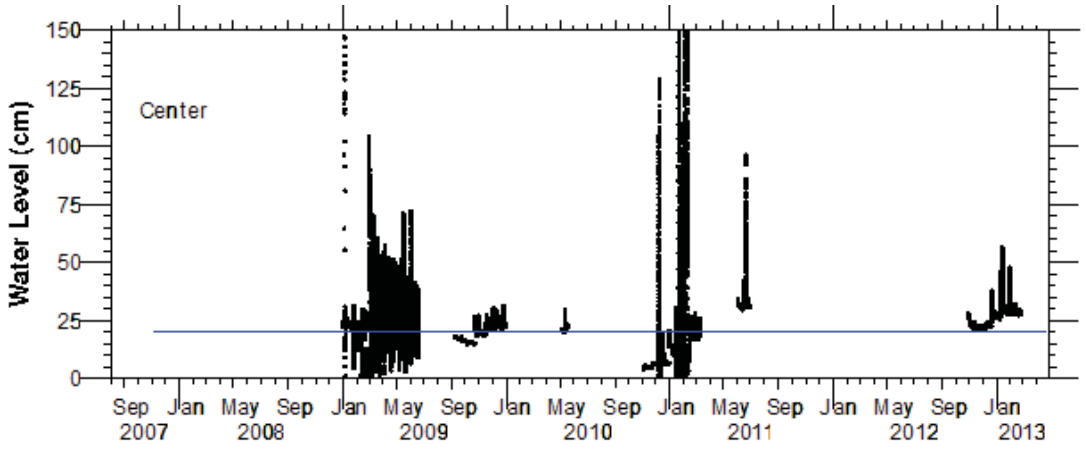

Figure 3-8. Observed stage height from center wetland's stilling wells for the time period from 8/1/2007 to 4/25/2013 at 15 minute record interval (data logger was installed in 12/1/2008). The blue line is the baseline where there is no surface water

3.5.3. Hydraulic gradient

The entire observed nested piezometer data from 7/24/2008 to 4/19/2013 is shown in Figure 3-9. The data points below the baseline for each piezometer were included to indicate that an observation was made, but that the piezometer was dry. For each depth, the lateral hydraulic gradient is shown in Figure 3-10. Only the data from 10/1/2007 to 9/30/2010 were used to calculate hydraulic gradient and vertical gradient in consistency with model simulation time period. The positive value means the water moves from upper landscape position to lower landscape position (toward the wetland). The surface layer (50 cm) shows that water moved toward the wetland most of time, when the hydraulic head was close to the surface. A flood in 2008 may have reversed flow direction at the adjacent area of the wetland. In the till layer (200 cm), water moved toward the wetland from both P1 and P2 in the spring. During summer, there is a reverse flow back to the upland (from P3 to P2).

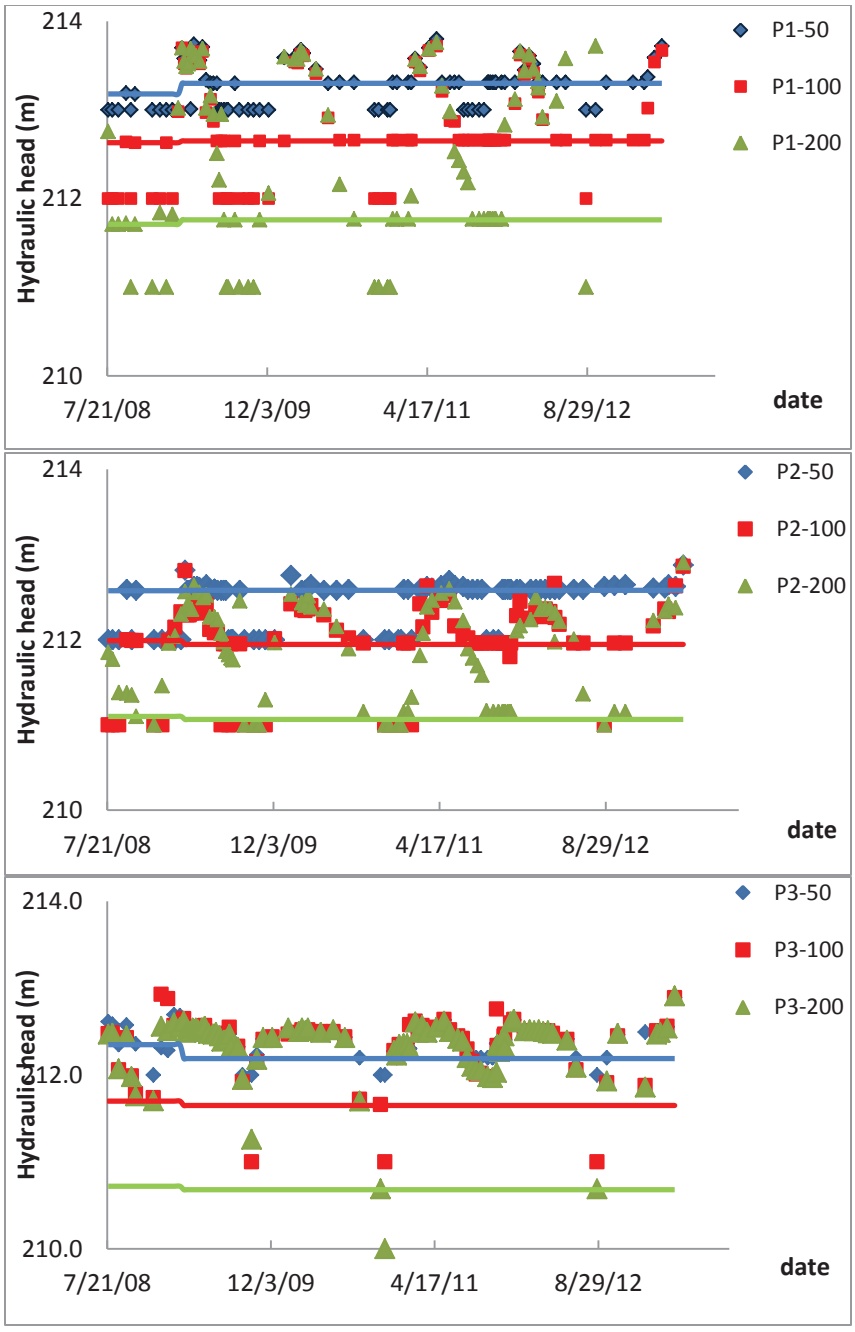

Figure 3-9. Hydraulic head in piezometers above the till layer (50 cm), at near till boundary (100cm) and in till layer (200cm) in different landscape positions with solid line indicated the bottom elevation of the piezometer. (P1:upper location; P2: middle; P3: near wetland)

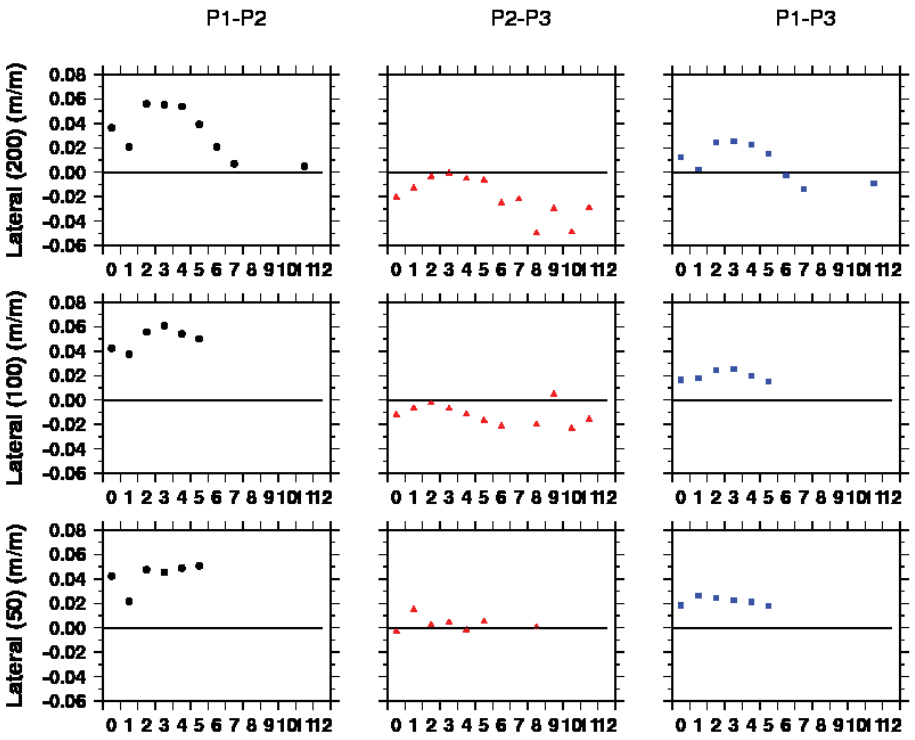

Figure 3-10. Monthly average lateral hydraulic gradient (2007-2010 water year) for piezometers at three depths: 50cm, 100cm and 200cm.

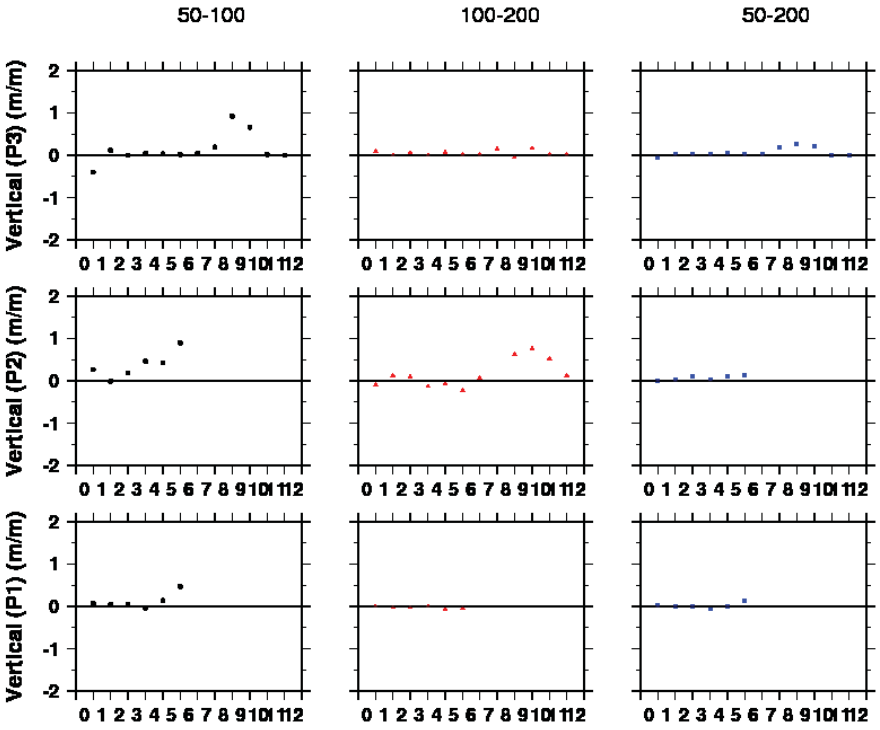

Figure 3-11. Monthly vertical hydraulic gradient for piezometers at three depths: 50 cm, 100 cm and 200 cm from 2007 to 2010 water year.

The monthly average vertical hydraulic gradient (Figure 3-11), illustrates that vertical water movement is small during time periods with high total hydraulic head conducive to lateral flow. When total head is lower, coinciding with the lateral flow reversal in the summer, water moves vertically downward through the till layer.

The simulated distributed water table depth from 10/1/2007 to 9/30/2010 for each landscape position estimated by the VIC model is used to describe the hydraulic gradient for different seasons, as shown in Figure 3-12. The water table position dropped to deeper layers in the summer and rose in spring. The high water table in the winter resulted in positive gradients toward the wetland during this time of year. Similar to the observed hydraulic gradient, as the water table drops, the wetland maintains a high water table in the lowest landscape position, resulting in a flow reversal during summer.

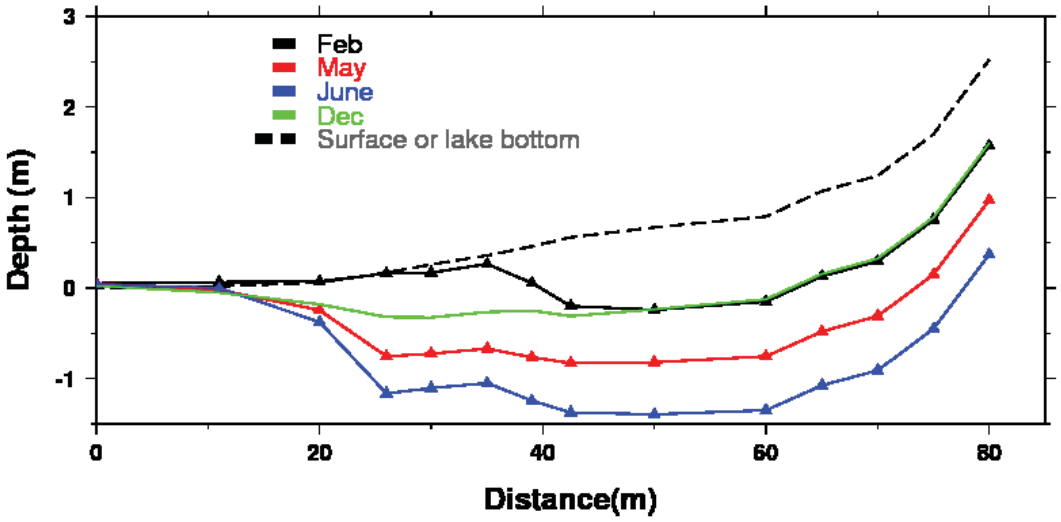

Figure 3-12. The average monthly distributed water table depth (Only show February, May, June and December) in the landscape position. Zero depth is the base when there is no water in the center of wetland

3.5.4. Water balance and water storage

The VIC model demonstrated reasonable performance in representing the complex hydrology of this small depressional wetland, including agricultural drainage inputs and subsurface/surface water interactions. The model can therefore be used to evaluate a cohesive water balance for the wetland itself. The basic water balance equation for the 1.3 ha wetland is as follows:

$$\Delta S = P + D + Q - O - ET$$

where P is the precipitation that fell on the wooded wetland area, D is the total water flowing through tile drains into Inlet A or B, Q is the inflow to the wetland from undrained contributing areas, O is the amount of surface water flowing out of the wetland thought the outlet channel, ET is the evapotranspiration, and ΔS is the change in wetland storage , including surface storage of ponded water and subsurface storage as soil moisture, over the time interval of interest. All variables are in meters.

Table 3-4. Numerical results from the water balance for this model simulation area for five time periods (average annual, average July to September, average October to December, average January to March, average April to June from 2007/10/1 to 2010/9/30)

	Annual	July to Sep	Oct to Dec	Jan to Mar	Apr to Jun
Inflows					
Precipitation (m)	1.11	0.23	0.29	0.19	0.4
Drainflow (m)	0.59	0.05	0.19	0.15	0.2
Q (m)	0.19	0.01	0.05	0.03	0.1
Outflows					
Outflow (m)	0.9	0.3	0.2	0.1	0.3
ET (m)	0.74	0.28	0.04	0.01	0.41
Change in Storage					
□S (m)	0.25	-0.29	0.29	0.26	-0.01

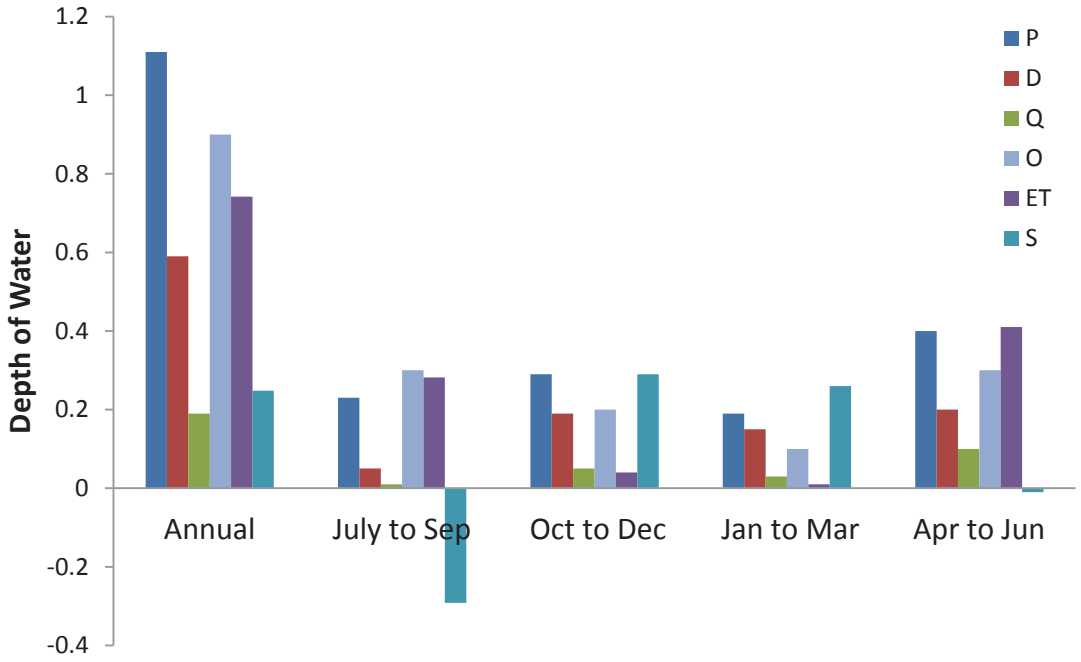

Figure 3-13. The simulated annual and seasonal water balance for the Oak's Wood Wetland from 10/1/2007-9/30/2010.

As the results show (Table 3-4 and Figure 3-13), tile drainage dominates the wetland water balance, especially during spring and early summer, accounting for 31% of annual input to the wetland. Evapotranspiration (39% of annual precipitation) takes over in the summer and fall due to plant growth and atmospheric demand. The positive values of ΔS are storing water in the wetland and ground, and the negative values are losing water in the ground. During winter and spring season, the soil and wetland stores water. During summer and fall, the soil and wetland lose the water.

Figure 3-14 shows the daily simulated water depth in the center of the wetland. The average monthly water level in the wetland shows higher water level in the early spring and also with larger surface water area (Figure 3-16). This Figure also shows that the wetland water volume varies from 0 to ~500 m^3 and the larger volume occurs in spring.

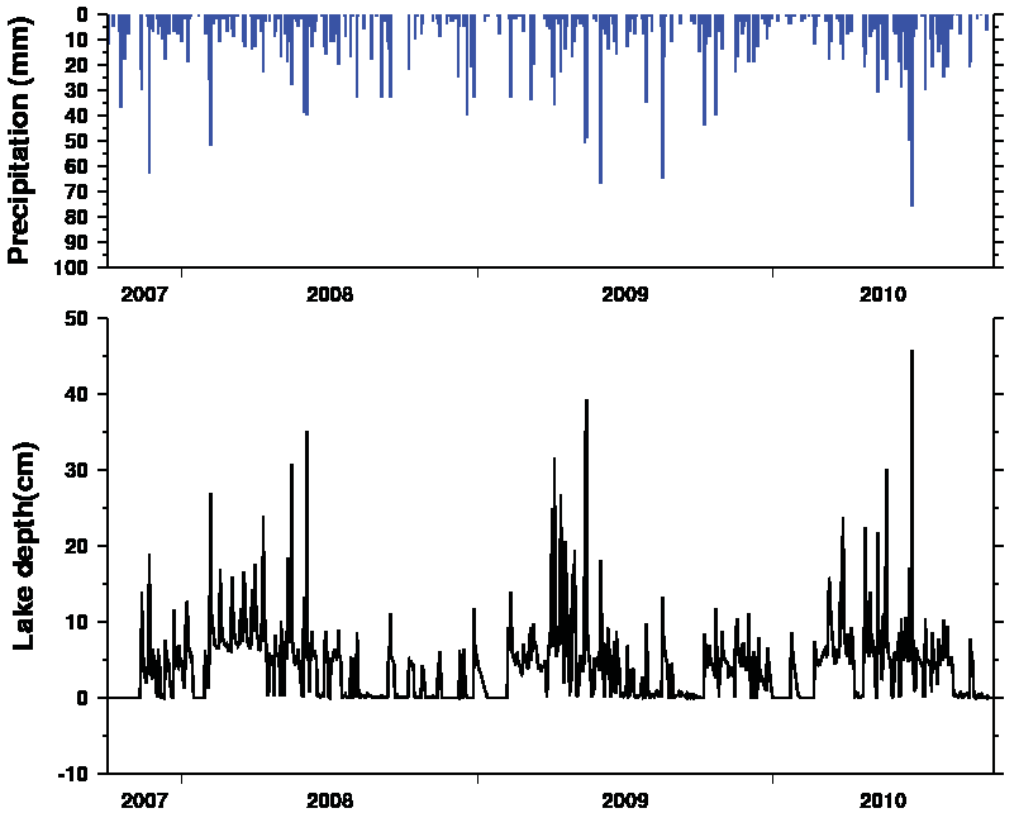

Figure 3-14. (Upper) the daily precipitation and (bottom) the simulated daily lake depth from 10/1/2007 to 9/30/2010.

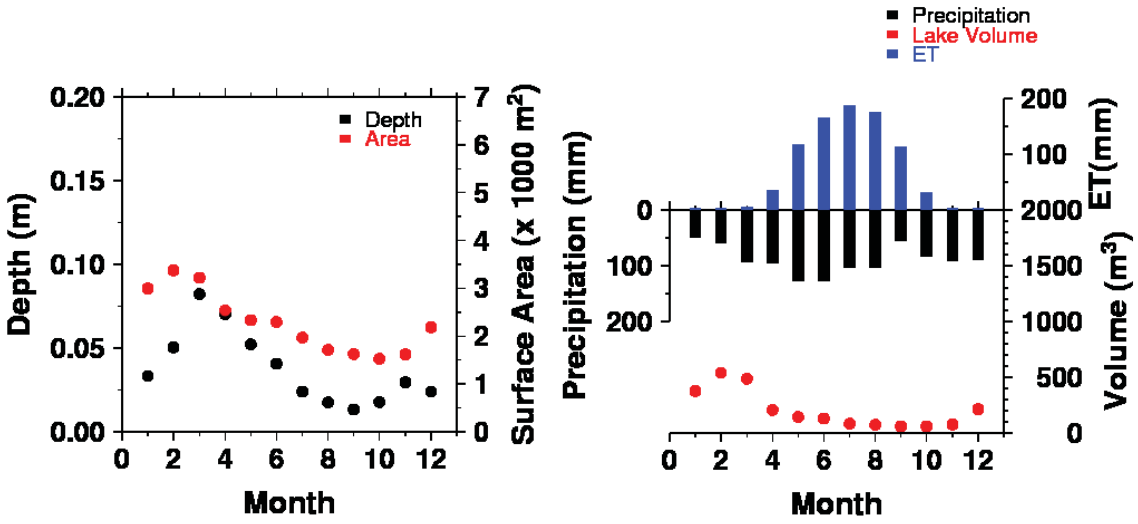

Figure 3-15. (Right) average monthly lake depth and average monthly lake surface area. (Left) average monthly precipitation, evapotranspiration and lake volume from 10/1/2007 to 9/30/2010.

3.6 **Conclusions**

The wetland at ACRE provides a way to study how a natural wetland responds to tile drainage from surrounding agricultural fields. The wetland receives 31% of its annual water budget from subsurface drainage. The wetland stores more water during the winter and spring season due to precipitation (and maybe the frozen ground) and loses water due to higher intense evapotranspiration during summer. The higher water level usually occurred in the end of winter and early spring.

The nested piezometer study also demonstrated the complex interaction with groundwater. As confirmed by model simulations, the subsurface flow generally moves towards the wetland during wetter periods. A gradient reversal occurring in the summer may make the wetland a source of subsurface water to surrounding area during dry periods. This reduces the outflow seen in the channel below the wetland, resulting in decreased summer baseflows. The VIC distributed water table algorithm was able to capture this non-linear water table relationship, a great advancement in our ability to represent wetland hydrology at large scale.

Major need for this study was to get predictions of daily inflow/outflow because we could not calculate loads with the incomplete data record. This model can be used to supplement water quality studies. This study was established to get a baseline look at the wetland and its attributes. This wetland will continue to be studied by moving forward with improving it as an ecosystem and as a filtering nutrient agent to reduce the nitrate load into the stream. The wetland at ACRE will hopefully become an educational study

feature so that others can learn how wetlands function and how wetlands work well in agricultural areas.

3.7 **References**

Alexander, R. B., Smith, R. A., Schwarz, G. E., Boyer, E. W., Nolan, J. V., and Brakebill, J. W., 2008, Differences in phosphorus and nitrogen delivery to the Gulf of Mexico from the Mississippi River Basin: Environmental Science and Technology, v. 42, no. 3, p. 822-830.

Algoazany, A. S., Kalita, P. K., Czapar, G. F., and Mitchell, J. K., 2007, Phosphorus transport through subsurface drainage and surface runoff from a flat watershed in east central Illinois, USA: Journal of Environmental Quality, v. 36, no. 3, p. 681-693.

Beauchamp, K. H., 1987, A history of drainage and drainage methods, *in* Pavelis, G. A., ed., Farm Drainage in the United States: History, Status, and Prospects: Washington D.C. , Economic Research Service, U.S. Department of Agriculture, Miscellaneous Publication Number 1455, p. 13- 29.

Brouder, S., Hofmann, B., Kladivko, E., Turco, R., Bongen, A., and Frankenberger, J., 2005, Interpreting Nitrate Concentration in Tile Drainage Water: Purdue Extension: Agronomy Guide AY-318-W.

Carter, Virginia, 1986,An overview of the hydrologic concerns related to wetlands in the United States: Canadian Journal of Botany, v. 64, no. 2, p. 364-374.

Conard, O., 2008, SAGA GIS v.2.0, System for Automated Geoscientific Analyses, http://www.saga-gis.org

Cowardin, L. M., Carter, V., Golet, F. C., and LaRoe, E. T., 1979, Classification of Wetlands and Deepwater Habitats of the United States, U.S. Fish and Wildlife Service, Office of Biological Services, FWS/OBS-79/31: Washington, D.C.

DeBusk, T. A., and DeBusk, W. F., 2001, Wetlands for water treatment, *in* Kent, D. M., ed., Applied Wetlands Science and Technology: Boca Raton, FL, Lewis Publishers, p. 241-279.

Fisher, J., and Acreman, M. C., 2004, Wetland nutrient removal: A review of the evidence: Hydrology and Earth System Sciences, v. 8, no. 4, p. 673-685.

Goolsby, D. A., Battaglin, W. A., Lawrence, G. B., Artz, R. S., Aulenbach, B. T., Hooper, R. P., Keeney, D. R., and Stensland, G. J., 1999, Flux and Sources of Nutrients in the Mississippi–Atchafalaya River Basin: Topic 3 Report for the Integrated Assessment on Hypoxia in the Gulf of Mexico, NOAA Coastal Ocean Program Decision Analysis Series No. 17, NOAA Coastal Ocean Program, Silver Spring, MD, 130 p.

Goolsby, D. A., Battaglin, W. A., Aulenbach, B. T., and Hooper, R. P., 2001, Nitrogen input to the Gulf of Mexico: Journal of Environmental Quality, v. 30, no. 2, p. 329-336.

Hatch, D., Gouling, K., and Murphy, D., 2002, Nitrogen, *in* Haygarth, P. M., and Jarvis, S. C., eds., Agriculture, Hydrology and Water Quality: Wallingford, UK, CABI Publishing, p. 7-27.

Heathwaite, A. L., and Dils, R. M., 2000, Characterising phosphorus loss in surface and subsurface hydrological pathways: The Science of the Total Environment, v. 251/252, p. 523-538.

Howarth, R. W., Sharpley, A., and Walker, D., 2002, Sources of nutrient pollution to coastal waters in the United States: Implications for achieving coastal water quality goals: Estuaries, v. 25, no. 4B, p. 656-676.

Jackson, W. A., Asniusseni, T. E., Hauser, E. W., and White, A. W., 1973, Nitrate in surface and subsurface flow from a small agricultural watershed: Journal of Environmental Quality, no. 2, p. 480-482.

Justic, D., Bierman, V. J., Scavia, D., and Hetland, R. D., 2007, Forecasting Gulf's hypoxia: The next 50 years?: Estuaries and Coasts, v. 30, no. 5, p. 791-801.

Kent, D. M., 2001, Evaluating wetland functions and values, *in* Kent, D. M., ed., Applied Wetlands Science and Technology: Boca Raton, FL, Lewis Publishers, p. 55-80.

Maidment, D. R., ed., 1993. *Handbook of Hydrology*, McGraw-Hill, New York

Mansell, R. S., S. A. Bloom, and Ge Sun, 2000, A model for wetland hydrology description and validation, soil science, 165:384-397

Mitsch, W. J., and Gosselink, J. G., 2007, Wetlands: Hoboken, NJ, Wiley, 582 p.5.1-5.20

Mitsch, W. J., Day, J. W., Zhang, L., and Lane, R. R., 2005, Nitrate-nitrogen retention in wetlands in the Mississippi river basin: Ecological Engineering, v. 24, no. 4, p. 267-278.

Naz, B. S., and Bowling, L. C., 2008, Automated identification of tile lines from remotely sensed data, Transactions of the American Society of Agricultural and Biological Engineers, ASABE. 51(6): 1937-1950.

Philips, B.D., R. W. Skaggs, and G.M. Chescheir. 2010. A method to determine lateral effect of a drainage ditch on wetland hydrology: Field Testing.

Rabalais, N. N., Turner, R. E., and Wiseman, W. J., Jr., 2002, Gulf of Mexico hypoxia, aka "The dead zone": Annual Review of Ecology and Systematics, v. 33, p. 235-263.

Ribaudo, M., and Johansson, R., 2006, Water quality - Impacts of agriculture, *in* Wiebe, K., and Gollehon, N., eds., Agricultural Resources and Environmental Indicators, 2006 Edition, Economic Information Bulletin 16, Economic Research Service, U.S. Department of Agriculture, p. 33-41.

Ritter, W. F., and Bergstrom, L., 2001, Nitrogen and water quality, *in* Ritter, W. F., and Shirmohammadi, A., eds., Agricultural Nonpoint Source Pollution: Watershed management and hydrology: Boca Raton, FL, Lewis Publishers, p. 59-89.

Sharpley, A. N., Chapra, S. C., Wedepohl, R., Sims, J. T., Daniel, T. C., and Reddy, K. R., 1994, Managing agricultural phosphorus for protection of surface waters: Issues and options: Journal of Environmental Quality, v. 23, no. 3, p. 437-451.

Skaggs, R. W., and Van Schilfgaarde, J., 1999, Agricultural Drainage, Agronomy: Madison, WI, American Society of Agronomy, Crop Science Society of America, and Soil Science Society of America.

Skaggs R.W., G.M. Chescheir, and B.D. Phillips. 2005. Method to determine lateral effects of a drainage ditch on wetland hydrology. Transactions of the ASAE, Vol. 48(2):577-584.

Sylvester, L.M., 2008, Characterization and analysis of a Natural wetland receiving Agricultural runoff. M.S. Thesis. Purdue University. West Lafayette, IN.

Tiner, R. W., 2005, In search of swampland: a wetland sourcebook and field guide: New Brunswick, NJ, Rutgers University Press, 330 p.

Turner, B. L., and Haygarth, P. M., 2000, Phosphorus forms and concentrations in leachate under four grassland soil types: Soil Science Society of America Journal, v. 64, no. 3, p. 1090-1099.

Vymazal, J., 2007, Removal of nutrients in various types of constructed wetlands: Science of the Total Environment, v. 380, no. 1-3, p. 48-65.

Watson, I., and Burnett, A. D., 1995, Hydrology: An Environmental Approach: Boca Raton, FL, CRC Press, Inc., 702 p.

Wayne, W. J., 1952, Map of Tippecanoe County, Indiana, Showing Thickness of Glacial Drift, Miscellaneous Map No. 2; Bloomington, IN, Indiana Geological Survey.

Willrich, T. L., 1969, Properties of tile drainage water, Completion report, Project A-013-IA: Iowa State Water Resour. Res. Inst., Iowa State University, Ames, Iowa.

Winter, T. C.1981, Uncertainties in estimating the water balance of lakes; Water Resources Bulletin, v. 17, no. 1, p. 82-115.

4. THE INFLUENCE OF AGRICULTURAL DRAINAGE ON CARBON EMISSIONS FROM CULTIVATED PEAT SOILS

4.1 Abstract

North temperate peatlands that historically experienced cold and saturated soil conditions are important potential sources of atmospheric methane and carbon dioxide owing to thousands of years of C fixation and peat accumulation with slow rates of decomposition. It has been estimated that about half of global wetlands have been lost due to intensive agricultural drainage, and expanding industrial and urban areas. Although considerable attention has focused on agricultural management practices that can increase the rate of soil carbon accumulation, the loss of carbon from cultivated organic soils may offset these gains. These regions also play an important role in global climate in part due to the potential for positive carbon-cycle feedbacks associated with the interaction between soil temperature and moisture. This study seeks to quantify the influence of water management on cultivated organic soils in northern Indiana. The Variable Infiltration Capacity (VIC) macroscale hydrologic model was modified to represent net primary productivity (NPP) and the influence of agricultural drainage on water table position. Methane and carbon dioxide emissions are simulated using soil temperature, water table position and NPP generated from the VIC model and evaluated using CO_2 flux measurements, combined with periodic measures of photosynthetic activity, water table

height and soil moisture measurements. In order to understand the changing environmental condition and carbon dynamics in managed peatlands from 1915-2007, we also investigate the thermal and moisture regimes, for both simulated drained and undrained conditions in the Kankakee River basin, Indiana.

4.2 **Introduction**

In recent years, growing awareness of earth's dynamic climate and the role of greenhouse gases such as CO_2 has resulted in a surge of interest in carbon emissions from northern peatlands (Bohn et al. 2007; Zhuang et al., 2004, 2006), as well as the potential for carbon sequestration in agricultural lands. At the intersection of these two topics, this work addresses the relative carbon balance of cultivated organic soils (muck soils) in the North Temperate Zone (Smith et al, 2002).

Peatlands are formed in low, wet places, where organic matter accumulates below the water table and decomposes more slowly than it accumulates (Jongedyk et al., 1950). Such natural wetlands (bogs, fens, swamps) are large natural sources of atmospheric methane (Matthews and Fung, 1987; Houghton et al., 2001), releasing an estimated 30 to 50 Tg CH_4 y-1 (Zhuang et al., 2004, 2006). Among the many soil, hydrologic and vegetation factors controlling carbon emissions, there are three major variables that control the rate and amount of methane emission from wetlands, including the availability and quality of high organic matter substrate and soil temperature (Christensen et al., 1996, 2003). Perhaps most important for cultivated organic soils, the position of the water table determines the extent of anaerobic soil, where methane is produced, and the aerobic soil zone, where methane production is restricted and carbon dioxide is produced,

primarily by near surface respiration by living roots and heterotrophic organisms (Elberling et al., 2008). Muck soils are composed of well-decomposed granular residue derived from peat parent materials following years of cultivation, weathering and oxidation (Dachnowski-Stokes A. 1933). As these muck soils are drained and exposed to oxygen in the atmosphere, microbial decomposition of organic matter is greatly enhanced and a significant portion of the organic carbon (~ 60%) may be irreversibly mineralized in the form of gaseous CO_2.

Wetland carbon emissions are therefore significantly affected by both agricultural activities and global climate change. For example, Bohn et al. (2007) showed that temperature and precipitation variability play an essential role in predicting methane emissions in northern Eurasia because of their direct influence on the position of the water table. In the conterminous United States, Wilen and Frayer (1990) demonstrated that the massive losses of wetlands from the 1950's to 1970's were primarily due to human activities. Agricultural development was responsible for 87% of wetland losses and 90% of the losses of forested wetlands. Agricultural drainage practices, such as surface ditches and subsurface drainage tiles (perforated PVC pipes buried beneath the root zone) are used to drain wetlands and improve annual crop yields. These drainage practices can increase the rate of water movement in the subsurface and lower the height of the surface water table. Consequently, the magnitude of total carbon emissions, including both carbon dioxide and methane, in cultivated organic soils is uncertain.

The overall purpose of this paper is to evaluate the role of agricultural drainage on the soil moisture and temperature regime of cultivated organic soils in the upper Midwestern

United States and estimate the impact on CO_2 and CH_4 emissions. In particular, we wish to address the control of soil water content on carbon exchange in the organic soils in northern Indiana and to determine if the soil water and carbon emissions from the landscape can be limited by controlling drainage into ditches. This will be accomplished using the Variable Infiltration Capacity (VIC) model as a tool for examining the hydrologic response to perturbation of relevant parameters and using a simplified carbon dioxide and methane model for examining the carbon dynamics.

4.3 **Study Site**

Much of the cultivated organic soils in Indiana are found in the Kankakee River floodplain in northern Indiana, part of the mesotrophic group of North American peatlands formed in wetlands along the southern extent of glacial drift between present day New Jersey and South Dakota (Dachnowski-Stokes A. 1933). The Kankakee River valley is a flat outwash plain covered with very deep, poorly drained soil formed from herbaceous organic material over sedimentary peat and sand deposits (see Figure 4-1). The 500,000 acre Grand Kankakee Marsh which once bordered the river was one of the largest continuous marshes in North America. The marsh was largely drained by 1922 to support agricultural settlement; presently the region is home to high agricultural production, including specialty crops such as perennial mint.

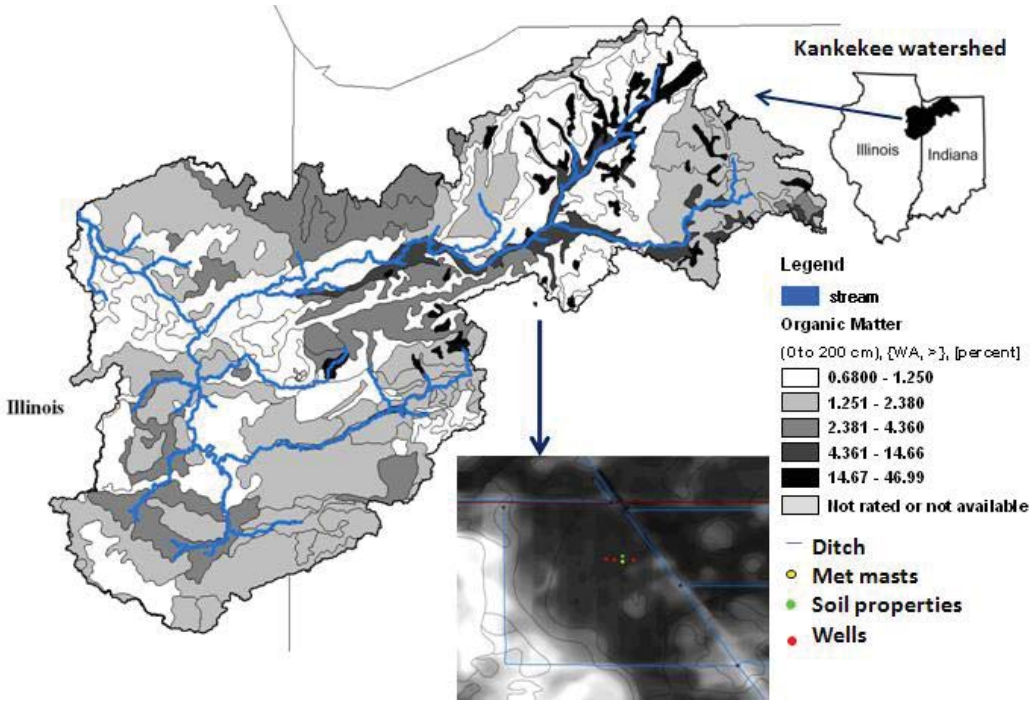

Figure 4-1. The Kankakee River basin in Illinois and Indiana, showing soil organic matter percent in the top 200 cm and the stream network. The field study site is also shown with locations of measured soil variables (green dot), including soil moisture and temperature at three depths, water table depth (red dots) at three locations and meteorological measurements (yellow dot).

The organic-rich soils in the Kankakee River floodplain contain at least 20-30% organic matter by weight. The depth of the muck soils is highly variable but a value on thickness of muck on the order of 50 cm is not uncommon. The drainage of these organic soils, while enhancing agricultural production has caused subsidence of the soils at rates greater than 7 cm/year in one location (Jongedyk et al., 1950) mainly due to the loss of water through drainage (primary subsidence) and loss of organic matter through increased decomposition rates (secondary subsidence) through shrinkage, compaction, and the oxidation process (Ewing and Vepraskas, 2006). Smith et al. (2002) estimated based on CENTURY model runs of the change in soil carbon that even with the increased adoption

of conservation practices over the past 10 to 20 years, the carbon sequestered in 99% of Indiana is overshadowed by increased CO_2 emissions from the 1% of cultivated organic soils. Concern regarding these high rates of soil organic matter decomposition under artificial drainage enhancement motivated an integrated field experiment to assess the carbon exchange rates that took place from May to October 2006 on a cooperative farmer's field planted with perennial mint, also shown in Figure 4-1. Soils at the site are classified as poorly drained Muston muck, with surface drainage ditches on three sides of the field. Field measurements conducted from May to October 2006 include 30 minute net radiation, air temperature, relative humidity, precipitation, wind speed, wind direction, soil moisture at four depths (5cm, 10cm, 20cm, 30 cm), soil temperature at three depths (2cm, 5cm 10cm), soil heat flux, and water table depth at 3 locations (well depth around 6 to 7ft deep) (Johnston et al., 2006). Carbon fluxes at 30-minute intervals were measured by the eddy-covariance micrometeorological method and methane fluxes were measured on one occasion using vent flux chambers.

Model simulations for the entire Kankakee River basin utilize observed surface meteorological data which includes daily precipitation, daily minimum and maximum temperature, and wind speed for the VIC model gridded 12 km for 1915-2007 based on the techniques in Maurer et al. (2002). The streamflow for Kankakee River is obtained from the U. S. Geological Survey (USGS) station at Wilmington, IL (station number 05527500). Drainage area is 5,510 square miles (13,338.44 km^2).

Land cover inputs and soil parameters are described in Yang et al. (2010), with three exceptions. In the Yang et al. (2010) dataset dominant soil type of each grid cell and

fractional vegetation coverage and vegetation characteristics were calculated from the Conterminous United States Multilayer Soil Characteristics Dataset for Regional Climate and Hydrology Modeling (CONUS SOIL) dataset (Miller, and White, 1998) and extracted from Wilson and Lindsey (2005) land use map. Most of these soil characteristics remained the same in this model set up, except for the calibration parameters that have known influence on drainage and water table depth response. The organic matter fraction of each soil layer was added as an additional model input, extracted from the Soil Survey Geographic Database (SSURGO) (Soil Survey Staff, 2006). Saturated hydraulic conductivity was calculated as a weighted average of the mineral soil values used by Yang et al. (2010) and a fixed organic saturated hydraulic conductivity of 1.2 cm/hr.

In addition, the soil and vegetation files from Yang et al. (2010) did not take the presence of subsurface drainage into account. To represent the impact of agricultural drainage practices in the Kankakee basin, it is necessary to identify those grid cells with artificial drainage improvements. Ale et al. (2010) developed a map of potentially drained land areas (areas with a high-likelihood of having regularly-spaced surface or subsurface drains) in Indiana, using a decision tree classifier based on land cover, surface slope and soil drainage class. This study extended this potential drainage map to cover Indiana, Illinois and Ohio and extracted the Kankakee watershed area (Figure 4-2). Grid cells that contained a majority of potentially drained land were considered to contain land suitable for agricultural drainage improvements, and were assigned a low maximum baseflow rate (to reflect pre-drainage conditions). All other grid cells were assumed to contain better drained soils and were assigned a higher maximum baseflow rate (based on general

calibration guide line for the VIC model). Two additional parameters are required to implement the drainage algorithm within the watershed, the drain depth and spacing for installed tiles. Rutkowski (2012) summarized the Indiana Drainage Guide (Franzmeier et al. 2001) and found that the recommended spacing ranged from 18-25 meter in Indiana, while depth ranged from 0.75 to 1m for tile drains. The most common drain depth is 0.9 meters and spacing is 20 m. In Kankakee, open ditches are also common infrastructure for drainage application. In an open ditch, the drain depth is considered the bottom of the ditch, which may be from 1-2 m below the soil surface in this area.

In this model set up, two scenarios (No-drainage and Drainage) were tested to estimate the agricultural drainage impact on hydrological response and carbon dynamics. The undrained scenario represented no agricultural drainage practices in all grid cells. The drained scenario represented agricultural drainage practices in the grid cells identified as having a majority of potentially drained area. For the drained area, non-corn cropland in these cells was assumed to have a drain spacing of 20 m and a depth of 0.9 m, corn cropland in these cells was assumed to have a drain spacing of 10m and a depth of 1.5m. (The deeper drain depth is intended to represent the open ditch effect.) For the undrained area, no agricultural drainage practices were simulated in these cells.

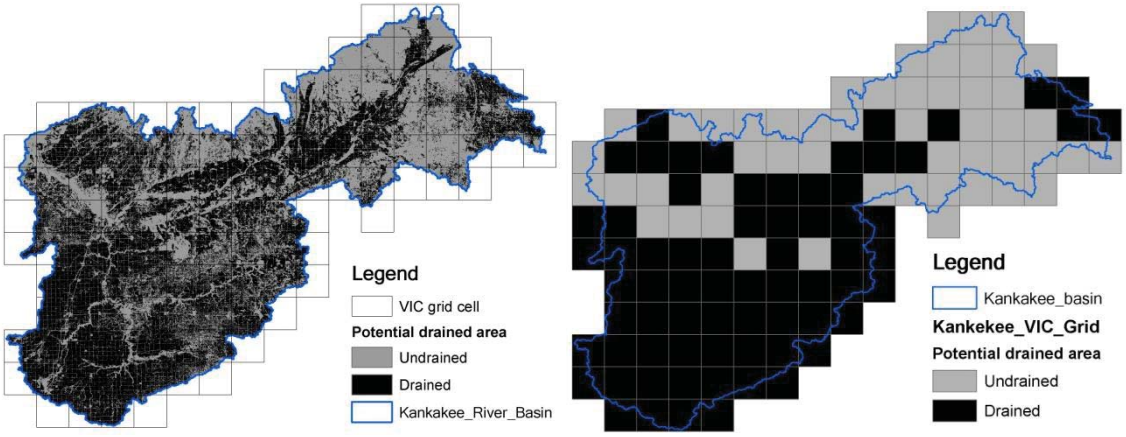

Figure 4-2. The potentially drained map used to create model input files, clipped to the Kankakee watershed at Wellington, IL. (Left) the potentially drained map in 56 m resolution; (right) VIC grid cells with a majority of drained land.

4.4 Land Surface Model Description

4.4.1. The VIC model

In order to create an integrated understanding of the hydrology of the soils with high organic matter content under intense artificial drainage application, the Variable Infiltration Capacity (VIC) hydrology model (Liang et al. 1994) is used to simulate the Kankakee watershed. As described in Chapter 2, the VIC model is a land surface scheme that closes a full water and energy balance for each computational unit. The model is typically applied for large regional simulations. The Kankakee watershed represents a unique case study with higher soil organic matter content and heavy open ditch drainage. This application serves as a case study to evaluate new model algorithms including:

- The organic matter fraction was represented for each soil layer;
- Water table representation using a drained to equilibrium profile; and
- Subsurface agricultural drainage from the surrounding fields.

The details of model development are described in chapter 2. The model requires four types of input data: meteorological observations, soil characteristics, vegetation and lake-wetland, each of which is described below section 4.6. The soil respiration and methane models are offline of the VIC model in order to evaluate the carbon dynamic with/without drainage applications. The soil respiration model and methane model are described below in section 4.5.

4.5 **Carbon Emissions Flux Estimation**

The most common terminology for describing the ecosystem carbon balance where input by assimilation is balanced by respiration with major carbon accumulation and losses taking place which bypass respiration is summarized in Figure 4-3. Gross primary production (GPP) is the CO_2 assimilation within the plant body where photosynthesis occurs and carbon enters ecosystem as the organic component or the rate at which energy is converted by photosynthetic and chemosynthetic autotrophs to organic substances. NPP is the balance between GPP and plant respiration (autotrophic respiration-R_a). Net ecosystem productivity (NEP or equivalent to negative sign of NEE-Net Ecosystem Carbon Exchange) includes heterotrophic soil respiration (R_h) and is mainly measured by eddy covariance methodology. Micro-meteorological measurement does not cover the respiration by harvest and by fire that are the main human land management components. The combined process with human land management has been termed Net biome productivity (NBP). In this study, we do not discuss the harvest and fire impacts. The carbon balance between each term can be represented in the following:

$$NPP = GPP - R_a \qquad (\mathbf{4\text{-}1})$$

$$NEP \text{ (or -NEE)} = NPP - R_h \quad (\mathbf{4\text{-}2})$$

$$NBP = NEP - (\text{respiration by fire or harvest}) \quad (\mathbf{4\text{-}3})$$

In this study, the major framework for assessing carbon fluxes couples the VIC model with the Biosphere-Energy-Transfer-Hydrology model (BETHY) (Knorr, 2000) and wetland methane model (Walter and Heinmann, 2000). The VIC model was modified to include BETHY components to compute the hourly NPP with a Farquhar formulation (Farquhar et al. 1980) with given meteorological fluxes, and VIC generated soil moisture and temperature (Bohn et al. 2007).

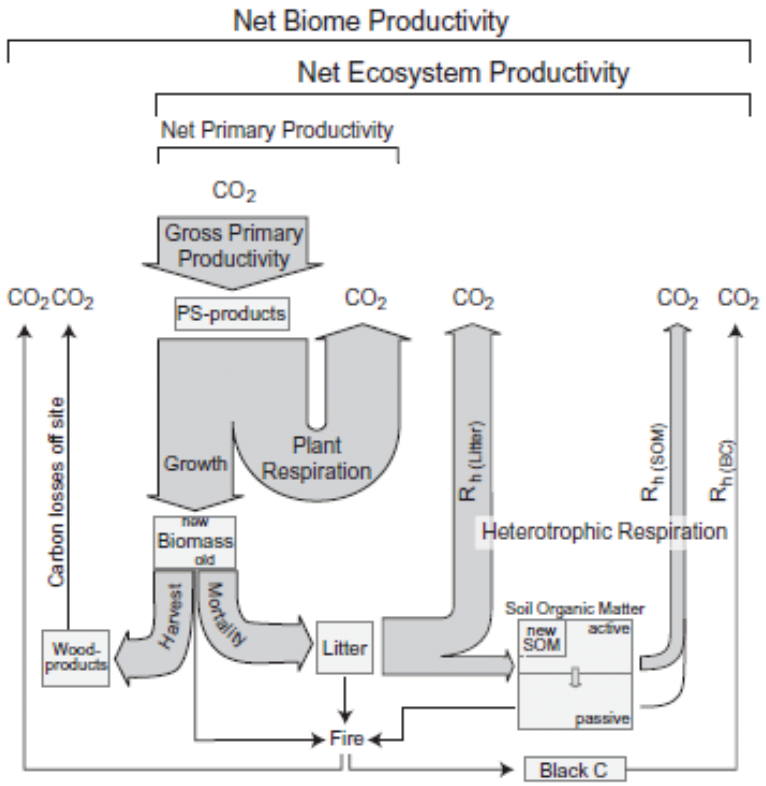

Figure 4-3. A conceptual scheme of the carbon flow through ecosystems with input by photosynthesis (Gross primary productivity) and C-losses from plant and soil respiration (courtesy from Schulze 2006)

4.5.1. Soil Respiration Model

In the soil respiration equation, there are three important factors for estimating the soil respiration rate. First is the soil temperature; second is precipitation; and third is NPP and the equation is shown below.

$$RES(t) = \frac{\int_{1year} NPP(t')dt'}{\int_{1year} f_e(t')dt' * Q_{10}^{\frac{T(t')}{10}} dt'} f_e(t) * Q_{10}^{\frac{T(t')}{10}} dt'$$

The effective moisture content equation is used for adjusting the actual evapotranspiration $f_e(t)$ (shown below); Q_{10} is the multiplicative factor describing the rise in respiration for a temperature increase of 10^oC; T is temperature at current step. Q_{10} is used to determine the soil respiration rate. When soil temperature is cold, the respiration rate is small. After certain point, the soil respiration rate is exponential increasing.

In order to speed up the calculation time, the soil respiration (CO_2) sub-model from the BETHY model (Knorr, 1997) is run off-line from the VIC model. The net CO_2 exchange with the atmosphere (NEP) is computed as the difference between soil respiration and NPP. Based on Raich and Porter (1995), the temperature is the most important factor determining the rate of soil respiration. Lloyd-Taylor constants (or Q_{10}) can be used for adjusting the soil temperature factor (Lloyd and Taylor, 1994). Evapotranspiration is a good approximation to soil respiration (Meentemeyer, 1978). In this study, the soil

moisture conditions are input as the ratio of actual to potential evapotranspiration. The optimal soil moisture and temperature was set 0.65 and 10^{o}C.

The VIC model already includes vegetation type, leaf area, plant structure, and population. Each vegetation type has an associated above- and below-ground litter pool. When litter decomposes a fraction, representing the highly labile fraction, is respired as CO_2 directly into the atmosphere. The remainder is converted into intermediate (active) and slow (passive) soil organic matter (SOM) pools (Foley, 1995). The Lund-Potsdam-Jena (JPL) Dynamic Global Vegetation Model included four soil carbon pools: above- and below- ground litter pool (labile carbon ~2year) and recalcitrant and stable soil pools with intermediate (~30 years) and slow (~1000 years) turnover times - the average time that carbon resides in a conceptual SOM pool also referred to as mean residence time (Stich et al. (2003) ;see Table 4-1). In this study, we only divide the soil carbon pool into litter, intermediate and slow carbon pools. Following Foley (1995), 70% of decomposed litter (assuming equal to NPP) goes directly into the atmosphere as CO_2 (f_{air}), the reminder (30%) enters the soil pools with 98.5% (f_{inter}) and 1.5 % (f_{slow}) of the remainder entering the intermediate and slow soil pools, respectively. The total heterotrophic respiration is the summation of carbon emissions from the litter pool and intermediate and slow soil pool decomposition:

$$Rh = Rh_{litter} * f_{air} + Rh_{intermediate} + Rh_{slow} \quad (\mathbf{4\text{-}4})$$

Where $Rh_{litter} * f_{air}$ is the flux of litter carbon's heterotrophic respiration to the atmosphere, $Rh_{intermediate}$ is the flux of intermediate Carbon's heterotrophic respiration

to the atmosphere, Rh_{slow} is the flux of slow Carbon's heterotrophic respiration to the atmosphere.

The Carbon pool for each component is updated in each timestep, as follows:

Litter Carbon += Litter Fall (assuming equals to NPP) – Rh_{litter}

Intermediate Carbon += f_{inter} * (Rh_{Litter} – Rh_{Litter}* f_{air}) – $Rh_{intermediate}$

Slow Carbon += f_{slow} * (Rh_{Litter} – Rh_{Litter}* f_{air}) – Rh_{slow} (**4-5**)

In order to spin up the calculation of carbon dioxide fluxes for each grid cell, this sub-model is run outside of the VIC model. The CO_2 model requires three forcings that are simulated by the VIC model: the daily ratio of actual to potential evapotranspiration for each soil layer (estimated by soil moisture), soil temperature, and NPP.

Table 4-1. Parameters and constants used in the BETHY soil respiration model.

Function	Abbreviation	Value	Description
Soil and litter decomposition	f_{air}	0.7	Fraction of the decomposed litter emitted as CO_2 to the atmosphere per time step
	f_{inter}	0.985	Fraction of decomposed litter's remainder entering the intermediate soil pool per time step
	f_{slow}	0.015	Fraction of decomposed litter's remainder entering the slow soil pool per time step.
	T_{litter}	2.86 yr	Litter turnover time at 10^oC
	T_{inter}	33.3 yr	Intermediate soil pool turnover time at 10^oC
	T_{slow}	1000 yr	Slow soil pool turnover time at 10^oC

*Turnover time: the average time that carbon resides in a conceptual SOM pool also referred to as mean residence time

4.5.2. Methane Model

The Walter and Heimann (2000) methane model consists of a hypothetical one-dimensional soil column divided into 1 cm thick parallel layers. The boundary between

anaerobic and aerobic soil zones is taken to be the position of the water table. Methane is only produced in layers below the water table; oxidation occurs in the layers above the water table. Methane transport into the atmosphere is represented by molecular diffusion through water or soil pores filled with air and standing water, bubble ebullition from depths where bubbles are produced to the water table and uptake through vegetation from the soil layer directly up to the atmosphere. The one-dimensional continuity equation of the entire soil/water column is solved numerically. The daily values of water table position, soil temperature profile and the NPP simulated by the VIC model provide the forcing of the methane model. The model outputs are the methane fluxes to the atmosphere and methane concentration in the soil profile.

4.6 **Model Calibration and Evaluation**

4.6.1. Field Scale

Similar to most physically-based hydrologic models, the VIC model has many parameters (soil physical properties, hydraulic properties, vegetation properties, etc.) that must be specified. Usually most parameters can be derived from field measurement, soil information databases and remote sensing observations. Application of the VIC model commonly involves calibration of four parameters: the infiltration parameter (bi), Ws (the fraction of maximum soil moisture of the third layer where non-linear baseflow occurs), Ds (the fraction of maximum baseflow velocity), and Dsmax (maximum baseflow velocity) which are the baseflow parameters. Calibration often involves the manual adjustment of these parameters via a trial and error procedure that leads to an acceptable match of model simulation with observations. After improving the representation of

organic matter fraction, water table estimation, and artificial drainage, two additional parameters need to be adjusted to fit the field observations. These are the bubbling pressure and the Brooks-Corey exponent for each soil layer. In order to more efficiently and accurately calibrate the model, the VIC model has been coupled with the Multi Objective COMplex evolution (MOCOM-UA) algorithm (Yapo et al., 1998) with two objective functions, the daily Nash-Sutcliffe efficiency and daily relative error between simulation and observation (Cherkauer et al., 2013; Shi et al., 2008). The model parameters and ranges used in the MOCUM-UA algorithm are listed in Table 2. These parameters were therefore adjusted during automatic calibration, producing a group of better parameter sets that were further adjusted by visually comparing the observed water table depth, soil moisture, and soil temperature. The final values of the calibrated parameters are also provided in Table 4-2.

Table 4-2. The range of six model parameters used in automatic field-scale calibration.

Parameter name (unit)	Abbreviation	Range	Calibrated Value
The infiltration parameter (N/A)	bi	0.00001 - 0.4	0.0001
The maximum baseflow velocity (mm/day)	Dsmax	0.00001 - 25	0.15
The fraction of maximum baseflow velocity (fraction)	Ds	0.00001 - 0.2	0.1
The fraction of maximum soil moisture content of third layer (fraction)	Ws	0.5 - 1.0	0.9
The exponent for each soil layer (N/A)	EXP	3.01- 20	3.67-7.6-7.82
The bubble pressure for each soil layer (cm)	Bubble	0.5 - 50	0.39-1.89-20.08

4.6.2. Watershed calibration and evaluation

The watershed calibration and evaluation involved the manual adjustment of soil parameters (bi, Dsmax, Ds, Ws, EXP, and Bubble), drain depth and drain spacing to

simulate daily surface runoff and subsurface baseflow and route the whole basin's streamflow in comparison with observed streamflow data at Wellington, IL for the calibration period (from 10/1/1996 to 9/30/2006) (Table 4-3). The model is then evaluated for the validation period (10/1/1985 to 9/30/1996) with no further adjustment of model parameters. For those grid cells that have poorly drained soil, based on the potentially drained land map (Ale, 2010), Dsmax is 0.5 mm/day after calibration. This represents the low conductivity of the soil prior to artificial drainage. It was assumed that most current agricultural drainage practices were in place during this period, so the drainage algorithm was activated during model calibration. Dsmax is increased internally to the model when the artificial drainage option is selected. Dsmax was set to 30 mm/day for the remaining grid cells that are assumed to not have artificial drainage. The drainage algorithm was not activated for well drained grid cell, therefore drain spacing and drain depth is 0.

Table 4-3. The range of six VIC model soil parameters and drainage parameters used in watershed scale

Parameter name (unit)	Abbreviation	Final Value after calibration
The infiltration parameter (N/A)	bi	0.0001
The maximum baseflow velocity (mm/day)	Dsmax	0.5 poorly drained soil 30 well drained soil
The fraction of maximum baseflow velocity (fraction)	Ds	0.1
The fraction of maximum soil moisture content of third layer (fraction)	Ws	0.95 poor drained soil 0.99 well drained soil
The exponent for each soil layer (N/A)	EXP*	3.39 -12.0185
The bubble pressure for each soil layer (cm)	Bubble*	6.0058 - 19.7661
Drain depth (m)	D	0 - 0.9
Drain spacing (m)	DS	0 - 20

* Those values are the range of value that used in each layer.

4.7 **Results**

4.7.1. Field Scale

4.7.1.1. Hydrological response with artificial drainage

The simulated and observed depth to water table and soil moisture for the field site is shown in Figure 4-4. In general, the simulated water table matches closely with the values observed in the three wells. The simulated soil moisture for layer two (10 to 61 cm) is slightly lower than observed soil moisture at 20 cm and 30cm. During the early growing season, the water table drops around 1 meter, coinciding with the period of maximum evapotranspiration. After harvest of the mint crop on July 10th (or Julian date 191) the water table maintains a shallower position and slightly higher soil moisture content. The observed water table depth and soil moisture also respond more quickly to precipitation events than simulated.

The study site is notable for its high organic matter content and low soil bulk density. Organic matter can act as an insulator with its low thermal conductivity and relatively high heat capacity modulating the transfer of energy from the atmosphere into the soil. To better evaluate the soil thermal properties used for organic matter, the observed daily soil temperature is used to evaluate the VIC model performance with/without the organic matter algorithm. The scatter plot of observed and simulated daily soil temperature (Figure 4-5a) shows that the simulation with organic matter is closer to the 1:1 line than the simulation without organic matter, which shows a bias at both high and low temperatures. As shown in Figure 4-5b) the simulation with organic matter has a smaller diurnal variation that more closely matches the observations. Overall, the simulation with organic matter has smaller daily fluctuation and closer representation of the seasonal trend than the simulation without organic matter (Figure 4-5c). This result shows that the model can perform better with the modifications to the soil thermal properties for high organic matter soil.

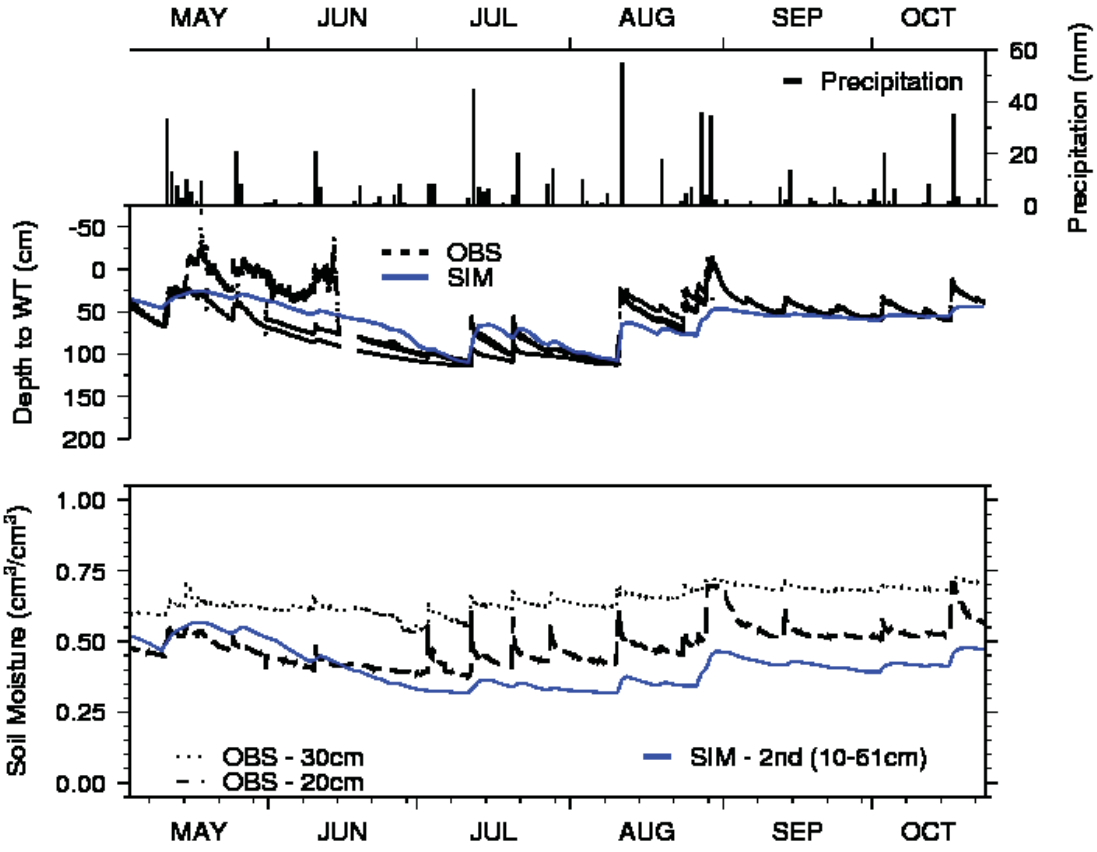

Figure 4-4: Simulated and observed soil water content for the field site (May-October 2006): precipitation (top), water table time series (middle), and soil moisture time series for the second soil layer (bottom)

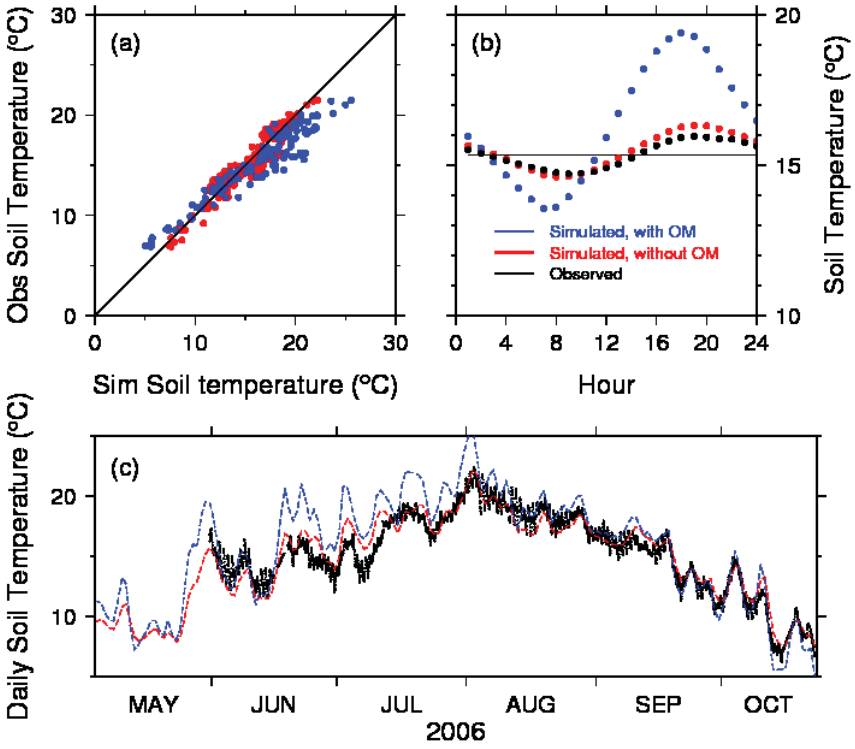

Figure 4-5: Simulated and observed 10 cm soil temperature at the field site, with and without organic fraction representation: a) scatter plot of daily temperatures b) mean diurnal cycle and c) daily time series.

4.7.1.2. Carbon fluxes (CO_2 and CH_4)

To evaluate the ability of the soil respiration model to capture variability in carbon dioxide emission, the observed and simulated daily carbon dioxide fluxes from the field site between May and October 2006 are shown in Figure 4-6. Carbon dioxide fluxes varied during this growing season. The highest daily flux (261.8 g/m^2d) was observed in the beginning of May, followed by a quick drop (Figure 4-6c). The second highest flux (229.7 g/m^2d) occurred in the middle of July. After harvest, the carbon dioxide flux decreases to less than 100 g/m^2d. Overall, the simulated daily carbon dioxide fluxes were slightly underestimated, primarily because the model did not capture the extreme highs.

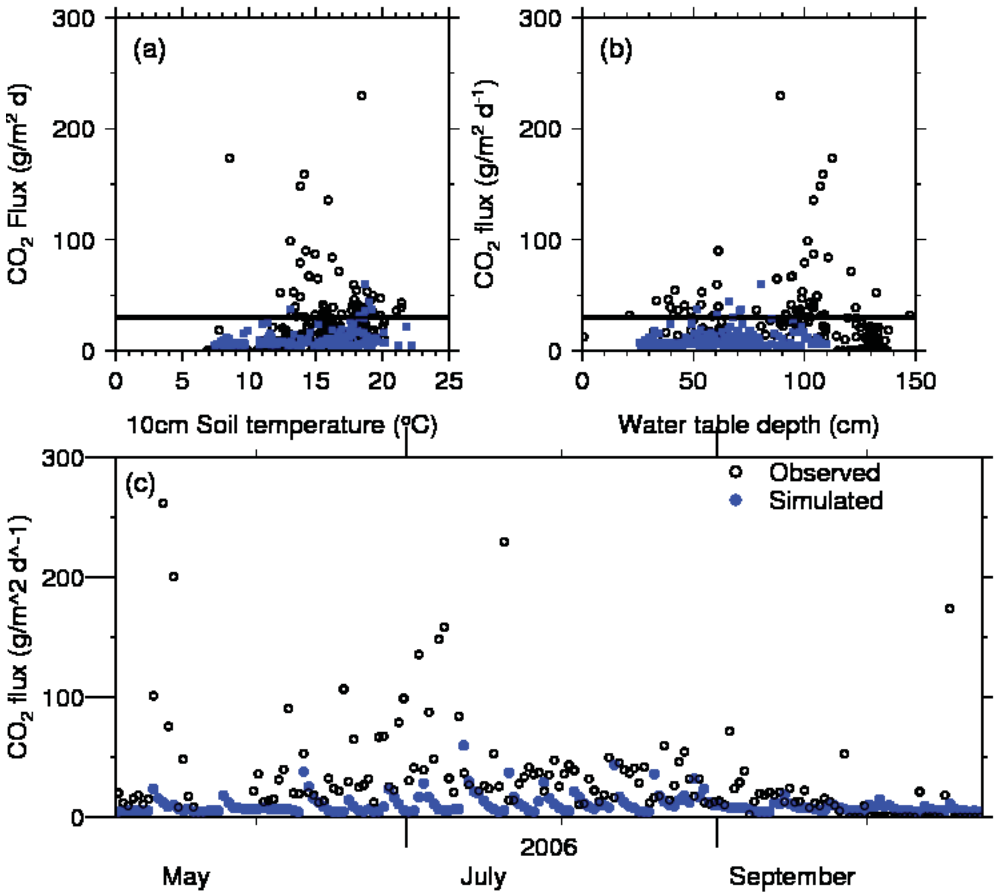

Figure 4-6: Observed and simulated daily CO_2 emissions from the field site: a) daily CO_2 flux versus 10 cm soil temperature-the, b) daily CO_2 flux versus water table position and c) daily time series of observed and simulated CO_2 flux. (The smooth line is the average CO_2 emissions).

Investigating the response of CO_2 fluxes to climate variability, a comparison of CO_2 flux versus the 10 cm soil temperature for observation in Figure 4-6a shows that observed carbon dioxide fluxes reached a maximum around ~15 ^{o}C. In contrast, the maximum simulated CO_2 fluxes during this period occurred with a 10 cm soil temperature of approximately 19 ^{o}C. The observed CO_2 emissions increase with deeper observed water table position and reach a maximum around 1 meter. For simulated carbon dioxide fluxes, there is little relationship with water table position.

Unfortunately observations of methane emissions from this field site were not available. To evaluate the responsiveness of the methane model framework, simulated daily CH_4 emissions from the field site between May 2006 and October 2006 are shown in Figure 4-7. The simulated daily methane fluxes show the strong impact of water table position. When the water table drops below a certain depth (~50 cm), the methane fluxes drop and stop emitting into the atmosphere. Methane emissions increase linearly with shallower water table depth. The response to soil temperature shows higher emissions for lower temperatures, but the signal is more mixed, potentially reflecting the fact that lower soil temperatures generally coincided with a higher water table. Overall, the majority of methane was emitted into the atmosphere before the growing season and after harvest under saturated conditions.

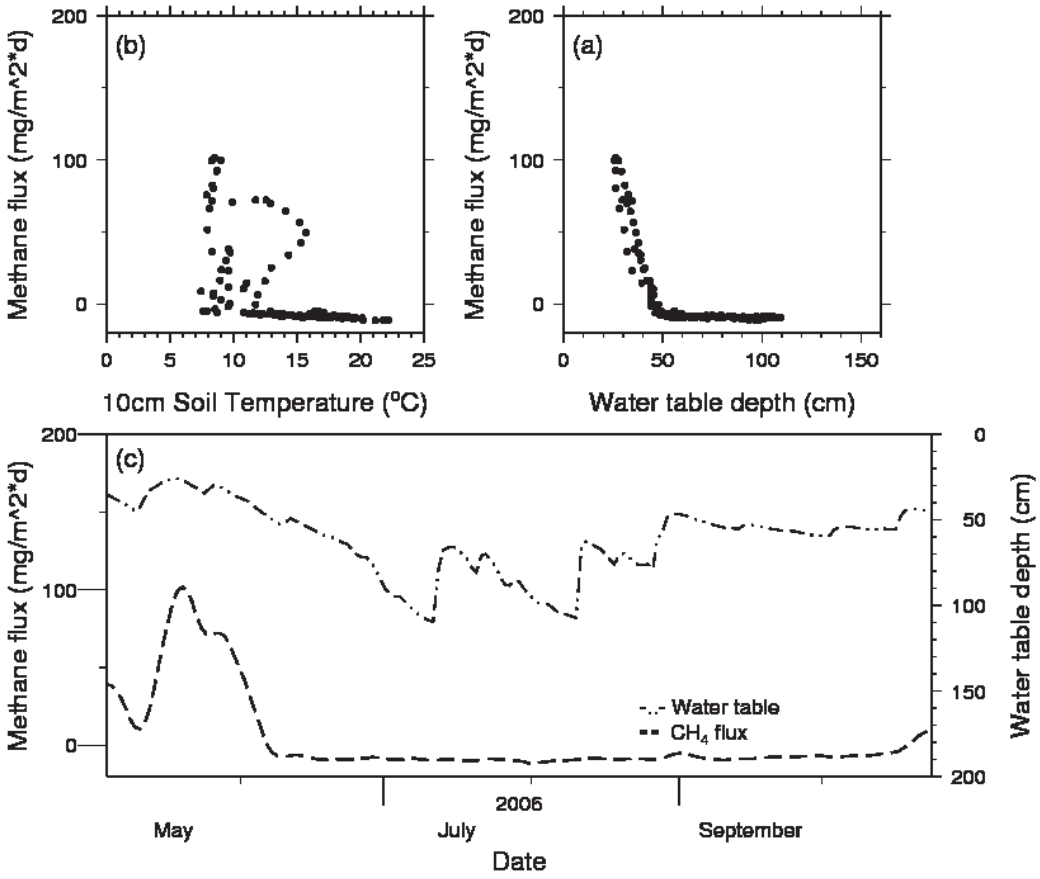

Figure 4-7: Simulated daily CH_4 emissions from the field site: a) daily CH_4 flux versus 10 cm soil temperature, b) daily CH_4 flux versus water table position and c) daily time series of observed and simulated CH_4 flux.

4.7.2. Watershed Scale

4.7.2.1. Streamflow calibration & evaluation

Daily streamflow during a portion of the calibration and validation period is shown in Figure 4-8. The daily Nash-Sutcliffe Index (NSE) for the calibration period (from 10/1/1996 to 9/30/2007) is 0.38, and 0.58 for the monthly flows. During the model validation period (10/1/1985 to 9/30/1996), the daily NSE is 0.22, and 0.34 for monthly flows. The percent bias (PBIAS) is 23.5% for calibration period and 34.2% for validation period. In general, model simulation can be judged as satisfactory if NSE >0.36 and if

PBIAS <25% for streamflow (Moriasi et al., 2007). The results show that the VIC model with drainage algorithm does a fair to satisfactory job of simulating streamflow, but underprediction of baseflow may be derived from anthropogenic influences in this mixed land use watershed and the stream network density that is altered by surface ditches.

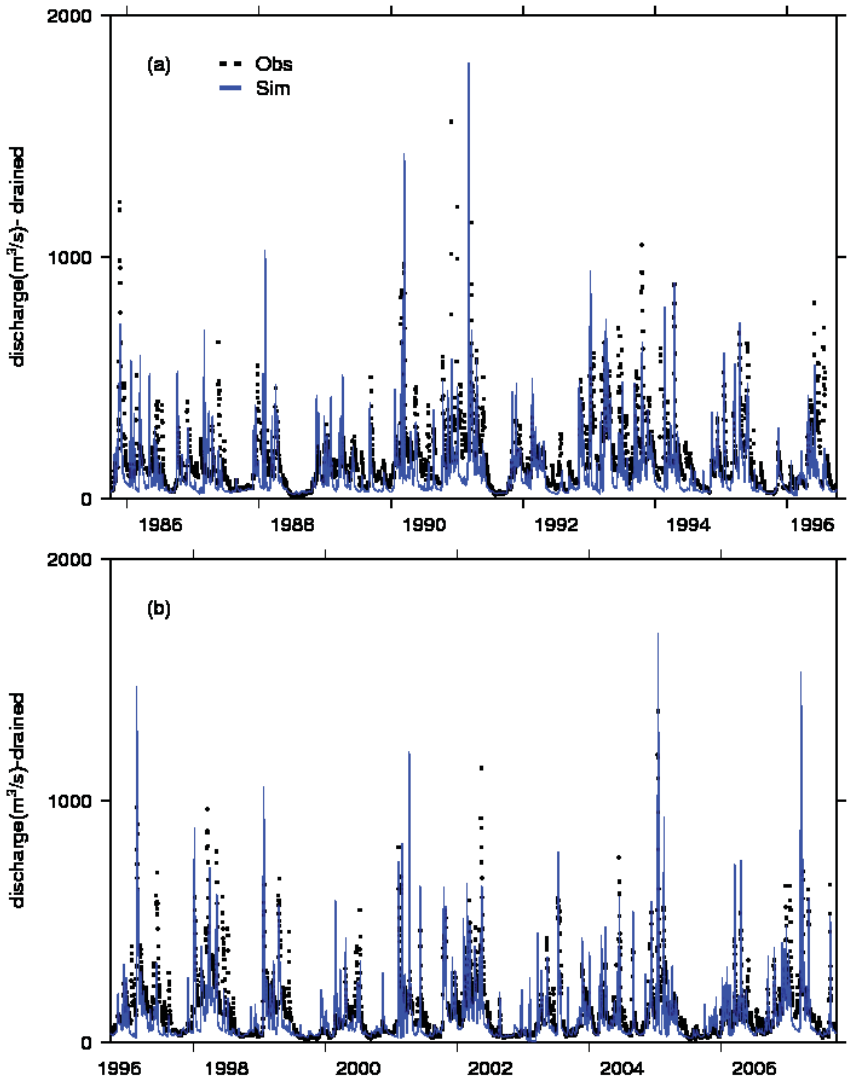

Figure 4-8: Observed and simulated streamflow for the Kankakee River above Wellington, IL for: a) the validation period (October 1985 – September 1996) and b) the calibration period (October 1996 – September 2007)

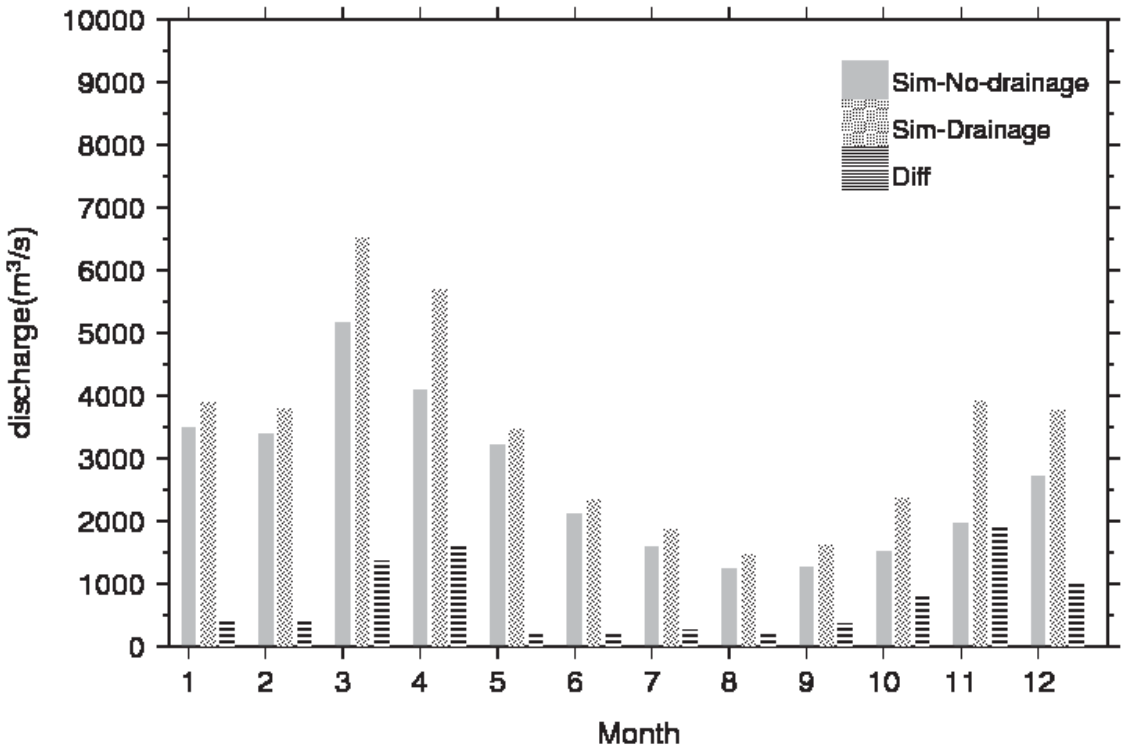

Figure 4-9: Simulated mean monthly streamflow for the Kankakee River above Wellington, IL for both Drainage and No-drainage conditions from 10/1/1985 to 9/30/2007.

4.7.2.2. Hydrologic response with/without drainage

In order to estimate the impact of agricultural drainage practices on the hydrological response and CO_2 and CH_4 emissions in this watershed, two scenarios were conducted: No-drainage (all grid cells assumed to contain no artificial drainage) and Drainage (grid cells identified as potentially-drained have a drain depth of 0.9 m and a drain spacing of 20m for the area with non-crop and a drain spacing of 10m and a depth of 1.5m for crop land. The model was calibrated for the Drainage scenario and model parameters were not adjusted for the No-drainage scenario. The daily Nash-Sutcliffe Index for the Drainage scenario is 0.38, and is 0.27 for the No-drainage scenario from 10/1/1996 to 9/30/2007. The monthly Nash-Sutcliffe Index for the Drainage scenarios is 0.59, and is 0.38 for No-

drainage scenarios. The PBIAS is 23.5% for Drainage scenarios and is 39.7% for No-drainage scenarios. The mean monthly simulated streamflow for the No-drainage and Drainage scenarios are shown in Figure 4-9. The No-drainage scenario has lower streamflow compared to the Drainage scenario in all months, especially in the winter and spring. The drainage application slightly reduces the surface runoff (range -3.5 % from -50.7%) and substantially increases the subsurface flow (including drainflow) (range 205.2 % from 897.3%) and increases streamflow (range from 31.4% to 191.5 %). In this case, the simulated lower subsurface flow contribution without drainage was not compensated by increased surface runoff because of the high water holding capacity of the muck soil throughout much of the watershed. The range of organic matter content in each grid in the watershed is from 0.2% to 26%. The grid cell with highest organic matter content tends to have lower runoff and baseflow for both Drainage and No-drainage scenarios, and lower variation (Figure 4-10). Meanwhile, the grid cell with lower organic matter content tends to have larger variation in the baseflow and runoff (Figure 4-11) with/without drainage application.

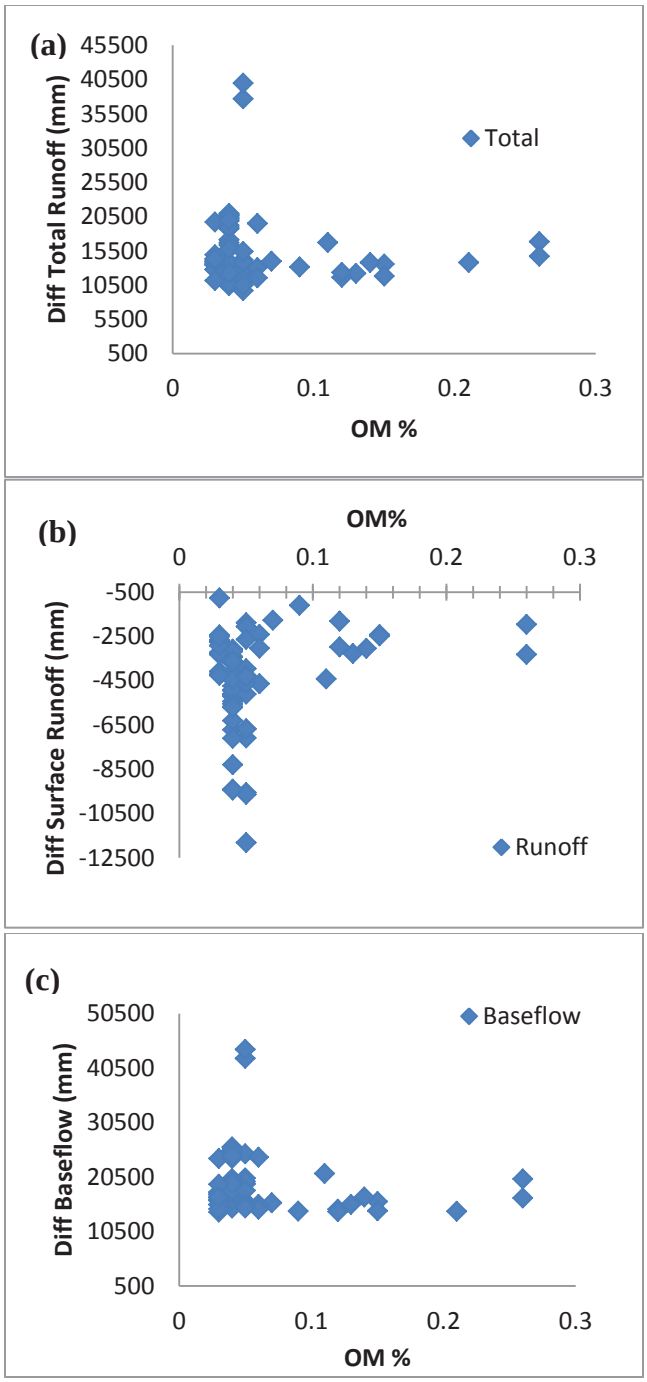

Figure 4-10. In those grid cells with poorly drained soils, a) the relationship between organic matter content and the difference of total runoff (surface runoff plus baseflow) between Drainage and No-drainage scenarios; b) the relationship between organic matter content and the difference of surface runoff between Drainage and No-drainage scenarios; and c) the relationship between organic matter content and the difference of baseflow between Drainage and No-drainage scenarios from 1915 to 2007.

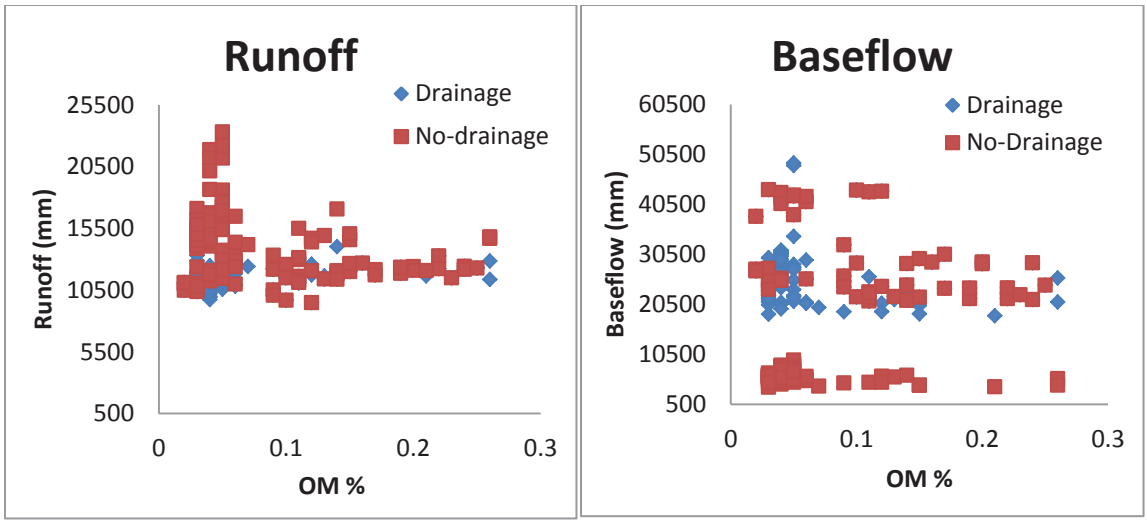

Figure 4-11. In all grid cells with poorly drained soil drainage class (Artificial Drainage) and well-drained soil drainage class (No-drainage). (left) the surface runoff vs organic matter content, (right) the baseflow vs organic matter content (those data point in orange box are those grid cell with well drained soils-meant no drainage). (Drained: Artificial Drainage; Undrained: No-drainage)

To investigate the hydrologic response and carbon dynamics with different drain spacing, the influence of drainage intensity on hydrology and carbon fluxes is explored in more detail for one representative grid cell with poorly drained soils in Figure 4-12. The results show that total moisture within the soil column and water table depth decreases with decreasing drain spacing. There is no significant difference for 20 cm soil temperature with different drain spacings, reflecting little moisture change at this depth. There is a slight difference in simulated NPP in August and September with different drain spacing. The wider spacing tends to have more NPP while having higher soil moisture, reflecting that NPP is limited in summer months when the soil moisture cannot satisfy the potential evapotranspiration needs of the crop. The carbon dioxide emission is strongly related to the amount of NPP. The methane emission decreases with decreasing drain spacing, reflecting the decline in water table. Note that some of the methane emission fluxes for

higher drainage intensities are actually negative due to the oxidation in the soil and this is the typical behavior for non-wetland soils (Nakano et al. 2004).

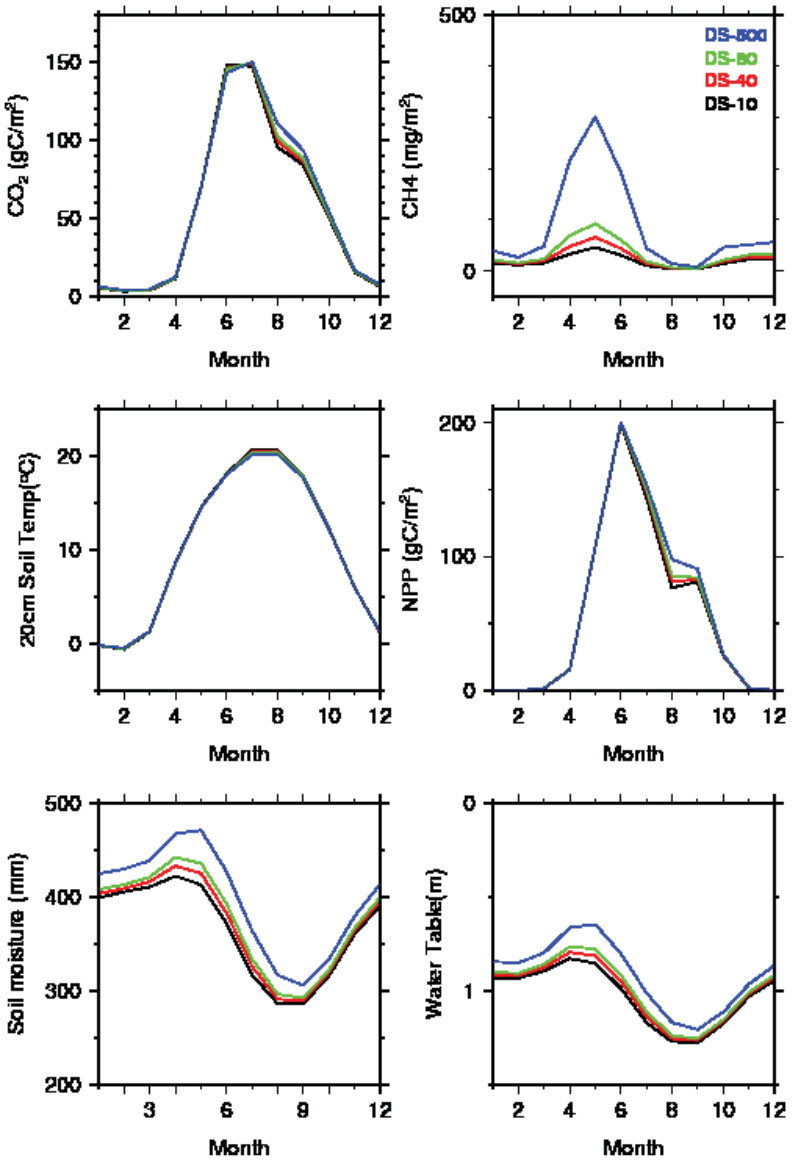

Figure 4-12: Mean monthly carbon fluxes (CO_2 and CH_4), soil temperature, NPP, total column soil moisture and water table depth for different drainage intensities for a grid cell centered at 41.5203 N, -86.1971 W with higher organic matter content from 1915 to 2007.

4.7.2.3. Evaluation of artificial drainage influence on Carbon dynamics in the Kankakee basin

To achieve the realistic initial soil carbon pools and reduce the computation time, a repeated offline spinup period from 1915 -2007 was used to find the long-term equilibrium carbon pool densities (defined by a net change in carbon pool storage of less than 0.1 g C/m^2 over this 91 year period) for the No-drainage scenario. It takes at least 1000 years to reach the equilibrium for all carbon pool storages. This equilibrium carbon pool storage was utilized as the initial carbon pool for both the No-drainage and Drainage scenarios. The carbon pools and simulated total CO_2 fluxes (total R_h fluxes) from 1915 to 2007 for both Drainage and No-drainage scenarios are shown in Figure 4-13. The No-drainage case had slightly higher litter carbon pools due to slightly higher NPP. The intermediate carbon pool depleted rapidly after drainage was "installed" at the start off the Drainage scenario. The slow carbon pool also depleted rapidly for the Drainage scenario. The No-drainage case had higher total carbon fluxes (R_h) than the Drainage case.

The total soil carbon pools for the entire Kankakee basin within 2 m was estimated to be 2,670 Tg C (2.67 Pg C) based on the SSURGO soil database (Figure 4-1). The initial simulated carbon pools for both the No-drainage scenario and Drainage scenario after spin-up was 816 Tg C/Y. The final simulated carbon pools for the No-drainage scenario are 816Tg C/Y, and for the Drainage scenario are 644 Tg C/Y. As expected, the net carbon pool loss for the No-drainage scenario was negligible, since these were the conditions used for model spin-up to equilibrium. For the Drainage scenario the net carbon pool loss was 172 Tg C/Y or 21% of the initial simulated pool.

The total accumulated simulated NPP and the CO_2 fluxes (R_h) for the Drainage scenario was 539 Tg C and 712 Tg C The total simulated NPP and CO_2 fluxes for the No-Drainage scenario was 863 Tg C and 863 Tg C from 1915 to 2007.

Figure 4-14 shows maps of the difference in average annual CO_2 (R_h) and CH_4 emissions between the No-drainage and Drainage scenarios within the Kankakee basin for the period 1915-1925 and 1995-2005. The spatial pattern reflects the pattern of the potentially drained area map, with no difference in simulated fluxes for grid cells without simulated agricultural drainage practices. Overall, annual average CO_2 fluxes (R_h) for 1995-2005 are smaller by around 100 g $C/m^2/d$ for the Drainage scenario (366 g $C/m^2/d$), reflecting the lower NPP associated with moisture stress in the summer months. These differences were larger earlier in the century. The difference in methane fluxes shows the opposite trend, with larger decreases due to drainage later in the century.

The 10 year average CO_2 emissions (R_h), total carbon pools (litter, intermediate, and slow), and methane emissions are shown in Figure 4-15. There is an increasing trend in 10 year average CO_2 emissions (R_h) for both scenarios. The 10 year average total carbon pools also increased slightly with time for the No-drainage scenario and implies there is carbon accumulation in the soil. The methane emissions for the Drainage scenario are close to zero.

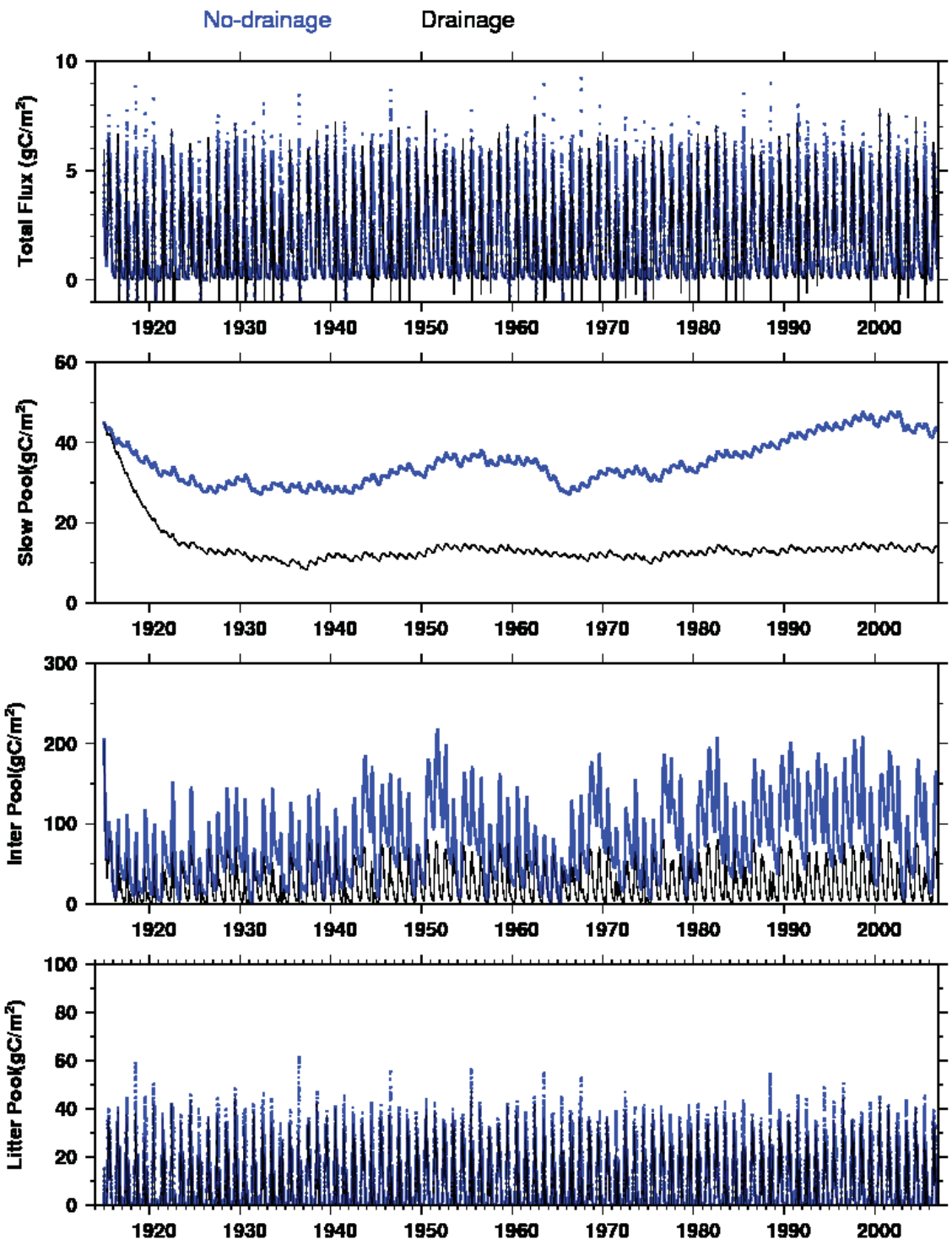

Figure 4-13: Total daily CO_2 fluxes (R_h) and Carbon pools (slow, intermediate, and litter) for a grid cell centered at 41.5203 N, -86.1971 W with higher organic matter content from 1915 to 2007.

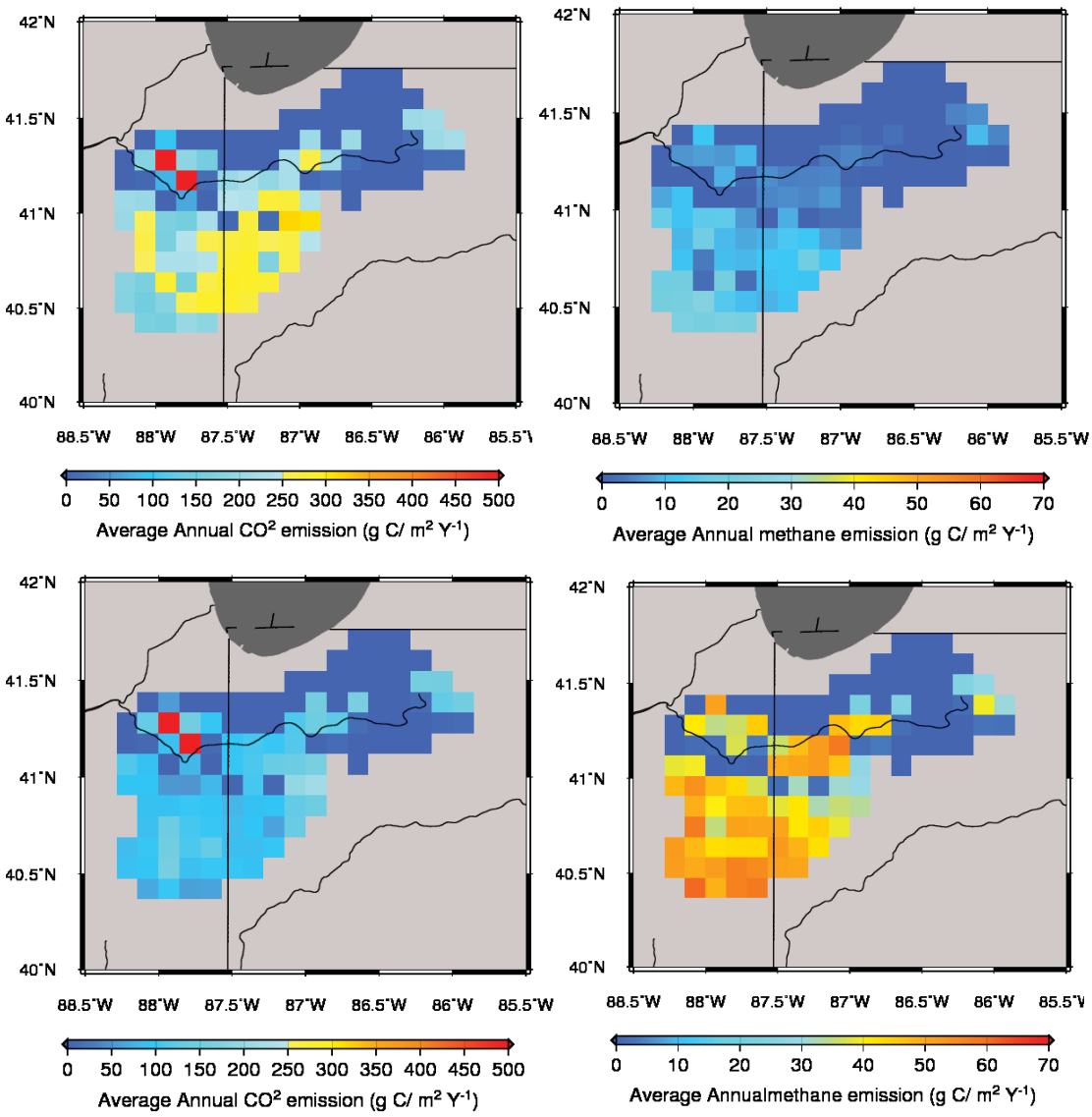

Figure 4-14: Spatial map of the difference in annual average carbon fluxes (Top:1915-1925; Bottom: 1995-2005) to the atmosphere for the No-drainage Scenario – Drainage Scenario for a) CO_2 emissions (R_h) and b) CH_4 emissions.

In the Kankakee River basin, the average annual CO_2 emissions (R_h) were estimated as 9.38 Tg C/Y for the No-drainage scenario and estimated 7.70 Tg C/Y for the Drainage scenario (Figure 4-16). The undrained grid cells on average have higher methane fluxes. The average annual CH_4 emission was estimated at 0.085 Tg C/Y for the No-drainage scenario and was estimated to be -0.03 Tg C/Y for the Drainage scenario (Figure 4-16).

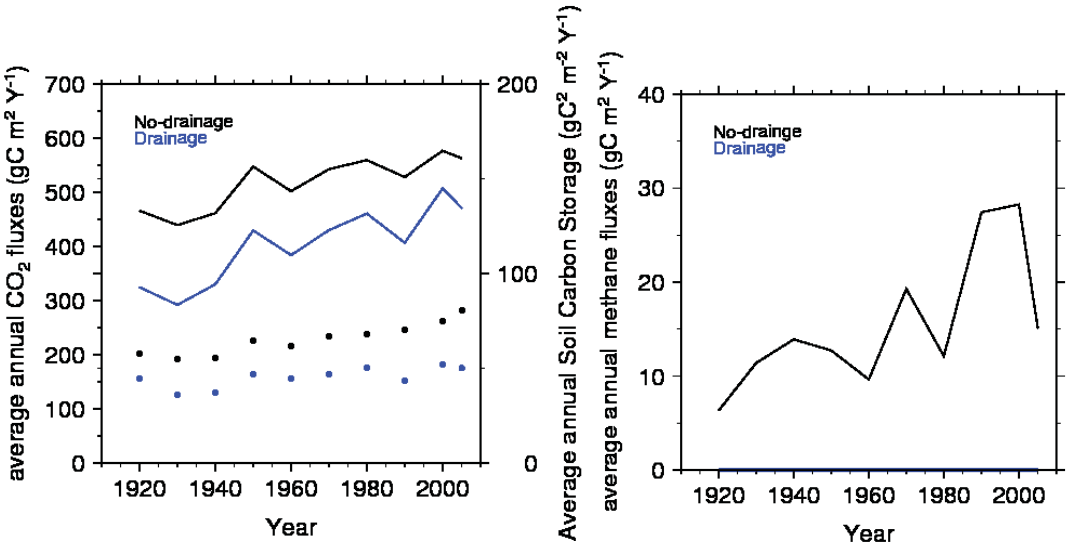

Figure 4-15. (Left) The 10 year average soil carbon pool (dot) and carbon dioxide emission (R_h) (solid line) for both scenarios; (Right) the 10 year average methane emissions for both scenarios for the whole basin.

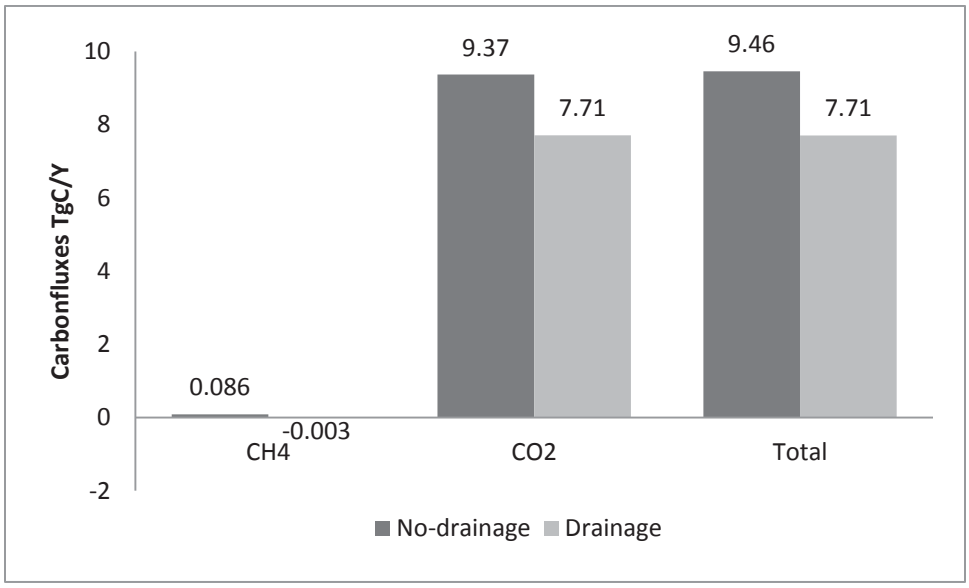

Figure 4-16: Difference in total carbon loss (average annual fluxes), drained versus undrained.

4.8 **Discussion**

Most of Indiana has been drained to increase cropland productivity since the 1800's. Based on the United State agricultural census reports, 44% of the total land area in Indiana was drained by 1930, and 48% by 1960 (USDCBC, 1932-1961). Agricultural

drainage (including open ditches and subsurface tiles) is used to lower the water table depth, improving conditions for crop growth and field access. In this paper, the VIC model was used to simulate the hydrologic response for a watershed with extensive drainage improvements. Overall, the simulations predict an increase in annual water yield with drainage, corresponding to a decrease in annual evapotranspiration and decreased soil moisture storage. Robinson and Rycroft (1999) showed the evapotranspiration slightly decreased after drainage in a clay soil and runoff significantly decreased, while subsurface flow significantly increased.

In this study, the same routing parameter file with stream network threshold of 2 km^2 was used for both Drainage and No-drainage scenarios. However, the open ditch drainage practices have increased the stream network density. Blann et al. (2009) showed that the natural channels have been straightened and deepened for surface drainage ditches with significant effects on the channel morphology, floodplain and riparian connectivity. The construction of main channel ditches through millions of acres of formerly low-lying marsh or wet prairie has resulted in the large-scale conversion from wetland mosaics to linear system. The extended stream network for drainage should be taken into account by using different stream network thresholds for streamflow routing of the Drainage scenario.

The average annual CH_4 emissions for the Drainage scenario with deeper water table depth resulted in a smaller emission flux compared to the No-drainage scenario. The methane emission range of No-drainage scenario was expected, and the simulated rates are comparable to the finding from Meng et al. (2012) who studied natural wetlands in

different locations such as Nanjing, China, Texas, US, and Japan. They observed mean fluxes around 200 mg CH_4 m^{-2} d^{-1} in Japan during the growing season.

The CO_2 emission was not expected to be higher in the No-drainage scenario than in the Drainage scenario. There are a couple of explanations for this. First, because VIC does not contain a dynamic crop-growth algorithm, there is no mechanism to reduce crop growth or water uptake under excess moisture stress conditions. Second, ET and NPP are limited under low moisture conditions. Simulated NPP is a function of actual evapotranspiration, so simulated NPP is higher for the No-drainage scenario where ET is essentially energy-limited and this higher NPP translates into higher CO_2 emissions (R_h). If the NPP were held to values simulated for the Drainage condition, the CO_2 emissions (R_h) simulated for the No-drainage scenario drop 22.17%, to a value only 0.03 % higher than the Drainage scenario. Although higher NPP in the No-drainage scenario was not what we expected in the Midwest cultivated region, Laine and Minkkinen (1996) studied natural mires with forest drainage in Finland and found that the long-term carbon accumulation rate of an undrained site was 21 g C /m^2/yr, while the drained site lost 14 g C /m^2/yr from pre-drainage carbon storage.

Even with fixed NPP values, the CO2 flux in the latter half of the century was lower for the Drainage scenario than the No-drainage scenario. As shown in Figure 4-12, the simulated carbon pool decomposes rapidly in the initial few years after drainage was 'introduced' in 1915. The intermediate carbon pool reaches a new equilibrium 5 years after the drainage simulation begins. It is not clear if the slow carbon pool reached a new equilibrium within the simulation period.

This shows that the carbon storage was substantially depleted after drainage was applied in this region. Once the carbon pools established a new, lower equilibrium, CO2 flux rates were also constrained to lower values. Hooijer et al. (2012) studied large tropical peat domes in Indonesia over 200 subsidence measurement sites and found higher carbon loss and land subsidence rates in the initial 5 years following conversion of forested tropical peatlands to other land uses by applying drainage practices. After drainage with increasing oxidation in soil, the contribution of oxidation to peat subsidence decreases over the first few years as primary consolidation and compaction diminish (Ewing and Vepraskas, 2006). The net carbon loss substantially decreases over this period as the rapidly decomposing most labile carbon compounds are consumed, leaving only recalcitrant carbon compounds. Stephens et al. (1984), investigating organic soil subsidence in the Netherlands, showed that the initial rapid shrinkage was due to desiccation or tillage or both after drainage practices were installed, and the following slow steady subsidence was mainly due to oxidation related to the amount of oxygen in the drained zone.

4.9 **Conclusions**

Addressing the hydrological aspect is critical to understanding the impact of agricultural activities in Indiana on the carbon balance and soil health. This study provides an initial assessment of the impact of intensive agricultural drainage on carbon dynamics in the Kankakee River basin, in Indiana and Illinois. The VIC model with one-way coupling to existing carbon dioxide and methane models provides a feasible modeling tool to estimate carbon emissions at the watershed scale and to better quantify the carbon loss

under agricultural drainage scenarios. Simulations of the Kankakee River basin from 1915-2007 for both a Drainage scenario (current conditions) and a No-drainage scenario with modern vegetation demonstrated the following:

- Annual streamflow increased by 32% with the introduction of drainage, particularly during the non-growing season, reflecting the overall decrease in soil moisture storage and evapotranspiration.
- Average CO_2 flux from 1915-2007 was 28.5% higher for the No-drainage scenario, largely due to the simulated increase in NPP with higher moisture conditions. Such an increase in NPP for a domestic crop may not be realistic. However, without the simulated increase in NPP, annual average CO2 flux for the No-drainage scenario is still 0.03 % higher than the Drainage scenario, due to the lower equilibrium organic matter content after years of drainage.
- Despite the lower average CO2 flux, organic matter was lost from all carbon pools very rapidly following the introduction of drainage, and reached a new equilibrium after greater than 92 years for the stable (slow) pool and 5 years for the recalcitrant (intermediate) pool. Between 1915-2007, ~21% of the initial simulated Carbon pool (816 Tg C/Y) was lost from the watershed due to oxidation for Drainage scenario, corresponding to a total potential subsidence of 42 cm for total soil depth 200 cm assuming soil density is constant.

We can conclude that these model simulations do support the high rate of subsidence previously reported for these high organic matter soils, but that most of this subsidence took place soon after the introduction of agricultural drainage. Such impacts should be quantified and considered in land use planning. Future work is needed to investigate the

potential for drainage water management or reduced periods of drainage to rebuild previously lost organic matter in these soils. Additional effort should also address the impact of excess water conditions on NPP in managed agriculture.

4.10 **References**

Blann K. L, J. L. Anderson, G. R. Sands, and B. Vondracek. 2009. Effects of Agricultural Drainage on Aquatic Ecosystems: A Review. Critical Reviews in Environmental Science and Technology, 39:909–1001, 2009 Copyright © Taylor & Francis Group,LLC. ISSN: 1064-3389 print / 1547-6537 online DOI: 10.1080/10643380801977966

Bohn, T. J., D. P. Lettenmaier, K. Sathulur, L. C. Bowling, E. Podest, K. C. McDonald, and T. Friborg (2007), Methane emissions from western Siberian wetlands: heterogeneity and sensitivity to climate change, Env. Res. Lett., 2, doi:10.1088/1748-9326/2/4/045015.

Bowling, L. C. and D. P. Lettenmaier, 2010. Modeling the effects of lakes and wetlands on the water balance of Arctic environments, Journal of Hydrometeorology, 11, 276-295.

Brooks, R. H., andf A. T. Corey. 1964. Hydraulic properties of Porous Media, *Hydrology paper 3*. Colorado State University, Fort Collins. Colo.

Cherkauer, K. A. and D. P. Lettenmaier, 1999. Hydrologic effects of frozen soils in the upper Mississippi River basin, J. Geophys. Res., 104(D16), 19,599-19,610, doi:10.1029/1999JD900337.

Cherkauer, K. A. and D. P. Lettenmaier 2003. Simulation of spatial variability in snow and frozen soil, J. Geophys. Res., 108(D22), 8858, doi:10.1029/2003JD003575.

Chiu, *C.*, L. C. Bowling, T. J. Bohn, R. H. Grant, and C. T. Johnston, 2009, Carbon dynamics in north temperate drained peatlands, AGU Fall meeting, San Francisco, CA.

Christensen, T. R., I. C. Prentice, J. Kalpan, A. Haxeltine, and S. Sitch, 1996. Methane flux from northern wetlands and tundra: An ecosystem source modeling approach, Tellus, ser. B, 48:652-661.

Christensen, T. R., A. Ekberg, L. Strom, M. Mastepanov, N. Panikov, M, Oquist, B. H. Sevenson, H. Nykanen, P. J. Martikainen, and H. Oskarsson, 2003. Factors controlling large scale variations in methane emission from wetlands. Geophys. Res. Lett., 30, 1414, doi:10.1029/2002GL016848.

Dachnowski-Stokes, A. 1933. Peat deposits in U.S.A. their characteristic profiles and classification. pp. 1–140. In K.V. Bürlow (ed.). Handbuch der Moorkunde, 7. Springer-Verlag, Berlin.

Elberling, B., Nordstrøm, C., Grøndahl, L., Søgaard, H., Friborg, T., Christensen, T.R., Ström, L., Marchand, F. and Nijs, I. 2008. High-Arctic Soil CO2 and CH4 Production Controlled by Temperature, Water , Freezing and Snow. *In Meltofte, H., Christensen, T. R., Elberling, B., Forchhammer, M.C. and Rasch, M. (eds.). High-Arctic Ecosystem Dynamics in a Changing Climate. Advances in Ecological Research 40: 441 – 472.*

Ewing, J. M. and M. J. Vepraskas, 2006 Estimating primary and sec- ondary subsidence in an organic soil 15, 20, and 30 yr after drainage, WETLANDS, 26, 119–130.

Farouki, O.T. 1981. Thermal properties of soils. CRREL Monograph. Vol. 81, no. 1, 134 pp.

Farguhar G. D., Von Caemmerer S. and J. A. Berry, 1980, A biochemical model of photosynthesis in the leaves of C3 species Planta. 149. 78-90.

Foley J. A., 1995, A equilibrium model of the terrestrial carbon budget, Tellus, 47B, 310-319.

Franzmeier, D.P, W.D. Hosteter, and R.E. Roeske, 2001, Drainage and Wet Soil Management: Drainage Recommendations for Indiana Soils.

Hooijer, A., Page, S., Jauhiainen, J., Lee, W. A., Lu, X. X., Idris, A., and Anshari, G. 2012. Subsidence and carbon loss in drained tropical peatlands, Biogeosciences, 9, 1053-1071, doi:10.5194/bg-9-1053-2012.

Houghton, J.T.; Ding, Y.; Griggs, D.J.; Noguer, M.; van der Linden, P.J.; Dai, X.; Maskell, K.; and Johnson, C.A., Climate Change 2001: The Scientific Basis, Contribution of Working Group I to the Third Assessment Report of the Intergovernmental Panel on Climate Change, Cambridge University Press, ISBN 0-521-80767-0

Laine, J., and Minkkinen, K., 1996. Effect of Forest Drainage on the Carbon Balance of a Mire: a case study. Scand. J. For. Res. 11:307-312.

Johansen.O., 1975. Thermal conductivity of soils Ph.D. thesis, CRREL Draft Transl. 637, 1977, Trondheim, Norway.

Johnston, C. T., R. Grant and L. C. Bowling. 2006. Influence of Water Management on Carbon Exchanges over Organic Soils.ASA-CSSA-SSSA International Meeting Indianapolis, IN, November 13, S11, Abstract 125-4.

Jongedyk, H.A., Hickok, R.B., Mayer, I.D. and N.K. Ellis, 1950. Subsidence of muck soils in northern Indiana. Purdue Univ. Agric., Exp. Sta., Spec. Circ., 366:1-10.

Lawrence, D.M. and A.G. Slater, 2008: Incorporating organic soil into a global climate model.Clim. Dyn., 30, doi:10.1007/s00382-007-0278-1.

Liang, X., D. P. Lettenmaier, E. F. Wood, and S. J. Burges, 1994. A Simple hydrologically Based Model of Land Surface Water and Energy Fluxes for GSMs, J. Geophys. Res., 99(D7), 14, 415-14, 428

Liang, X., E. F. Wood, and D. P. Lettenmaier, 1999. Modeling ground heat flux in land surface parameterization schemes, J. Geophys. Res., 104(D8), 9581-9600.

Lloyd, J. and J. A. Taylor, 1994. On the temperature dependence of soil respiration. Functional Ecology, 8, 315-323.

Lohmann, D., R. Nolte-Holube, and E. Raschke, 1996: A large-scale horizontal routing model to be coupled to land surface parametrization schemes, *Tellus*, 48(A), 708-721.

Lohmann, D., E. Raschke, B. Nijssen and D. P. Lettenmaier, 1998: Regional scale hydrology: I. Formulation of the VIC-2L model coupled to a routing model, *Hydrol. Sci. J.*, 43(1), 131-141.

Knorr, W., 1997. Satellite Remote Sensing and Modelling of the Global CO2 Exchange of Land Vegetation: A Synthesis Study. Ph.D. Thesis. Max-Planck-Institut für Meteorologie, Hamburg.

Matthews, E., and I. Fung, 1987. Methane emission from natural wetland: global distribution, area, and environmental characteristics of sources. Glob. Biogeochem. Cycle, 1:61-86.

Meentemeyer, V. 1978. Macroclimate and lignin control of litter decomposition rates. Ecology, 59, 465-472.

Maurer, E. P., A. W. Wood, J. C. Adam, D. P. Lettenmaier, and B. Nijssen, 2002. A long-term hydrologically based dataset of land surface fluxes and states for the conterminous United States. J. Climate, 15, 3237–3251.

Miller, D.A. and R.A. White, 1998. A Conterminous United States Multi-Layer Soil Characteristics Data Set for Regional Climate and Hydrology Modeling. *Earth Interactions*, 2. [Available on-line at http://EarthInteractions.org]

Moriasi, D. N., J.G. Arnold, M. W. Van Liew, R. L. Bingner, R. D. Harmel, T. L. Veith, 2007, Model evaluation guidelines for systematic quantification of Accuracy in watershed simulations. Transactions of ASABE. Vol 50-3. pp. 885-900.

Nakano, T., G. Inoue and M. Fukuda, 2004, Methane consumption and soil respiration by a birch forest soil in West Siberia, Tellus, B, 56, 223-9.

Raich, J.W. and Potter C.S. 1995. Global patterns of carbon dioxide emissions from soils. Global Biogeochem. Cycles, 9, 23-36.

Robinson, M. & Rycroft, D.W. (1999). The impact of drainage on streamflow. Chap 23 In: Skaggs R.W. and J. van Schilfgaarde (eds.) *Agricultural Drainage*. Agronomy Monograph No 38. American Society of Agronomy / Crop science Society of America / Soil Science Society of America. Madison, Wisconsin, USA. pp 767-800. Library of Congress Catalogue Number 99-073092.

Rutkowski, S. M., 2012. Role of climate variability on subsurface drainage and streamflow patterns in agricultural watersheds, Master of Science in Engineering Thesis, Purdue University.

Sathulur, K., 2008. The spatial distribution of water table position in northern Eurasian wetlands using the Variable Infiltration Capacity Model, Master of Science in Engineering Thesis, Purdue University.

Schelze, E. D. 2006. Biological control of the terrestrial carbon sink. Biogeosciences, 3, 147-166.

Sitch S., B. Smith, I. C. Prentice, A. Arneth, A. Bondeau, W. Cramer, J.O. Kaplan, S. Levis, W. Luch, M. T. Sykes, K. Thonicke, and Venevsky S., 2003. Evaluation of ecosystem dynamics, plant geography and terrestrial carbon cycling in the LPJ dynamic global vegetation model .Global Change Biology, 9, 161-185.

Smith, P., J. Brenner, K. Paustian, G. Bluhm, J. Cipra, M. Easter, E. T. Elliott, K. Killian, D. Lamm, J.Schuler, and Williams, S., 2002. Quantifying the change in greenhouse gas emissions due to natural resource conservation practice application in Indiana. Final report to the Indiana Conservation Partnership. Colorado State University Natural Resource Ecology Laboratory and USDA Natural Resources Conservation Service, Fort Collins, CO, USA

Soil Survey Staff, Natural Resources Conservation Service, United States Department of Agriculture. Soil Survey Geographic (SSURGO) Database for Indiana, Illinois, and Ohio. Available online at http://soildatamart.nrcs.usda.gov.

Walter, B.P., and M. Heimann, 2000: A process-based, climate-sensitive model to derive methane emissions from natural wetlands: Application to five wetland sites, sensitivity to model parameters, and climate. *Global Biogeochem. Cycles*, 14, 745-76, doi:10.1029/1999GB001204.

Wilen, B. O., and W. E. Frayer, 1990, Status and trends of U.S. wetlands and deepwater habitats. Forest Ecology and Management, Volumes 33-34, P. 181-192.

Wilson, J. S. and G. H. Lindsey, 2005, Socioeconomic correlates and environmental impacts of urban development in a central Indiana landscape. Journal of Urban Planning and Development-Asce, 131,159-169.

Yang G., L.C. Bowling, K. A. Cherkauer, B. C. Pijanowski, and D. Niyogi (2010), Hydroclimatic Response of Watersheds to Urban Intensity- An Observational and Modeling Based Analysis for the White River Basin, Indiana, J. Hydrometeorology, 11(1), 122-138.

Yang, G., L. C. Bowling; K. A Cherkauer, and B. C Pijanowski (2011), The impact of urban development on hydrologic regime from catchment to basin scales, Landscape and Urban Planning, doi: 10.1016/j.landurbplan.2011.08.003.

Yapo, P., H. Gupta, and S. Sorooshian, 1998: Multi-objective global optimization for hydrologic models, *J. Hydrology*, 204(1), 83-97.

Zhuang, Q., J. M. Melillo, D. W. Wicklighter, R. G. Prinn, A. D. McGuire, P. A. Steudler, B. S. Felzer, and S. Hu, 2004. Methane fluxes between terrestrial ecosystems and the atmosphere at northern high latitudes during the past century: A retrospective analysis with a process-based biogeochemistry model. Global Biogeochem. Cycles. 18, GB3010, doi:10.1029/2004GB002239.

Zhuang, Q., J. M. Melillo, M.C. Sarofim, D. W. kicklighter, A. D. McGurie, B. S. Felzer, A. Sokolove, R. G. Prinn, P. A. Steudler and S. Hu, 2006. CO_2 and CH_4 exchanges between land ecosystems and the atmosphere in northern high latitudes over the 21st century. Geophys. Res. Lett. 33, L17403, doi:10.1029/2006GL026972.

5. THE IMPACT OF SURFACE AND SUBSURFACR DRAINAGE IN THE HYDROLOGIC REGIME OF THE NORTHERN WABASH RIVER

5.1 Abstract

Wetlands are hydrologically dynamic systems which have the potential to improve water quality, reduce the risk of flood, and provide habitat for wildlife. Unfortunately, many of the wetlands in the North Central United States have been lost or degraded due to human impacts primarily associated with agriculture and urban or suburban development over the past several decades. Agricultural drainage practices such as surface ditches or subsurface tiles are used to lower the water table depth, reduce the degree of water saturation and increase the crop yield in cultivated areas. The rate of water movement away from the critical zone is increased and further alters streamflow and decreases the duration of soil saturation across wide areas. In this study, the Variable Infiltration Capacity (VIC) hydrology model is used to quantify the combined affects of surface and subsurface drainage in a region with large surface storage capacity in terms of depressional wetlands. The results show that temporary surface storage in wetlands reduces streamflow flashiness by 11% and peak flows by 4% relative to the simulations with no wetlands. Low flows and flow distribution were reduced by 3% and increased by 1%, respectively. Subsurface drainage increased peak streamflow by 4% and flashiness by 1% and reduced flow distribution by 3%. .

5.2 **Introduction**

Most of the land located in the US Midwest region was occupied with prairies and wetlands in the 1800's due to lower permeable soils – a reminder of prehistoric glacier activity. Since European settlement in this region, agricultural drainage practices, such as surface drainage (open ditches), and subsurface tile drainage (tile drains), have been intensively applied. By increasing the speed of water moving out of and off of the soil, these practices lower the water table position and alter streamflow timing. According to data compiled by the USGS (2010; NHDPlus), most of Indiana has been drained over 25% and some areas of northern Indiana have been drained more than 75%. Dahl (1990) showed that 87% of total original wetlands were lost by 1980.

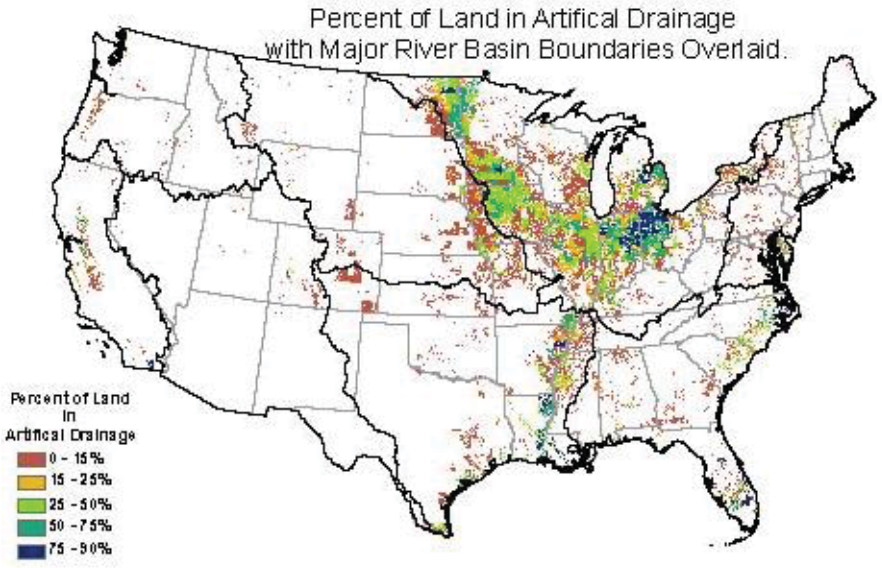

Figure 5-1: Attributes for NHDPlus Catchments (Version 1.1) in the Conterminous United States: Artificial Drainage (1992) and Irrigation Types (1997) U. S. Geological Survey (2010).

Kumar et al. (2009) analyzed 31 USGS gauging stations in Indiana having more than 50 years or more continuous unregulated streamflow records and showed there is an increasing trend in low and medium flow conditions across Indiana. The northern region

also showed increasing trends in high flow conditions. They suggested that the subsurface tile drains may play a role in the streamflow trends and that further investigation involving hydrologic simulation that considers soil moisture condition, slope, drainage space, and agricultural practices was warranted. In contrast, Rutkowski (2012) demonstrated that the trends in low flows could be reproduced using a hydrology model with fixed drainage extent, suggesting a climate origin. It is generally agreed that extensions to the surface drainage network through dredging, straightening and ditch excavation generally decrease lag time and increases runoff response and peak flows downstream. Bailey and Bree (1981) reported that surface ditch enhancements in S. Ireland decreased lag time and increased flood peaks by 60% for the three-year flood.

The influence of subsurface drainage on peak streamflow and timing is somewhat more debated. The subsurface tile drains provide more temporary storage in the poorly drained soil by constant/gradually removing extra water from the soil profile between rain events, providing a buffer zone between rainfall and streamflow response (Figure 5-2 a&b). The relative speed of transport through the tile drains can mean the difference between peak flow increases and decreases (Robinson, 1990). The function of wetlands provides temporary extra surface water storage which reduces runoff during storm events, and decreases baseflow to streams by making more open water available for evapotranspiration and discharge to the surrounding soil (Novitzki, 1978) (Figure 5-2 c). We hypothesize that when tile drains are installed into areas of historic wetlands, this wetland surface storage cannot be utilized as effectively. The magnitude of peak flow is increased due to faster water movement even with increased soil storage, the lag time between a storm event and peak flow is increased relative to the undrained case.

The Variable Infiltration Capacity (VIC) model has experienced intensive development to improve representation of wetland hydrology, including a lake and wetland algorithm (Bowling and Lettenmaier, 2010), a surface/subsurface water exchange algorithm (Chiu et al., in prep) and a subsurface drainage algorithm (Chiu and Rutkowski, In preparation; Rutkowski, 2012). This study utilized this modified VIC model to simulate streamflow response of drained wetlands in the northern Wabash River, IN. The intensive drainage system in the northern Wabash watersheds has increased available soil pore space, decreased surface water storage, and increased subsurface flow, and reduced wetland and lake extent. The objective of this study is to evaluate the role of anthropogenic modifications to drainage conditions on streamflow variability in the northern Wabash River basin. The historic impact of surface and subsurface drainage networks will be addressed through digital mapping of tile drainage extent, analysis of observed streamflow and hydrologic simulation of the watershed using two drainage networks: natural (pre-settlement), and modern which includes surface drainage ditches.

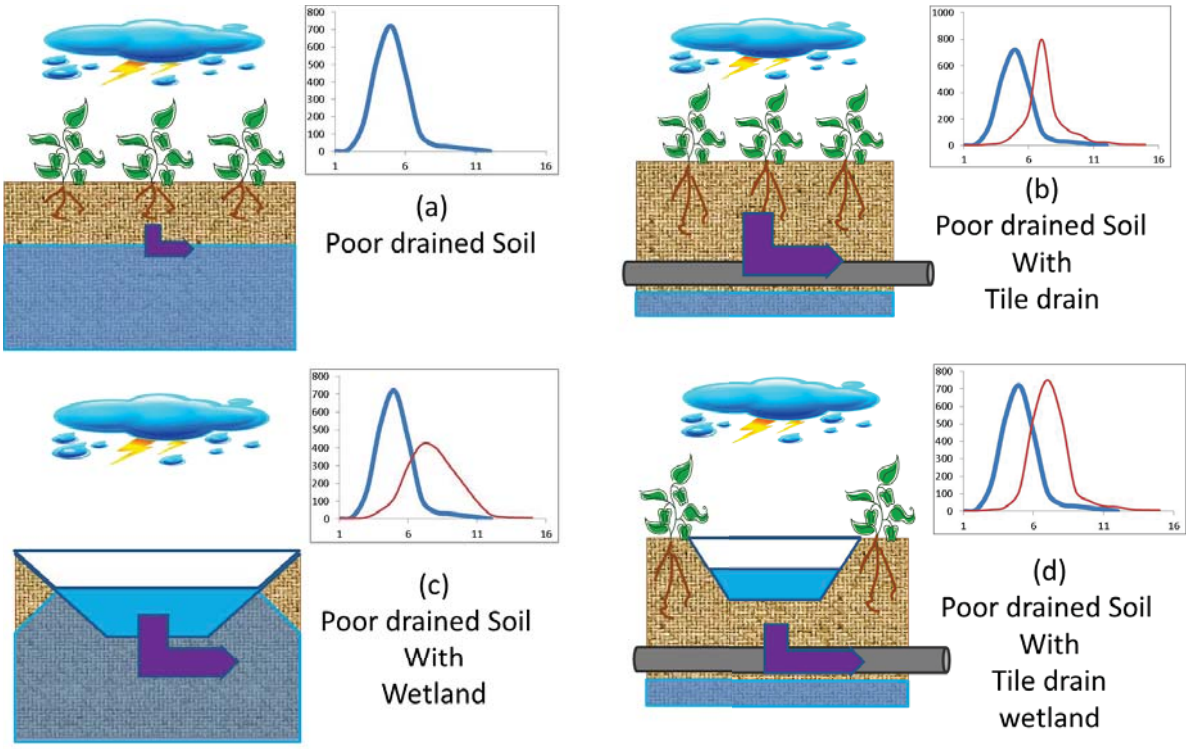

Figure 5-2. Illustration of hypothesis regarding tile-drained and wetland hydrology, showing water table position and streamflow response for: (a) poorly drained soil; rainfall events generate an immediate and large runoff response from saturated soils, (b) poorly drained soil with tile drainage application,, (c) poorly drained soil with a depressional wetland providing surface water storage and (d) poorly drained soil with tile drain and wetland storage.

5.3 **Study Site Description**

The Wabash River watershed is the largest watershed in Indiana (Figure 5-3). Here we focus on the Wabash above Vincennes, IN, upstream of the confluence with the White River (which is influenced by urban land use, as well as karst geology). The soils of the Upper Wabash mostly formed from Wisconsinan glacial till, glacial outwash, and recently deposited alluvium, resulting in a very low-gradient, poorly drained landscape subject to seasonal frost. Agriculture is the predominant land use in the upper Wabash River Basin. The land use of the Wabash River basin began to significantly change from mixed woodland (and some prairie) dominated by small lakes and wetlands to agriculture

in the mid-1800s. Most wetland areas were drained to facilitate better crop production and make them suitable for living.

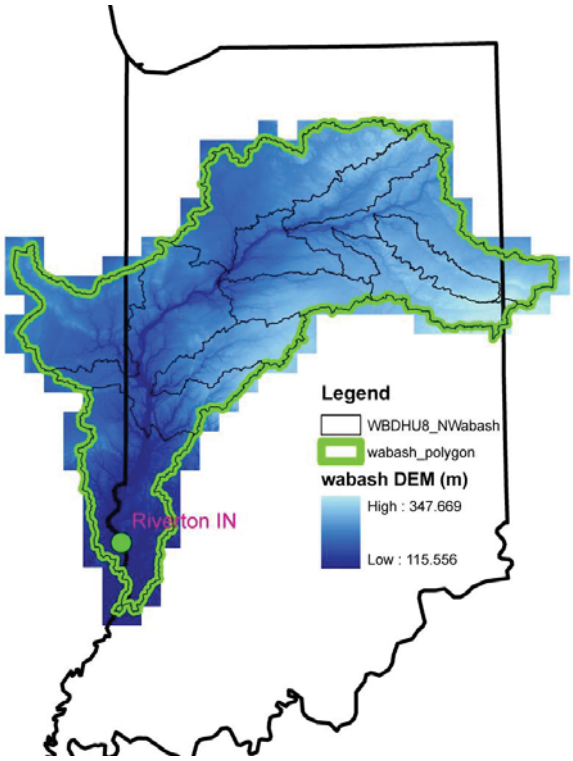

Figure 5-3. The watershed boundary of northern Wabash River basin (Green) and the three USGS gage stations at Riverton, IN.

Wilen and Frayer (1990) demonstrated that the massive losses of wetlands in the conterminous United States from the 1950's to 1970's were primarily due to human activities. Agricultural development was responsible for 87% of wetland losses and 90% of the losses of forested wetlands. Urban and other development caused only 8% and 5% of the losses, respectively. Forested-wetland losses caused by urban development and other industrial development were 6% and 4%, respectively. Agricultural drainage (such as ditches and subsurface tile) is mainly used to lower water table depth, and increase the rate of water movement flowing away from the land. Loss of wetlands can result in

changes in flood timing and an increase in the magnitude and likelihood of severe and costly flood damage occurring in low-lying areas of a basin.

The historical record of daily streamflow at Memorial Bridge at Vincennes, IN only has a few years of data, starting in January 2009. A previous gauging station at Vincennes, a short distance upstream with a drainage area of 35,498 km^2, was in operation from 1929-2004. Because of the gap in data record that was not identified until after the model was set-up, the historical record of daily streamflow from the Wabash River at Riverton, IN was used. This data is available from October 1, 1938 through the present day (USGS Gage: 03342000). The drainage area is 34,086 km^2. Model simulations were rescaled by the ratio of the drainage areas to account for this discrepancy in model simulated area. A 59 year time period (10/1/1948-9/30/2007) will be used for this study, which utilizes the majority of the available measured streamflow and extends through the end of available meteorological data for the model simulations (9/30/2007). Nine years of streamflow data from 10/1/1998 to 9/30/2007 was used to calibrate the VIC model, while observed streamflow data from 10/1/1988 to 9/30/1998 was used for model evaluation. The streamflow data from the last 18 years is used for this process because the model set-up was intended to capture current conditions, including the current extent of drained agricultural land.

5.4 **Methodology**

As described above, the VIC model was evaluated for current conditions, before being used to explore the influence of wetland storage and drainage practices on streamflow hydrology. Therefore, the VIC model with the subsurface drainage algorithm and

wetland algorithm with subsurface exchange were both activated. Detailed descriptions of these algorithms can be found in Chapter 2. Subsequently the model was run for the full 59 year record with different scenario options, as described in Section 5.4.5.

5.4.1. Model input files

The surface meteorological data includes observed daily precipitation, daily minimum and maximum temperature, and wind speed for 1/1/1915-12/31/2007 gridded to 12 km spatial resolution by Yang et al. (2010). The temperature and precipitation was derived from National Climatic Data Center (NCDC) summary of the day observations. Daily average wind speed data was obtained from the National Center for Environmental Prediction – National Center for Atmospheric Research (NCEP-NCAR) reanalysis fields (Yang et al., 2010; Kalnay et eal., 1996). Unfortunately, this observed meteorological dataset did not cover the Ohio portion of the northern Wabash River basin. An additional dataset created by Sinha et al. (2010), based on the same station observations was used to cover those Ohio areas by using the closest grid cell's data. This data is at 1/8 degree resolution (latitude/longitude) including daily precipitation, daily minimum and maximum air temperature, and daily wind speed from 1/1/1915 to 12/31/2007 (Figure 5-4).

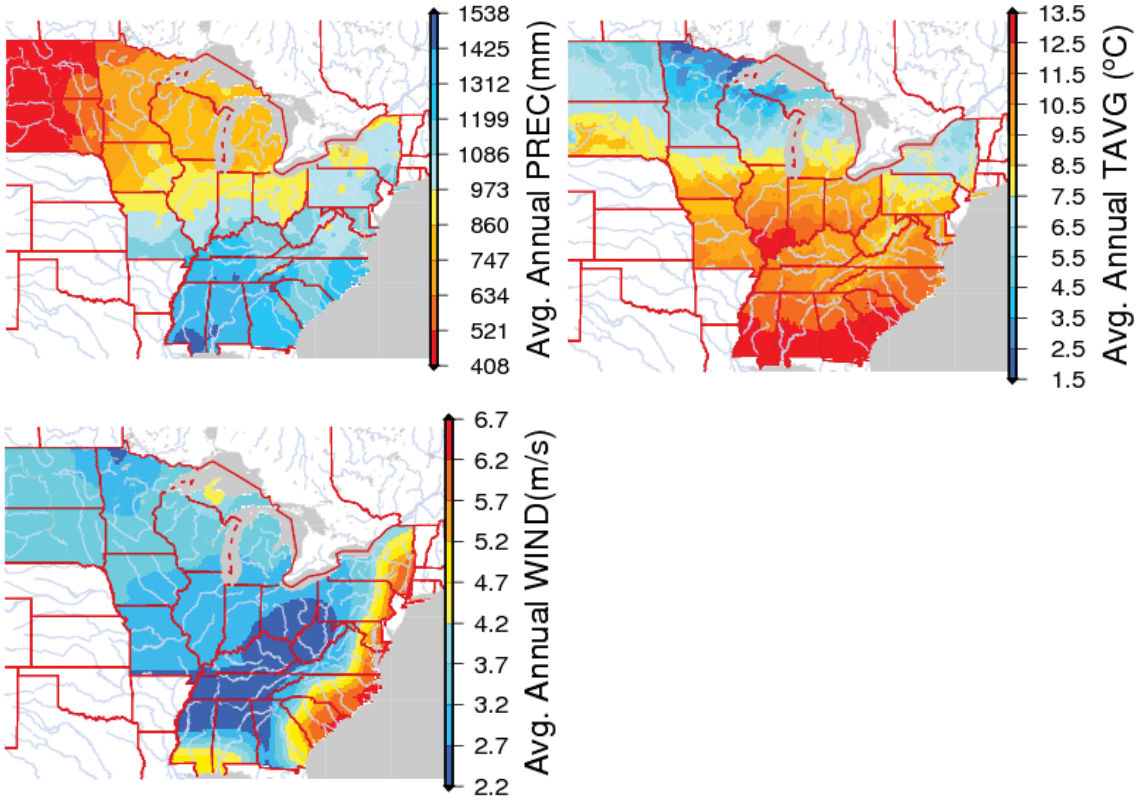

Figure 5-4. Map of average annual precipitation, average annual daily air temperature, and average annual wind speed for the Midwest and eastern coast (Sinha et al., 2010).

The VIC model requires several soil physical parameters describing the soil water characteristics, bulk density and conductivity for the majority soil type of each model grid cell. The 12 km resolution soil parameter file compiled by Yang et al. (2010) based on the CONUS gridded STATSGO data (Miller and White 1998) was clipped to the northern Wabash River basin to use, and the missing Ohio portion was filled using data from nearby grid cells based on the soil drainage class (Figure 5-5.c).

Some of the parameters were altered from the Yang et al. (2010) dataset. The depths for each soil layer were set 0.1, 0.3 and 1.6 m and the baseflow parameters were held constant at Ds = 0.001 and Ws = 0.99. In order to have better representation of soil water

characteristics and improve representation of spatial variability of empirical parameters in this watershed, the following parameter estimates were also changed:

- Soil water characteristics: For consistency, water content at the critical point (Wcr; 70% of field capacity) and wilting point (Wpwp) are calculated from the Brooks-Corey equation (Rawls et al., 1993). The pore-size distribution (λ) is calculated from the Brooks-Corey exponent in the Yang et al. (2010) data. Bubbling pressure and residual moisture content were determined using a look-up table based on soil texture (Rawls et al., 1993).

- Empirical parameters: The infiltration parameter, b_i and maximum baseflow rate, Dsmax, are typically calibration parameters for the VIC model and were held constant for all model grid cells by Yang et al. (2010). In order to increase the representation of spatial variability, these parameters were estimated as a function of soil conductivity (K_s), as follows:

$$b_i = \square 4.55 e^{\square 5} K_s + 0.419 \quad (\mathbf{5\text{-}1})$$

$$Ds_{\max} = K_s \tan \square d_b / a \quad (\mathbf{5\text{-}2})$$

Where tan β is the average land surface slope (0.05) and a is the average drainage area per unit contour length for an agricultural field (365). The final parameter distributions are shown in Figure 5-5.

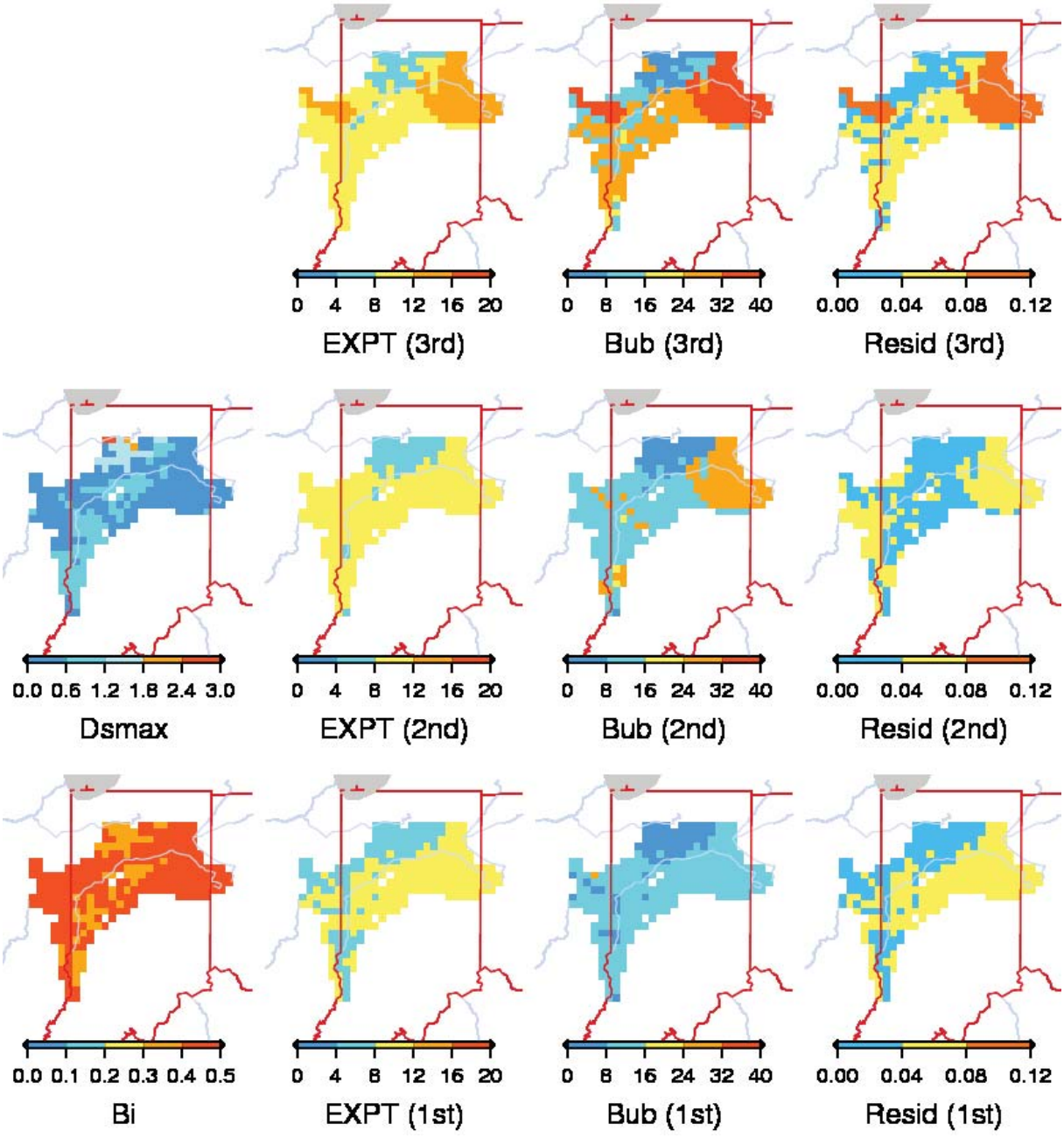

Figure 5-5. Spatial variation of the input soil parameters map showing the infiltration parameter-b_i (no unit), maximum baseflow rate-Dsmax (mm/day), and Brooks-Corey exponent (EXPT) (no unit), bubbling pressure (BUB) (cm), and residual moisture content (Resid) (fraction) for each soil layer in the northern Wabash River Basin.

The VIC model allows specification of multiple land use fractions for each grid cell. In the new VIC drainage algorithm, drain spacing and depth are specified for each

vegetation fraction (with a drain depth of 0 m indicating no drainage). Land use fractions were determined based on the Wilson (1993) land cover dataset for Indiana, with fractional coverage for 12 km grid cells as determined by Yang et al. (2010). The Yang et al. (2010) vegetation fractions were used as the base to create a new vegetation parameter file with two drainage variables (drain spacing and drain depth). The current extent of potentially subsurface drained land in the northern Wabash River basin was determined using the decision tree analysis developed by Naz and Bowling (2009), based on terrain slope and soil drainage classes from the higher resolution SSURGO database and land use maps (Figure 5-6). The National Agricultural Statistics Service (NASS) land use map has a resolution of 56 m. For consistency, the DEM (10 m resolution) and soil drain class (shape file converted to raster) were resampled to 56 m.

First, the fraction of crop area for each grid cell was extracted from the Yang et al. (2010) vegetation file. Second, the fraction of drained area for each grid cell was calculated from the potentially drained area map (Figure 5-6(d)). It is assumed that all of the drained area fraction should be crop land; the non-crop is assumed to be undrained. The remaining fraction of crop land is not drained. So for example, for a grid cell where the majority of area is crop (80%) and 20 % is woodland; if 60% is drained and 40% undrained it will have three vegetation types:

- 20% woodland vegetation with no drainage (spacing: 0 m and depth: 0 m)
- 20% crop with no drainage (spacing: 0 m and depth: 0 m)
- 60% crop with drainage (spacing: 18 m and depth: 1 m)

All drained area is assigned a mean drain spacing of 18 m and drain depth of 1 m, decided by the criteria of Indiana Drainage Guide (Franzmeier et al., 2001), used in IN state's extension recommendation.

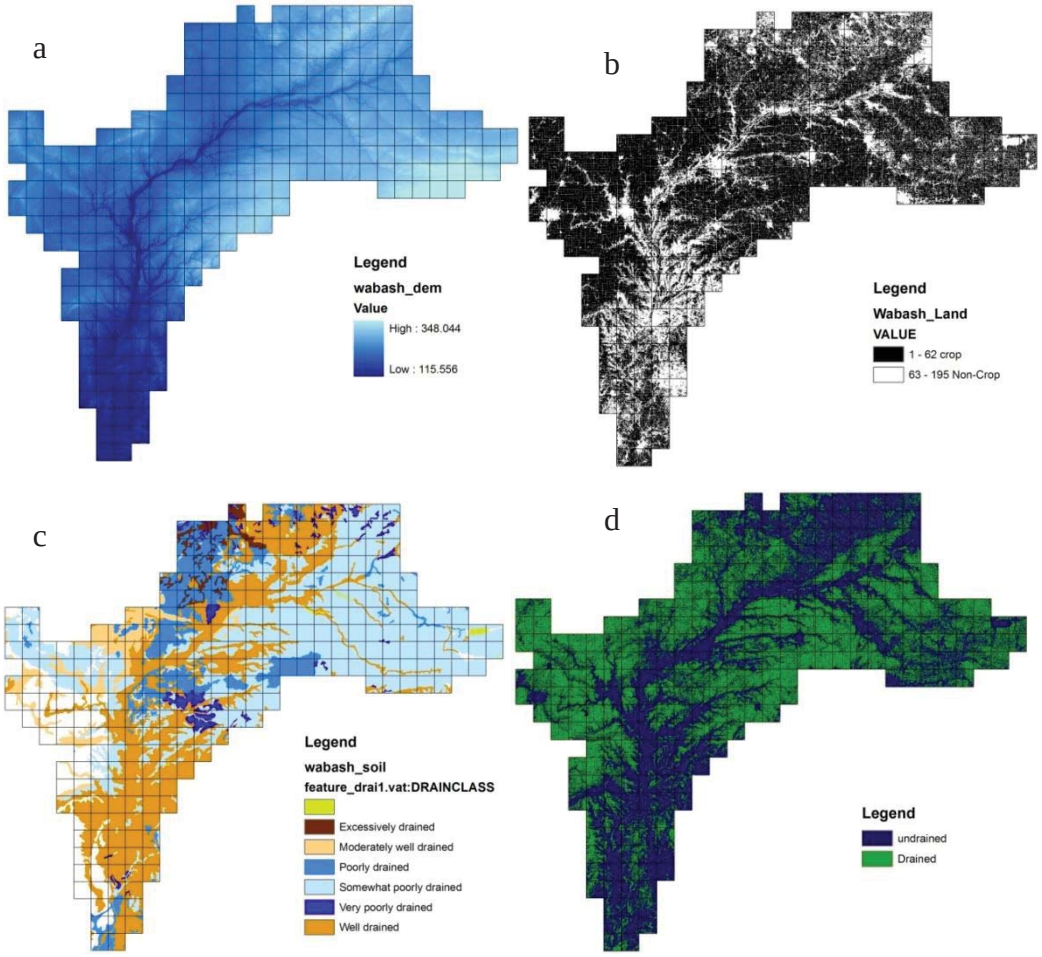

Figure 5-6. Spatial data layers (at 56 m resolution) used to define subsurface drainage inputs to the VIC mdoel for the northern Wabash River basin (a) DEM; (b) Land Use Map (NASS); (c) Soil drain class (SSURGO); and (d) Potentially drained area map.

5.4.2. Lake Parameterization

Lake/wetland parameters describe the variation in surface water extent with depth, as well as the slope and topographic index of each node, as described in Chapter 2. These

are generated based on two inputs of DEM and wetland vegetation class map, to specify wetland location. In this case, the mask for wetland vegetation class locations in the northern Wabash river basin was determined using the soil drainage class map (Figure 5-5(c)) and depressional areas (sinks) from the DEM. The wetland extent mask file is generated by assuming that wetlands exist in depressions underlain by poorly or very poorly drained soil class.

5.4.3. Routing model parameter

Yang et al. (2011) developed a GIS-based routing model that preserves the spatially distributed travel time information in a finer-resolution flow network than the VIC model grid cell size. By using a finer resolution DEM to generate a stream network the cell response functions (CRFs) can be derived for each VIC model grid cells as their unit hydrograph. Streamflow is calculated by convolution integral of the runoff for all VIC cells with their CRFs. This GIS-based unit hydrograph approach makes the model more responsive to drainage network enhancement.

The historic impact of surface drainage networks will be addressed using two drainage networks for streamflow routing: natural (pre-settlement), and modern, which includes extension of the streamflow network by surface ditches (and in some cases subsurface tile mains). These two routing model parameter files (natural and modern) were set-up by using different contributing area thresholds to generate the stream network in ArcGIS.

It is not always clear which of the existing streams and ditches in the State are natural streams that have been dredged and straightened, versus artificial ditches that were constructed. In order to have an idea of the natural (pre-drainage) stream network extent,

the estimated stream network from watershed delineation, National Hydrography Dataset (NHD) and Tippecanoe Drainage Map were compared. As shown in Figure 5-7, both the NHD and Tippecanoe Drainage Map make some distinction between ‘natural waterways’ and ‘regulated’ or ‘maintained’ ditches. Based on visual comparison for the natural waterway extent (Figures 5-7; 5-8) and drainage density comparison for a portion of western Tippecanoe County from the NHD database (for current condition) (Figure 5-9 and Table 5-1), the contributing area threshold for stream generation was set to 400 grid cells (4 km^2) for the historical condition, and 100 grid cells (1 km^2) for the current condition. The DEM resolution was 100 m.

Table 5-1. Summary of the stream drainage density in western Tippecanoe County (with an area of 1533.91 km^2) with different stream threshold and NHD database.

No. Cells of threshold	Contributing Length (km)	Drainage Density (km/km^2)
NHD	1269.6	0.83
50	1707.4	1.11
100	1238.2	0.81
200	892.8	0.58
300	737.5	0.48
400	650.8	0.42

Note: The NHD have stream & ditch overlay and only visual comparison of the ‘stream’ extent were used to determine the threshold for historical condition

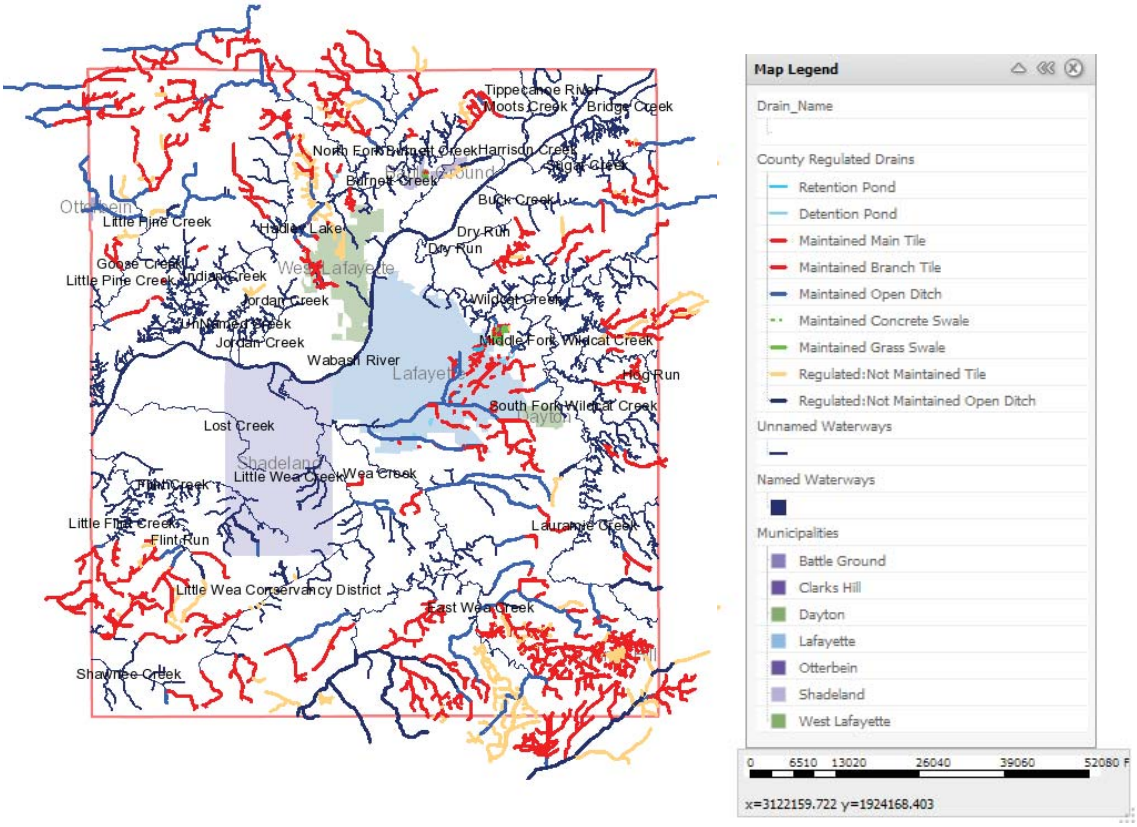

Figure 5-7. Tippecanoe Drainage Map from Tippecanoe County website (http://www.tippecanoe.in.gov/eGov/apps/services/index.egov?view=detail;id=95)

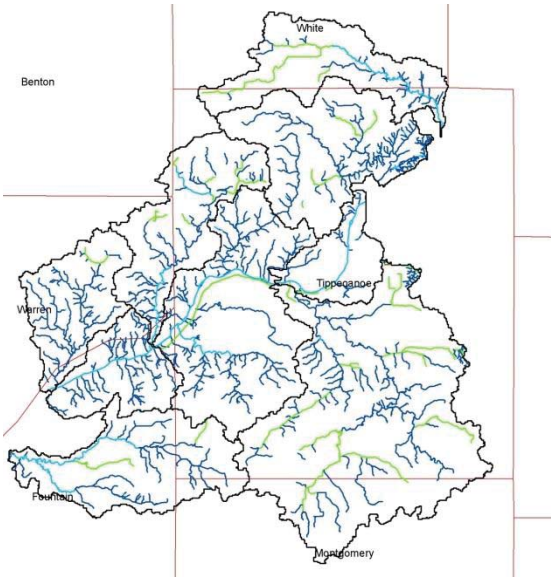

Figure 5-8. An example of the current stream and surface ditch extent in western Tippecanoe County from the NHD database

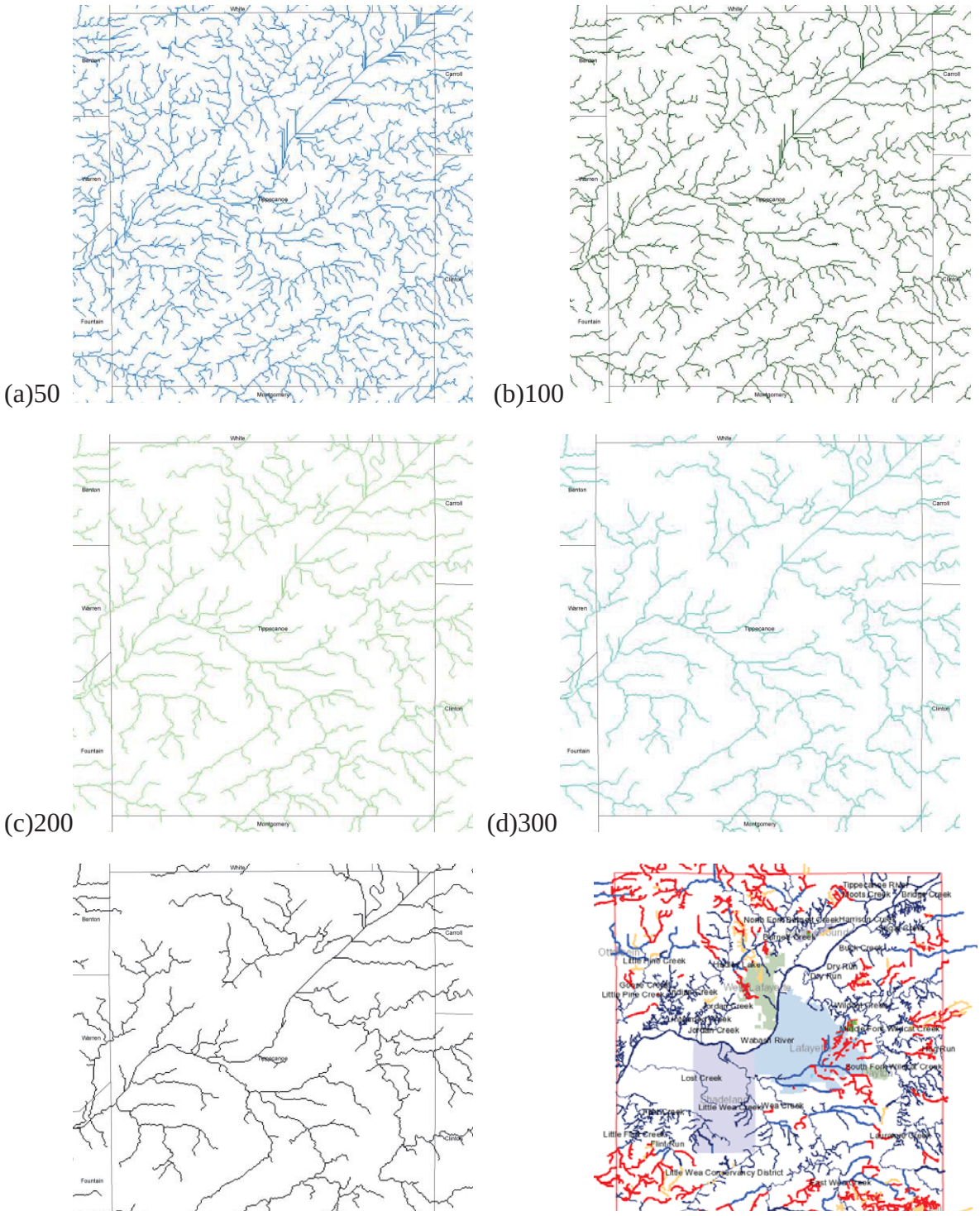

Figure 5-9. The stream network map with different stream threshold (a) 50 number of cell (0.5 km^2); (b) 100 number of cell (1 km^2); (b) 200 number of cell (2 km^2); (b) 300 number of cell (3 km^2); (b) 400 number of cell (4 km^2) and (f) the current stream and tile network map from the Tippecanoe County GIS website.

5.4.4. Calibration and Evaluation

Application of the VIC model commonly involves calibration of four parameters: the infiltration parameter (bi); Ws (the fraction of maximum soil moisture of the third layer when non-linear baseflow occurs), Ds (the fraction of maximum baseflow velocity), and Dsmax (maximum baseflow velocity) which are the baseflow parameters. Calibration involves the manual adjustment of these parameters via a trial and error procedure that leads to an acceptable match of model simulation with observations (Table 5-2). Nine years of observed streamflow from 10/1/1998 to 9/30/2007 was used to calibrate the VIC model with the subsurface drainage and wetland SEA algorithms, while 10/1/1988 to 9/30/1998 was used for model evaluation.

Table 5-2. Parameters used for calibrating the subsurface drainage algorithm.

Parameters	Initial value range	Calibrated value
Bi	0.338-0.415	0.338-0.415
Ds	0.001	0.001
Dsmax	0.0144 - 0.285	0.144-2.85
Ws	0.99	0.999

Nash-Sutcliff coefficient of efficiency (NSE) is common and widely used to evaluate model performance (Nash and Sutcliffe, 1970). The NSE is calculated as follows:

$$NSE = 1 - \frac{\sum_{i=1}^{n} (Q_{obs,i} - Q_{sim,i})^2}{\sum_{i=1}^{n} (Q_{obs,i} - Q_{obs,mean})^2} \quad \textbf{(5-3)}$$

Where, $Q_{obs,i}$ is the observed daily streamflow, $Q_{sim,i}$ is the simulated daily streamflow from the VIC model and routing model, and $Q_{obs,mean}$ is the mean observed daily

streamflow during the study period (calibration or evaluation). An NSE greater than 0.75 is considered to be a good fit to observation. An NSE between 0.36 and 0.75, the simulation is considered to have a satisfactory fit to observation (Motovilov et al., 1999; Moroasi et al., 2007).

Percent bias (PBIAS) is used to measure the average tendency of simulated data to be larger or smaller than their observed counterparts (Moroasi et al, 2007). The optimal value of PBIAS is 0.0 to low magnitude values indicating a better fit of model simulation. The positive value shows model is overestimation and negative value is underestimation. PBIAS is shown as following:

$$PBIAS = \frac{\sum_{i=1}^{n}(Y_{sim,i} - Y_{obs,i}) * 100}{\sum_{i=1}^{n}(Y_{obs,i})} \quad (\mathbf{5\text{-}4})$$

The ratio of root mean square error (RMSE) to the observed standard deviation ratio (RSR) includes a measure of error index statistics normalized by the standard deviation (Moroasi et al, 2007). The optimal value is 0 indicating zero RMSE or residual variation and the lower RSR, the lower RMSE, and the better model simulation performance. RSR is calculated as the ratio of RMSE and standard deviation of observation as shown in the following:

$$RSR = \frac{RMSE}{STDEV_{obs}} = \frac{\sqrt{\sum_{i=1}^{n}(Y_{obs,i} - Y_{sim,i})}}{\sqrt{\sum_{i=1}^{n}(Y_{obs,i} - Y_{obs-mean})^2}} \quad (\mathbf{5\text{-}5})$$

The hydrologic metrics shown in Table 5-3 have been widely used as measures of the hydrologic regime that may be important to ecosystem stability (Konrad and Booth, 2005). The most widely used low-flow index in the United States is the 10 year 7-day-average low (Riggs et al., 1980). It is used to remove the impacts of single day streamflow outliers. In this study, annual seven day low flow values were determined by the minimum of the 7- day moving average series for 59 year periods. The annual maxima series was created by selecting the single highest discharge value per year.

Table 5-3. Hydrologic metrics used for streamflow analysis for observed and simulated data

Category	Name
Low Flow	Seven-Day Minimum Flow
Mean Flow	Mean Annual Flow
High Flow	Annual maximum flow
Streamflow Variability	Richards-Baker Flashiness Index (RBI)
Streamflow Distribution	TQmean

Richards-Baker Flashiness Index (RBI) is used to quantify variation in streamflow response to storm events, particularly short-term changes. High streamflow RBI values (or flashiness) indicates sensitivity in flow changes from storm events and is an important indicator of hydrologic regime (Baker et al., 2004). The index is calculated by dividing the sum of the absolute value of day to day changes in daily discharge volume by total discharge volume for each year, as follows:

$$RBI = \frac{\sum_{i=1}^{n-1} | Q_{i+1} - Q_i |}{\sum_{i=1}^{n} Q_i} \qquad (\mathbf{5\text{-}6})$$

Where Q_i is daily discharge volume for day i, and n is the number of days in a year.

In order to test flow distribution, the fraction of time that daily streamflow exceeds mean streamflow for each year (TQmean) is calculated as follows (Konrad and Booth, 2002; Yang, 2011):

$$TQmean = \frac{number\ of\ days\ that\ streamflow\ greater\ than\ mean\ streamflow}{days\ in\ a\ year\ (365\ or\ 366)} \quad (5\text{-}7)$$

The redistribution of water from baseflow to stormflow in a stream can reduce the period of streamflow exceeding the mean streamflow, and result in decreasing TQmean values (Konrad and Booth, 2005).

5.4.5. Factor Separation Analysis

Model comparisons often evaluate the influence of only one factor, but in this study we are interested in the combined and individual impact of wetland (depression area) storage and subsurface drainage. In order to obtain the pure contribution of any factor to any predicted field and the contributions due to the mutual interaction among two or more factors, the simple factor separation method developed by Stein and Alpert (1993) is utilized. This isolates the change in the hydrologic metrics listed in Table 5-3 due to subsurface drainage and wetland storage. For example, the control simulation (f_0) represents the average annual hydrologic metric (scalar) of simulated streamflow for the base VIC simulation without utilizing the drainage algorithm or the wetland algorithm. Experiment 1 utilizes the drainage algorithm (f_1) to simulate streamflow. Experiment 2 utilized the wetland algorithm (f_2) to simulate streamflow. The interaction simulation (f_{12}) includes both drainage and wetlands (Table 5-4). The individual components are

then calculated from the accumulated average annual metric as follows (Stein and Alpert, 1993):

$$\hat{f}_0 = f_0;$$

$$\hat{f}_1 = f_1 - f_0;$$

$$\hat{f}_2 = f_2 - f_0;$$

$$\hat{f}_{12} = f_{12} - (f_1 + f_2) + f_0 \quad \textbf{(5-8)}$$

Table 5-4. The four experiments for factor separation analysis at a daily time step, the modern, higher stream network density 1km^2 was used for routing model in all scenarios

Experiment		Hydrologic Metric
Baseline	No Drainage & No Wetland	f_0
1	Drainage	f_1
2	Wetland	f_2
Interaction	Drainage & Wetland	f_{12}

5.4.6. Stream network density test

To evaluate the effect of stream network density on streamflow in the Northern Wabash River watershed, the calibrated model will be applied for the entire 59 years meteorological data at a three hour time step and with four experiment scenarios (Table 5-5). The scenarios will be run 1) with and without tile drainage, and 2) with natural and modern stream network extent to quantify the interplay between tile drainage, storage capacity and residence time for local soil conditions. Wetlands are represented in all four scenarios.

Table 5-5. The four experiment sets for different stream network density (modern or historical) and drainage algorithm (with or without).

Model option / Routing parameter	Drainage Wetlands	No Drainage Wetlands
Modern network (1 km^2 threshold)	1	3
Natural network (4 km^2 threshold)	2	4

Note: The modern network was used for the calibration, evaluation and factor separation analysis

5.5 **Results and Discussions**

5.5.1. Model Evaluation

The daily observed and simulated hydrograph for the calibration period are shown in Figure 5-10. Observed streamflow data from 10/1/1988 to 9/30/1998 was used to independently evaluate the VIC model. The daily observed and simulated hydrograph are shown in Figure 5-11. Visually, the simulation appears to fit the observations well during the calibration period. The simulated streamflow did not catch the high peak response well during the evaluation period. The daily NSE, RSR and PBAIS values for calibration and evaluation are summarized in Table 5-6. The calibration values were in the satisfactory range. The validation period from 1988 to 1998 water years yields a slight decrease in NSE of 0.32, RSR increased from 0.77 to 0.83 and PBAIS increased from 19.58 to 25.12. The average annual total runoff depth for observation and simulation from 10/1/1948 to 9/30/2007 is shown in Table 5-7. The results showed that simulation underestimates total runoff.

Table 5-6. The summary of statistics results for calibration and evaluation.

	NSE	PBAIS	RSR
Calibration Period (10/1/1998 to 9/30/2007)	0.40	-19.58	0.77
Evaluation Period (10/1/1988 to 9/30/1998)	0.32	-25.12	0.83

Table 5-7. Comparison of simulated and observed total runoff depth from 10/1/1948 to 9/30/2007.

	Observation	Simulation
(Drainage Area) km^2	34086	35706
Average annual streamflow (m^3/s) (1948-2007)	366.5	276.8
Total runoff depth (m/year) (1948-2007 average)	0.34	0.24

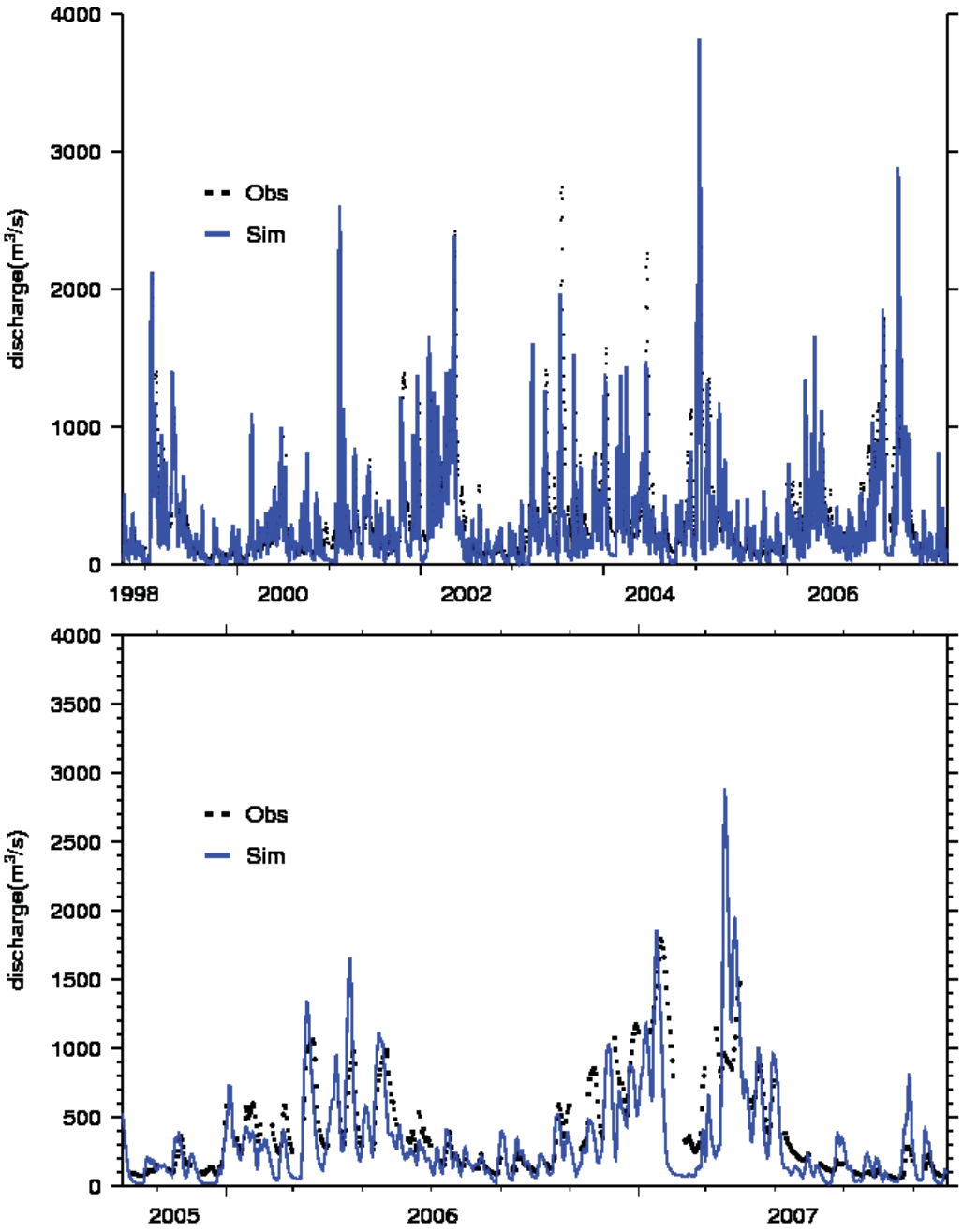

Figure 5-10. (Upper) Observed daily streamflow and simulated daily streamflow from 10/1/1998 to 9/30/2007; with (bottom) a short time period (10/1/2005 to 9/30/2007)

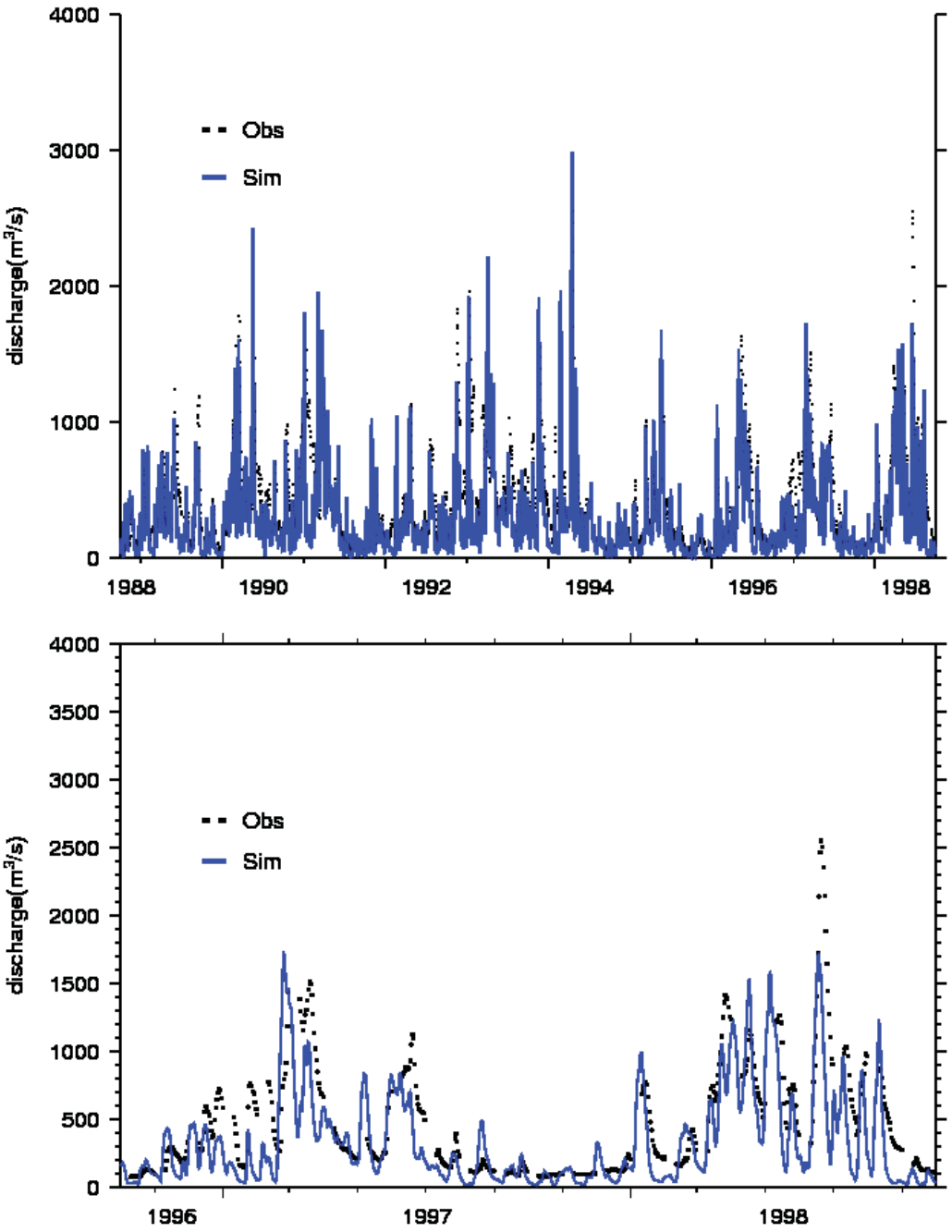

Figure 5-11. (Upper) Observed daily streamflow and simulated daily streamflow from 10/1/1988 to 9/30/1998 with (Bottom) a short time period (10/1/1996 to 9/30/1998)

The average annual precipitation, runoff, baseflow, drainflow, water table depth, soil moisture for each layer, evapotranspiration, open water volume and fraction from 1998 to

2007 (water years) for the calibration simulation are shown in Figure 5-12. The average precipitation (about 1200 mm/year) for the northern Wabash River basin is similar across the domain with a lower value at the northern part of the watershed. The area with lower values of average annual surface runoff has lower soil moisture content in all three layers and higher baseflow values. This indicates that the more available soil pore space is used as a buffer to reduce the runoff and increase the baseflow volume. The spatial pattern in drainflow also reflects the pattern in surface runoff, where areas with higher surface runoff have lower drainflow. The areas with higher surface water fraction and volume also have lower surface runoff values. This indicates that wetlands/lake can provide more temporal surface storage and reduce the runoff magnitude. The relationship with soil moisture is much more difficult to discern, reflecting the fact that drainage lowers soil moisture content, but at the same time soils with higher subsurface moisture can generate more drainflow. The mean water table depth is strongly influenced by the exponent value and bubbling pressure. This implies that those parameters need to be carefully chosen. Overall, the higher exponent and bubbling pressure result in much lower water table (Figure 5-5).

5.5.2. Factor Separation Analysis

The effect of both lake/wetland extent and subsurface drainage was analyzed by factor separation approach and results are shown in Table 5-8. The average annual observation was also analyzed for all metrics: low flow, mean flow, high flow, RBI and TQmean. Observed low flow and mean flow are higher than the simulated low flow and mean flow

value, while the simulated average RBI overpredicts the observed average annual RBI value. The model has much more flashiness compared to observation.

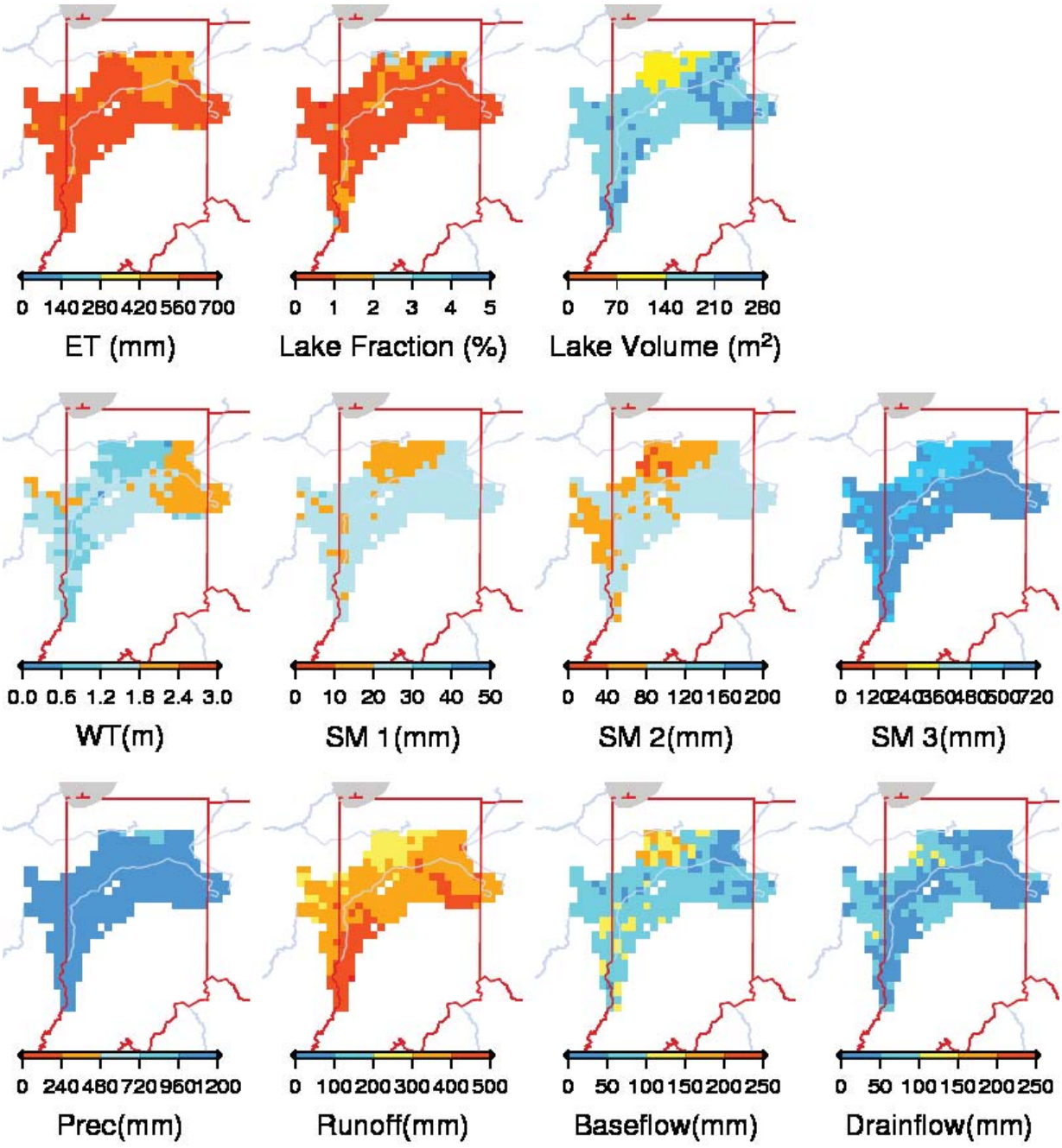

Figure 5-12. Average annual precipitation, runoff, baseflow, drainflow, water table (WT), first layer soil moisture content (SM1), second layer soil moisture (SM2), third layer soil moisture (SM3), evapotranspiration (ET), lake area fraction and lake volume from 10/1/1998 to 9/30/2007.

The drainage simulation increases the magnitude of mean and high flow, increases RBI and decreases the flow duration and low flow. All of these changes are consistent with what we would expect from urbanization. We hypothesized that peak flows would increase with subsurface drainage and the simulation shows the similar change. This indicates that in the model simulation the subsurface drains tend to increase the rate of water transport to the stream, despite increasing available soil pore space and decreasing surface runoff. The results showed that the watershed average mean surface runoff increased 0.11 % with drainage compared to no drainage and no wetlands.

Table 5-8. The average annual of all metrics- low flow, mean flow, high flow, RBI and TQmean for components of drainage algorithm, subsurface exchange algorithm.

	Low flow (m^3/s)	Mean (m^3/s)	Average High flow (m^3/s)	RBI (daily)	TQmean
Observation	34.286	363.947	1837.569	0.094	0.327
$f_0 = \hat{f}_0$ (No wetlands & No drainage)	5.516	262.123	1930.500	0.205	0.332
f_1 Drainage	5.488	262.412	2013.490	0.207	0.322
f_2 Wetlands	5.300	262.903	1852.620	0.183	0.335
f_{12} (Wetlands + Drainage)	5.273	262.193	1938.330	0.186	0.324
$\hat{f}_1$ Drainage factor	-0.028	0.289	82.990	0.002	-0.010
$\hat{f}_2$ Wetlands factor	-0.216	0.780	-77.880	-0.022	0.004
$\hat{f}_{12}$ (Wetlands + Drainage factor)	0.001	-0.999	2.720	0.001	-0.001

For the wetland factor, the simulated streamflow has lower low flow, high flow, and RBI, and higher mean flow and TQmean. This implies that wetland has strong influence on attenuating the streamflow hydrograph, lowering peak flow and increasing the flow duration. A decrease in annual minimum flow is at first surprising, but this reflects that wetland storage in the late summer serves to recharge ground water rather than being released downstream (see Chapter 3).

The interaction factor reflects the non-additive relationship that results when subsurface drainage is installed in a landscape with extensive surface water depressional storage, which is the case in the Wabash River basin. Most notably, adding subsurface drains to a wetland landscape tends to increase peak flows by a greater factor than adding drains to a flat landscape. This reflects the fact that drainage has a greater impact on streamflow lag time, because surface runoff was not a dominant flow pathway in the undrained system because of wetland storage (Figure 5-2d).

5.5.3. Analysis of Surface Network Extension

Streamflow metrics were averaged over the 59 year analysis period and compared between with/without drainage and stream threshold 1 km^2 or 4 km^2 (Table 5-9 and Table 5-10) to evaluate the impact of drainage and network density on simulated streamflow for both a 3 hour routing model time step and a daily time step. In all cases, the increased stream density increases RBI and high flows. For RBI, stream density (5 % increase) has a greater influence than does subsurface drainage representation (2% increase) for both the 3 hour and daily time step. The reverse is true for high flow, where the ditch network increased peak flows by 3%, but subsurface drainage increased them by 5%.

Table 5-9. Average for RBI and TQmean of streamflow network density analysis for all 59 years of analysis time period with 3 hour time step.

	RBI (3 hourly)	Average High flow (m^3/s)
Scenario 1 (Drain -1km^2)	0.024	245.9
Scenario 2 (Drain – 4 km^2)	0.023	239.3
Scenario 3 (No Drain -1 km^2)	0.024	235.1
Scenario 4 (No Drain -4 km^2)	0.023	228.6

Table 5-10. Average for RBI and TQmean of streamflow network density analysis for all 59 years of analysis time period with daily time step.

	RBI (3 hourly)	Average High flow (m^3/s)
Scenario 1 (Drain -1km^2)	0.186	1938.3
Scenario 2 (Drain – 4 km^2)	0.178	1888.2
Scenario 3 (No Drain -1 km^2)	0.183	1852.6
Scenario 4 (No Drain -4 km^2)	0.174	1805.3

5.6 **Conclusions**

In this study, the Variable Infiltration Capacity (VIC) hydrology model was used to quantify the combined effects of surface and subsurface drainage in a region with large surface storage capacity in terms of depressional wetlands. The model was calibrated and validated for a 20 year period reflecting current extent of subsurface drains and surface ditches. The model did a reasonable job in simulating streamflow during the calibration and validation periods. Factor separation analysis provides a quantitative approach to investigate the influence between several factors such as subsurface drainage and wetland extent. The results showed the following:

- Wetlands provides temporary surface storage, reducing streamflow flashiness by 11% and peak flows by 4% relative to the simulations with no wetlands. Low flows and mean annual flow were reduced by 4% and increased less than 1%, respectively.
- Subsurface drainage increased peak streamflow by 4% and flashiness by1% and reduced flow distribution by 3%. The direction of change was generally consistent with that of urbanization.
- The interaction of wetlands and subsurface drainage resulted in a small (0.1%) increase in peak flow and decrease in flow distribution (0.3%), reinforcing the idea of a reduced ability to utilize surface storage capacity in depressional wetlands with subsurface drainage.

The stream network density analysis used different thresholds to create the routing parameter files for natural and modern stream/ditch network extents. Increasing stream network density increased the flashiness and high flow values. The VIC model with surface drainage and wetland algorithm provides a valuable tool for scientists to study agricultural activity, the wetland restoration, and even the flooding in the Midwest.

5.7 **References**

Ale, S and L.C. Bowling. 2010. Estimating potentially subsurface drained areas in Indiana and their influence on streamflow pattern. National Water Conference. Hilton Head, SC.

Bailey, A.D. and T. Bree, 1981, Effect of improved land drainage on river flows. In: Flood Studies Report – 5 Years On. Thomas Telford, London, 131-42.

Baker, D.B., P. Richards, T.L. Loftus, and J.W. Kramer. 2004. A New Flashiness Index: Characteristics and Applications to Midwestern Rivers and Streams. Journal of the American Water Resources Association 40(2):503 – 522, http://www.awra.org/jawra/papers/J03095.html

Bowling, L. C**.** and D. P. Lettenmaier, 2010. Modeling the effects of lakes and wetlands on the water balance of Arctic environments, Journal of Hydrometeorology, 11, 276-295.

Dahl, T. E. 1990. Wetlands loss in the United States 1780's to 1980's. US Department of the Interior, Fish and Wildlife services, Washington, DC. 21pp.

Franzmeier, D.P, Hosteter, W.D., and Roeske, R.E. (2001) Drainage and Wet Soil Management: Drainage Recommendations for Indiana Soils.

Kalnay, E., and Coauthors (1996). The NCEP/NCAR 40-year reanalysis project. Bulletin of the American Meteorological Society, 77(3), 437-471.

Konrad, C. P., and Booth, D. B. 2002.Hydrologic trends associated with urban development for selected streams in the Puget Sound basin, Western Washinton. U. S. Geological Survey Water-Resources Investigations Report 02-4040, Tacoma, Washington.

Konrad, C. P., and Booth, D. B. 2005. Hydrologic Changes in Urban Streams and Their Ecological Significance. Paper presented at the American Fisheries Society Symposium.

Kumar, S., V. Merwade, J.H. Kam, and K. Thurner. 2009. Streamflow trends in Indiana: Effects of long term persistence, precipitation and subsurface drains. J. of Hydrology. 374: 171-183.

Maurer, E. P., A. W. Wood, J. C. Adam, D. P. Lettenmaier, and B. Nijssen, 2002. A long-term hydrologically based dataset of land surface fluxes and states for the conterminous United States. J. Climate, 15, 3237–3251

Miller, D.A. and R.A. White, 1998: A Conterminous United States Multi-Layer Soil Characteristics Data Set for Regional Climate and Hydrology Modeling. *Earth Interactions,* **2.** [Available on-line at http://EarthInteractions.org]

Moriasi, D. N, J. G. Arnold, M. W. Van Liew, R. L. Binger, R. D. Harmel, and T. L. Veith,, 2007, Model evaluation guidelines for systematic quantification of accuracy in watershed simulation, ASABE, 50(3):885-900.

Motovilov, Y., G. L.Gottschalk, K. Engeland, and A. Rodhe, 1999. Validation of a distributed hydrological model against spatial observations. Agricultural and Forest Meteorology, 98(9):257-277.

Nash, J. E. and J. V. Sutcliffe, 1970. River flow forecasting through conceptual models part I – A discussion of principles. J. of Hydrology. 10:282-290.

Novitzki, R. P., 1978. Hydrologic characteristics of Wisconsin's wetland and their influence on floods, streamflow and sediment. In: Wetland Functions and Values: The state of our understanding , Proceeding of the National Symposium on Wetlands. American Water Resource Association, pp.377-388.

Rawls et al., Infiltration and Soil Water Movement, In: *Handbook of Hydrology*, D. Maidment (ed.), 1993

Riggs, H. C.1980. "Characteristics of low flows" J. Hydraul. Eng. 106(5): 717-731.

Robinson, M. 1990, Impact of improved land drainage on river flows. Report No. 113. Institue of Hydrology, UK.

Stein, U., and P. Alpert. 1993. Factor separation in numerical simulations. J. Atm. Sci., 50: 2107-2115.

U. S. Geological Survey. 2010. Attributes for NHDPlus Catchments (Version 1.1) in the Conterminous United States: Artificial Drainage (1992) and Irrigation Types (1997). Available online: http://water.usgs.gov/GIS/metadata/usgswrd/XML/nhd_adrain.xml

Yang G., L.C. Bowling, K. A. Cherkauer, B. C. Pijanowski, and D. Niyogi. 2010. Hydroclimatic Response of Watersheds to Urban Intensity- An Observational and Modeling Based Analysis for the White River Basin, Indiana, J. Hydrometeorology, 11(1), 122-138.

Yang, G. X., Bowling, L. C., Cherkauer, K. A., and Pijanowski, B. C. 2011. The impact of urban development on hydrologic regime from catchment to basin scales. *Landscape and Urban Planning*, *103*(2), 237-247. doi: 10.1016/j.landurbplan.2011.08.003

6. CONCLUSIONS AND RECOMMENDATIONS FOR FUTURE WORK

6.1 Summary

The overall goal of this research was to understand the interaction of surface and subsurface hydrology, surface energy balance and carbon dynamics with surface physical properties in northern wetlands heavily influence by human activity. This study primarily focuses on the continued development of a land surface model for northern wetlands and utilized directly observed measurements to i) evaluate the model performance and ii) quantify the relationship between surface water, energy balance and carbon dynamics in agricultural wetlands.

The Variable Infiltration Capacity (VIC) model developments were presented in Chapter 2. First, the organic matter fraction was taken into account in the model framework to represent the effect of organic matter on soil moisture regime and thermal properties. This modification provides the ability to investigate soil with high organic matter content such as peat land, swamp, or marsh. Second, the equilibrium water table algorithm is used to improve the previous water table calculation. This algorithm considers the soil's ability to store and release water as a function of soil suction (or matric potential) determined by the water table position. This drained volume calculation determines how the water table moves when a given amount of water is removed or added to the soil column. Third, a new drainage algorithm was developed in the VIC model to estimate subsurface tile drainage using the classic drainflow ellipse equation which is solved in

terms of VIC input parameters, by equating the Arno baseflow curve with the ellipse equation during maximum flow conditions, based on input drain spacing and drain depth. Fourth, the distributed water table algorithm estimates the water table depth at different landscape positions. The subsurface/surface moisture exchange option for the lake and wetland algorithm uses the distributed water table to calculate subsurface moisture exchange between open water and the adjacent soil. Finally, a lake-wetland parameterization was developed using the generalized topographic index and multiflow directional algorithm to prepare a wetland parameter file in order to estimate the distributed water table depth for each landscape position.

The enhanced VIC wetland model was used to explore three case studies related to agricultural drainage and wetland interactions, as summarized below,

6.1.1. Natural Wetland Study

A continuously monitored natural wetland at the Agronomy Center for Research and Education (ACRE) was used to study the surface and subsurface hydrology of wetlands, as well as the effect of tile drainage, as discussed in Chapter 3. The main objective of this study was to investigate the hydrology and physical characteristics of the wetland. A second objective was to evaluate the performance of the modified VIC model using this natural wetland surrounded with dense agricultural tile drainage applications, as a representative test case. The observed and simulated hydraulic gradient showed general water movement towards the wetland from higher elevations, especially during the wetter periods of the year, and a reversal of the direction of movement during the drier periods

of the year. The surrounding tile drainage accounts for 31% of water that enters the wetland, based on the simulation results.

The model was also used to simulate the lake depth, and reproduced the limited field observations well. The simulated results show that the area and volume of the wetland expands to maximum in early spring due to reduced evapotranspiration, accumulated snow melt, and heavy seasonal precipitation and shrinks to minimum during the fall due to plant growth and high evapotranspiration. This model now provides a really promising modeling tool for simulating the extent of lakes or wetlands and groundwater recharge.

6.1.2. Watershed with high organic matter peatland

In chapter 4, the study focused on the north temperate peatlands that have been gradually lost due to intensive agricultural drainage, and expanding industrial and urban areas. These regions also play an important role in global climate in part due to the potential for positive carbon-cycle feedbacks associated with the interaction between soil temperature and moisture. The water table position usually acts as the dominant control on methane (CH_4) and carbon dioxide (CO_2) emissions in such drained wetlands. The modified VIC model with organic matter fraction and drainage algorithm was used to evaluate the role of drainage condition on soil moisture and temperature regime and also CO_2 and CH_4 emissions in the Kankakee River watershed.

The field scale study results showed a significant improvement in soil temperature when simulated with organic matter fraction compared to simulation without organic matter fraction. The water table simulations successfully capture the fluctuation of observed water table depth with storm events. However, the equilibrium water table algorithm is

very sensitive to the range of the Brooks-Corey exponent and bubbling pressure, which requires caution.

At the watershed scale, the results showed a significant increase in streamflow with the introduction of drainage particularly during the growing season reflecting the overall decrease in soil moisture and evapotranspiration, demonstrating the capability of model with drainage algorithm. Results showed that the No-drainage scenario has higher average CO_2 fluxes from 1915 to 2007 due to the simulated increase in NPP with higher moisture conditions. This increase in NPP for a domestic crop is not realistic. This needs to be further investigated in order to estimate the right NPP with higher moisture condition. Despite the lower average CO_2 fluxes in the Drainage scenario, most of the organic matter was lost rapidly from the muck soil within the first 10 years of the installation of surface drainage (open ditches) and reached a new equilibrium for slow (stable) and intermediate (recalcitrant) soil pools. This shows similarity with the field study conducted by Hooijer et al. (2012) in a drained tropical peatland and implies the carbon loss will be faster right after drainage introduction.

6.1.3. Pre-settlement wetlands with intensive agricultural drainage practices

The northern Wabash River basin was utilized to evaluate the role of anthropogenic modifications to drainage conditions on streamflow variability in chapter 5. The intense drainage system in the northern Wabash watersheds has reduced the extent of lakes and wetlands and increased the variability of the streamflow patterns compared with their pre-drainage condition. The modified VIC model was used to study streamflow response to wetland drainage, and evaluate the historic impact of surface drainage network density on

streamflow regimes within the Wabash River basin. The calibration results showed that the modified model can represent the streamflow with a satisfactorily. Once again the simulated water table depths, and therefore drainflow predictions, were strongly influenced by the choice of exponent and bubbling pressure.

The factor separation analysis showed that wetlands have reduced the Richard-Baker flashiness Index (RBI), reduced high flows, and slightly increased the flow distribution. This finding is expected since the wetlands provide more surface water storage. Subsurface drainage increased the high flow, mean flow, and RBI, and reduced the low flow and flow duration. The findings of Rutkoski et al. (2012) showed the same hydrologic response in upper White River with intense tile drainage. The additional stream network density analysis showed that the simulation with lower stream drainage density had lower peak flows and smaller RBI. Overall, the addition of subsurface and surface drainage to the Wabash River basins is estimated to have increased peak flows by over 7%.

6.2 **Hypotheses validation**

Several scientific questions and hypotheses were proposed in Chapter 1. These responses are summarized here:

1. What is the role of natural, depressional wetlands in the Wisconsin till plain that are heavily influenced by agricultural drainage in recharging local soil moisture and ground water?

Hypothesis: groundwater flow and subsurface drainage from the adjacent land areas both serve to recharge surface water storage in wetlands during the winter and spring; however during the drier summer season wetlands serve to recharge local soil moisture, reducing streamflow at the outlet.

The field and modeling study at ACRE showed groundwater flow from the wetland to the upland in the summer and the opposite in winter. Wetland expansion occurred in the winter as a result of this inflow and the shrinking of wetland extent and the cessation of baseflow inflow in the summer. Similarly, simulations for the Wabash River basin showed a reduction in summer low flow in the simulation with wetlands, relative to simulations with no wetlands.

2. How has organic matter content and depth, which affects thermal and hydraulic properties, and drainage conditions affected the surface thermal and moisture regime in managed peatlands in Northern Indiana over the past several decades? Furthermore, how have agricultural drainage applications affected methane and carbon dioxide emissions from these high organic matter soils?

Hypothesis: Soils with high organic matter content with high drainage have lower average annual surface moisture and higher annual surface temperature, resulting in higher annual CO_2 emissions and lower methane emissions. Furthermore northern wetlands experiencing intense human activities such as cultivation and drainage experience faster organic matter degradation rates.

The results in the Kankakee River basin study presented in Chapter 4 showed that drained muck soils with high organic matter had lower average annual surface moisture and slightly higher surface temperature compared to simulations without drain practices, as hypothesized. While the simulations did not show an increasing magnitude of CO_2 emissions with drainage, due to the simulated reduction in net primary production (NPP), the drained muck soils did experience faster organic matter degradation especially for intermediate soil pools and slow soil carbon pools.

3. How have agricultural applications such as surface ditches or subsurface tiles altered hydrological patterns and reduced the magnitude (volume and duration) of surface water storage in the Wabash River Basin, Indiana?

Hypothesis: The use of drainage has decreased surface water storage, increased subsurface flow and lowered the water table depth, consequently increasing stream flashiness and flood frequency.

The study of the Wabash River basin in Indiana showed that the use of tile drainage has reduced the surface flow (runoff) due to more available pore space in the soil profile. The chapter 4 results also showed the tile drainage can significantly lower the water table depth. The results show that temporary surface storage in wetlands reduces streamflow flashiness by 11% and peak flows by 4% relative to the simulations with no wetlands. Low flows and mean annual flow were also reduced by 4% and 1%, respectively. Changes in streamflow metrics due to subsurface drainage were generally less than 1%, while surface drainage enhancements increased peak flows by 4% and streamflow flashiness by 1%.

6.3 **Significance of Study**

The important of this study is to develop the model that can work in areas with high organic matter content soil, wetland environment and tile drainage for studying the hydrologic impacts of wetland and tile drainage, and carbon dynamics.

- Sub-grid moisture dynamics

  The significance on the enhanced wetland model described here is the ability to represent sub-grid variability in moisture conditions – both vertically and horizontally – to better represent moisture variability and extremes. There is a well-known positive relationship between water table depth and methane emissions. Many carbon models only have simple hydrology schemes that cannot represent the sub-grid variability in moisture exchange represented by the enhanced VIC model. The distributed water table depth function can even better to present the wetland class's water table depth for each sub-grid at each time step. The modified distributed water

table depth function is a powerful and essential tool for understanding the spatial variation of methane emissions due to its positive relationship with water table depth. The modified distributed water table depth and wetland-lake algorithm can calculate the lake area and the time period that the area was saturated or covered open water. This is also an applicable tool to study the extent and the duration of wetland inundation and will provide the best aspect in hydrology for studying carbon dynamics especially in those area strongly influenced by seasonal saturation (inundation).

- Subsurface drainage

  Drainage application in Midwest is really common agricultural practices for removing excess water in soil profile to increase crop yield. The modified drainage algorithm in the VIC model is a valuable tool for quantifying the volume of drainflow into streams (or wetland or lake), investigating the hydrologic response with different drainage density, and tile drain depth and further this can be used to understand the nutrient loading with available water quality data from Midwest farmland. This improvement also helps to clarify the debate of tile drainage effects in stream hydrologic responses. In this study, the model showed that tile drainage increased the rate of subsurface water movement increasing the peak streamflow. The combined subsurface tile drainage and wetland algorithm can also provide a useful tool for scientists to investigate, and quantify the impacts of wetland restoration above existing drained landscapes. Further, it can provide a tool to estimate the impact of wetland loss (or restoration) on the risk of the flooding.

- Wetland Hydrology

  Many studies have already shown that there is lateral flow between wetlands and adjacent area. In some situations what is less understood are the watershed level implications of this exchange. Both model and observed results in chapter 4 showed that the water discharges into wetland during wetter period of year and recharges surrounding area during drier period of year in a natural, depressional wetland that receives excess water from drainflow. It also showed that there is reduced outflow during summer when water recharges the adjacent area. In chapter 5, we also have found that annual minimum flow was decreased due to this soil moisture recharge. The modified VIC model has the ability to quantify the timing of wetland expansion, wetland area and the volume of water entering and leaving wetlands. This model now can provide an insight and even a quantitative tool for those studies that investigate the nutrient loading into wetland, pollutants removal from a wetland, and even the carbon dynamics study (such as methane emission, NO_3 emission) in area affected by drainage application.

6.4 **Future Work**

The ACRE field study was conducted for 7 years with monitoring conducted by several graduate students. Only three years of observations were used to evaluate model performance due to lack of filled meteorological data and the impact of a drought event in 2012. More observations are still needed to complete the understanding of the wetland function within a tile drained landscape. There are many opportunities to further explore this wetland. This research provides a promising hydrology model and a starting point for

water quality study with measured water samples such as Nitrate, Nitrite and phosphate. This study can provide an initial evaluation for nutrient loading of ACRE's wetland and the role of anaerobic processes in nutrient retention by merging simulated discharge with observed water quality data.

The equilibrium water table depth algorithm is sensitive to the choice of exponent and bubbling pressure parameter. However, field observations of bubbling pressure and the exponent are limited. In order to have better soil water retention curve, improvements are needed in our ability to parameterize soil water characteristic models using soil physical properties such as soil texture, clay content, sand content, and soil density.

The drainage algorithm has the ability to simulate the monthly drainflow and controls the drainflow by adjusting the drain depth. The drainage water management (DWM) conservation practice was not explored in this study, although it could be. The modified model also provides a useful tool for water quality study for reducing the nutrient loading into the stream through DWM. Information on the control section in the field is needed to build up the decision for raising the water table for providing more water for plant to use and lowering the water table for releasing extra water from the soil profile.

The poor response of simulated NPP to moisture condition for croplands was identified in chapter 4. Incorporating dynamic vegetation growth, such as the new VIC-CropSyst coupled model developed by colleagues at Washington State University would be an improvement for carbon dynamics study. However, even the CropSyst model does not limit biomass growth in the presence of excess water stress, so that improvement is still needed. Field methane data is needed to calibrate and evaluate the simulated methane

emissions. A soil subsidence study is needed to study the subsidence associated with carbon emissions from high organic matter soil.

VITA

VITA

Chun-mei Chiu

Education

2007-2013 Ph. D., Department of Agronomy, Purdue University-West Lafayette.
Thesis Advisor: L. C. Bowling. Thesis: OBSERVATION-BASED ALGORITHM DEVELOPMENT FOR SUBSURFACE HYDROLOGY IN NORTHERN TEMPERATE WETLANDS
2006 – 2007 Ph. D., Department of Soil Science, University of Wisconsin-Madison.
2002 – 2004 M. S., Agricultural Chemistry, National Taiwan University (NTU).
Thesis Advisor: Z. S. Chen. Thesis: Characteristics and Pedogenesis of the Sandy and Loamy Spodosols in Chushan region in Chiayi.
1998 – 2002 B. S., Soil and Environmental Sciences, National Chung-Hsing University (NCHU).

Professional Activities

Research Assistant:

Hydrologic Impacts Group, Department of Agronomy, Purdue University.
1/2007 -12/2009 Project: An integrated understanding of the terrestrial water and energy cycles across the NEESPI domain through observations and modeling; funded by National Aeronautics and Space Administration.

Soil Survey and Classification Lab, Department of Agricultural Chemistry, National Taiwan University.
8/2005-12/2005Project: The Evaluation of the phytoremediation of heavy metal contaminated soils in Chang-Hua cropped pollution control site; funded by Environmental Protection Administration.
8/2004-7/2005 Project: Effects of northeastern monsoon on carbon and nitrogen mineralization and their dynamics in Nanjenshan forest ecosystem; funded by Environmental Protection Administration.
8/2003-7/2004 Project: Soil Genesis and Soil Solution Chemistry of Coarse Textural Spodosols in Alishan Area (I); funded by National Science Council.

Teaching Assistant:

Purdue University
Fall 2012: Soil Ecology Lab (Undergrad course)
Spring 2011 & 2012 & 2013: Environmental Hydrology Lab. (Undergrad & Grad course)
Fall 2010: Soil Classification, Genesis, and Survey. (Undergrad & Grad course)
National Taiwan University
2002-2003: Soil Chemistry in Department of Agricultural Chemistry. (Undergrad course)

Awards and Honors:

2009 Travel grant - Frederick N. Andrews Environmental Grant, Purdue University, West Lafayette, IN.

2008 Travel grant - Ninth International Conference on Permafrost, Fairbanks, AK.

2006 Travel grant - Taipei Economic and Cultural Office in Chicago, IL